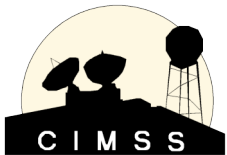


# Application of PCA to Hyperspectral Data for Noise Characterization, Noise Filtering and Instrument Monitoring

---

Paolo Antonelli, Dave Tobin, Hank Revercomb, Dave Turner, Steve Dutcher, Ben Howell, Bob Knuteson, Ken Vinson  
CIMSS/SSEC/UW-Madison

Seminar on Recent developments in the use of satellite observations in numerical weather prediction  
ECMWF  
3-7 September 2007



# Questions we are trying to answer

---

- What is the impact of PCA on hyperspectral IR data?
  - data compression;
  - estimation of the Information Loss;
  - noise reduction.
- What information is embedded in the Principal Components?
  - noise estimation and characterization;
  - Instrument monitoring.
- What are the current and future applications of PCA to hyperspectral data?
  - IASI data analysis;
  - Data inversion;
  - Forward Models.

# Data Compression Problem

---

- Generally there are two dimensions along which a compression scheme may be measured: algorithm complexity and amount of compression;
- When data compression is used in a data transmission application, the goal is speed. Speed of transmission depends upon the number of bits sent, the time required for the encoder to generate the coded message, and the time required for the decoder to recover the original ensemble;
- When dealing with hyperspectral data compression there is a third dimension that becomes relevant: impact of compression on observation noise;
- This means that when data is compressed, the goal is to reduce redundancy, leaving only the informational content.

# Data compression/Noise filter Problem

---

$$L_{\text{obs}}(\mathbf{v}) = L_{\text{atm}}(\mathbf{v}) + \eta(\mathbf{v})$$

$$\Omega = B(L_{\text{obs}}(\mathbf{v})) \text{ and } L_{\text{est}}(\mathbf{v}) = Q(\Omega)$$

$$\text{Find } F = BQ \text{ such that: } L_{\text{est}}(\mathbf{v}) = F(L_{\text{obs}}(\mathbf{v}))$$

$$\text{With minimal Estimation Errors: } EE(\mathbf{v}) = L_{\text{est}}(\mathbf{v}) - L_{\text{atm}}(\mathbf{v})$$

**MMSE**

For noise filter only purposes if  $S = \text{cov}(\eta)$  and  $R = \text{cov}(L_{\text{atm}})$  are known, the optimal linear filter in the least square sense is

$$F = R(R + S)^{-1}$$

**PCA**

$$L_{\text{est}}(\mathbf{v}) = P(L_{\text{obs}}(\mathbf{v})) \text{ where } P = BQ$$

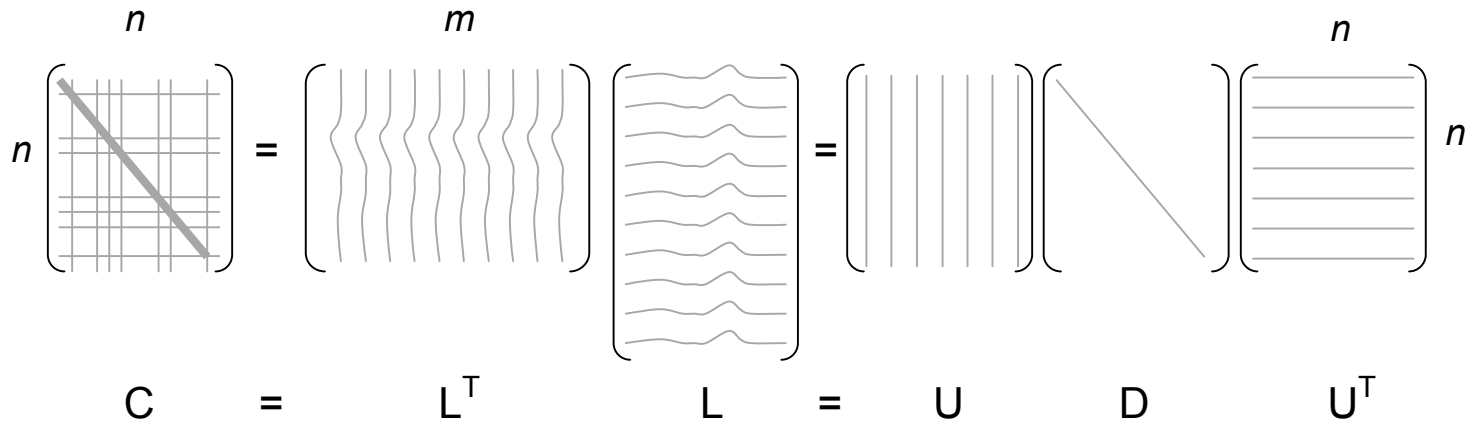


# Application of PCA to hyperspectral data

---

- Normalize each spectrum  $L_{\text{obs}}$  by estimated Noise Equivalent Radiance;
- Derive the Principal Components from observations (Eigenfunctions of Covariance Matrix of dependent  $L_{\text{obs}}$ );
- Project each  $L_{\text{obs}}$  onto PCs;
- Compress the data retaining only  $N_t$  PCs;
- Estimate noise normalized signal ( $L_{\text{est}}$ ) by expanding the compressed data;
- Remove normalization.

# Terms, Equations



## Variable

$n$

## Description

number of channels

$m$

number of spectra

$L = N_{\text{orig}}/NEN_{\text{init}}$

noise normalized spectra

$C = L^T L = U D U^T$

covariance matrix of S

D

eigenvalues

U

eigenvectors

$\hat{U}$

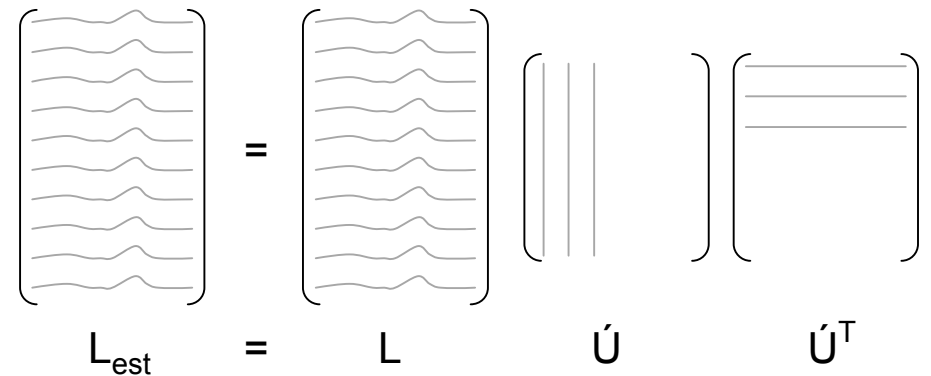
truncated eigenvector matrix

$n_T$

number of eigenvectors in  $\hat{U}$

$L_{\text{est}} = L \hat{U} \hat{U}^T NEN_{\text{init}}$

reconstructed spectra



# Compression and Noise Reduction

---

After Noise Normalization data:  $\sigma_i=1 \quad \forall i$

Original space:  $\Phi^2 = \sum \sigma_j^2 = N \quad j=1, \dots, N$

Reduced space:  $\Gamma^2 = \sum \sigma_j^2 = N_t \quad j=1, \dots, N_t$

Noise Reduction Factor (NRF)

$$\gamma = \sqrt{\Phi^2 / \Gamma^2} = \sqrt{N / N_t}$$

# Useful Quantities

---

Estimation Error (**EE**): difference between noise free and filtered signals;

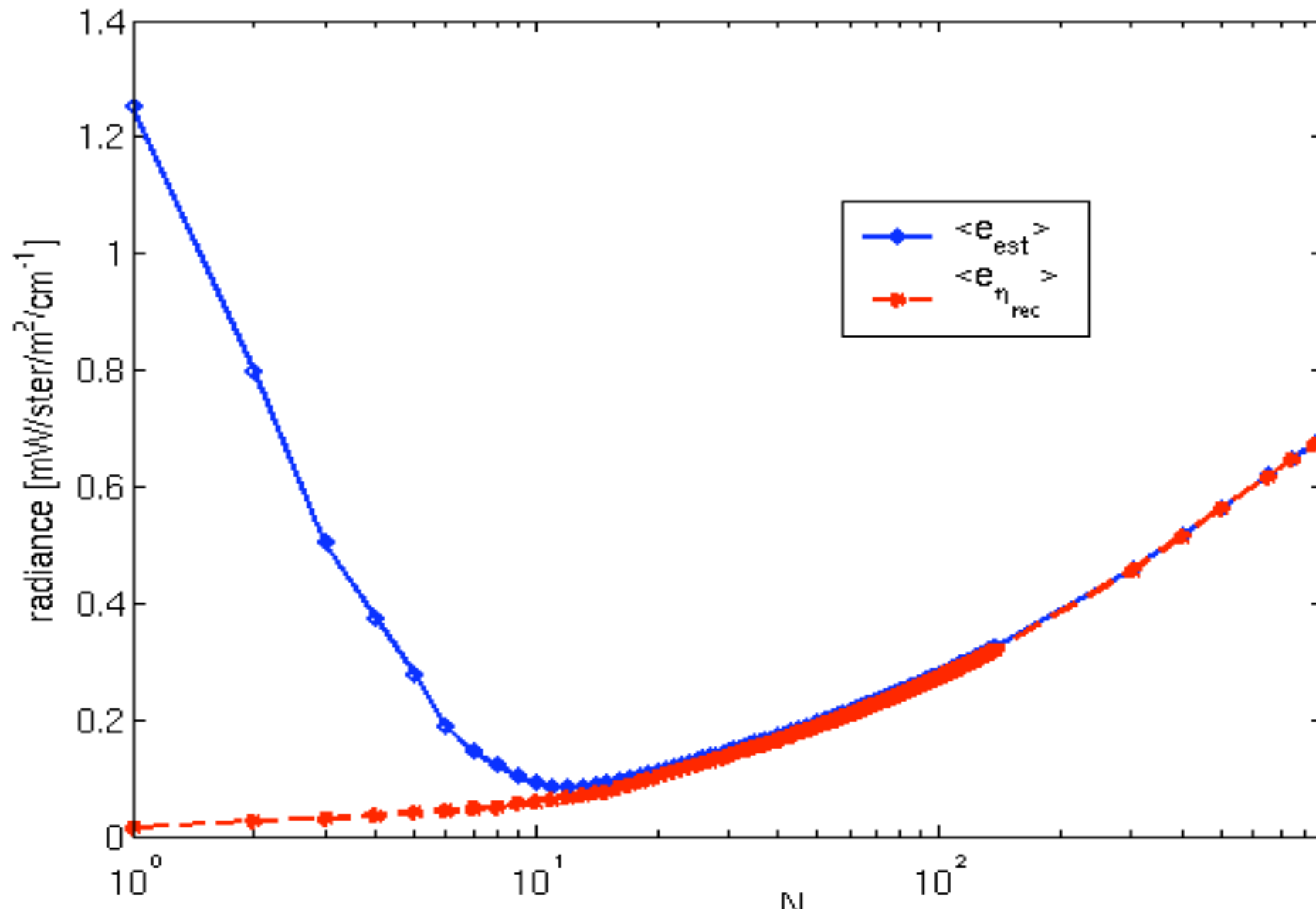
Atmospheric Information Loss (**AIL**): difference between noise free signal before and after filtering;

Reconstructed Noise (**RN**): noise signal after filtering;

Reconstruction Residuals (**RR**): difference between observed signal before and after filtering;

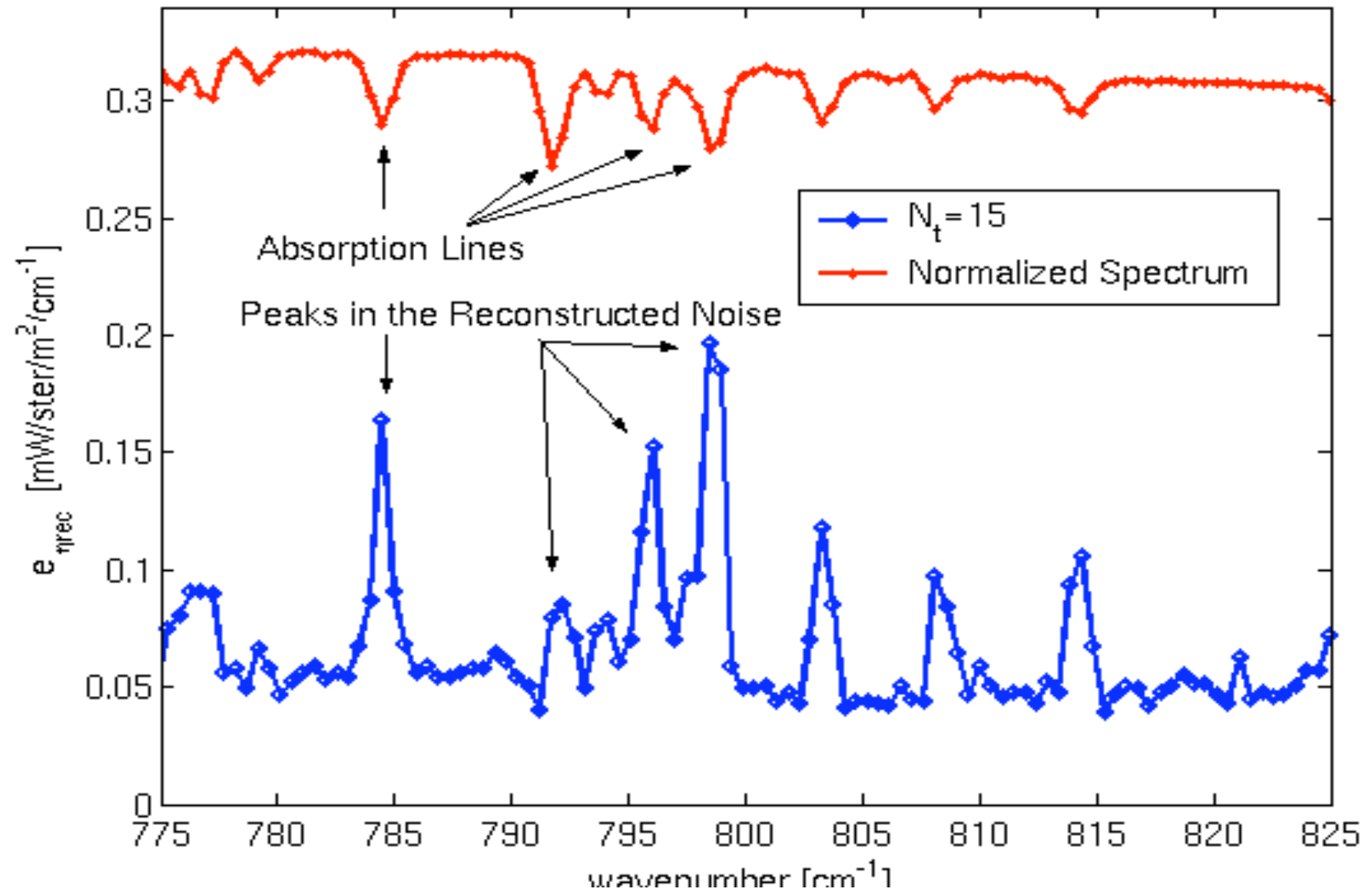
# EE vs RN

On simulated data

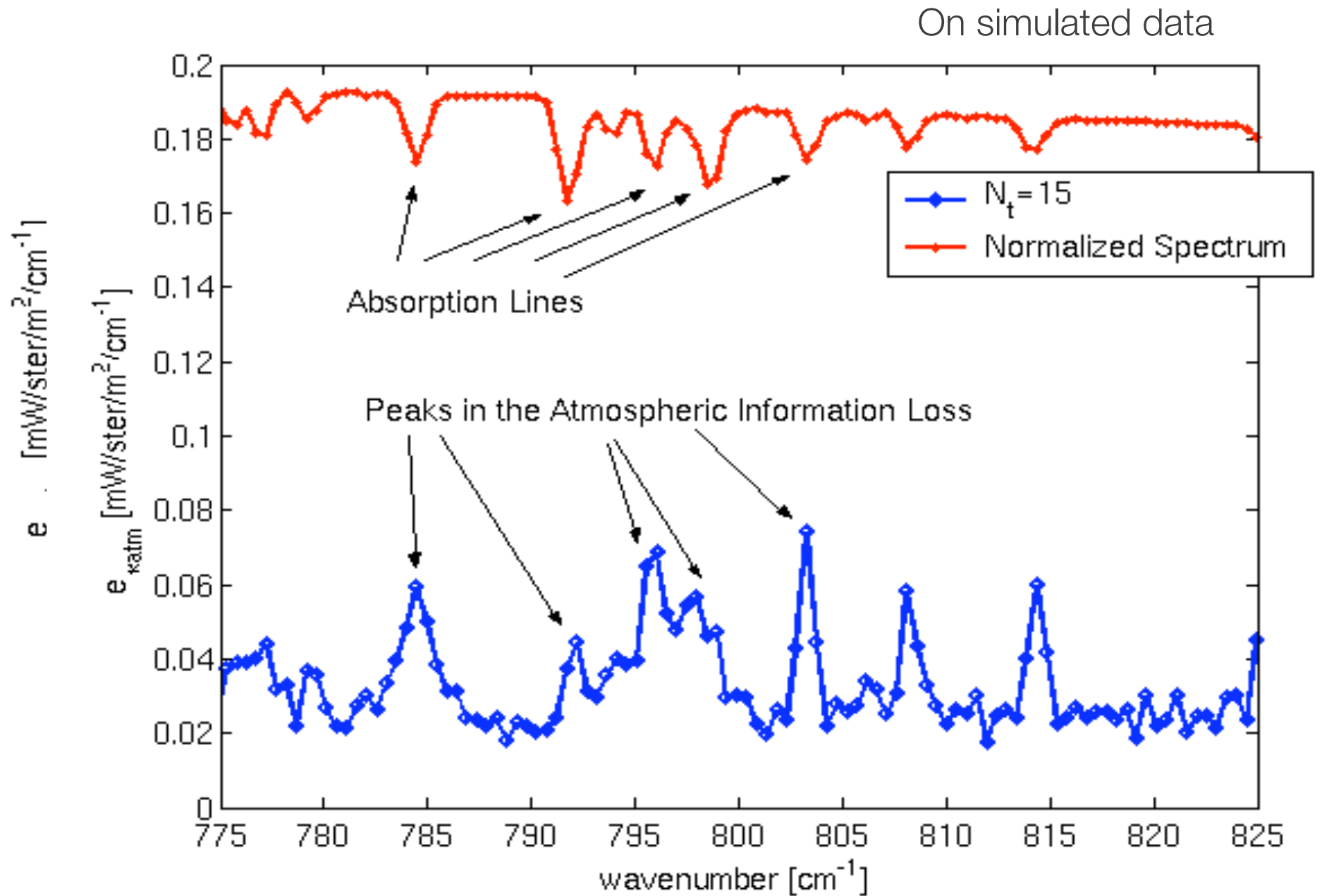


# Correlation in RN

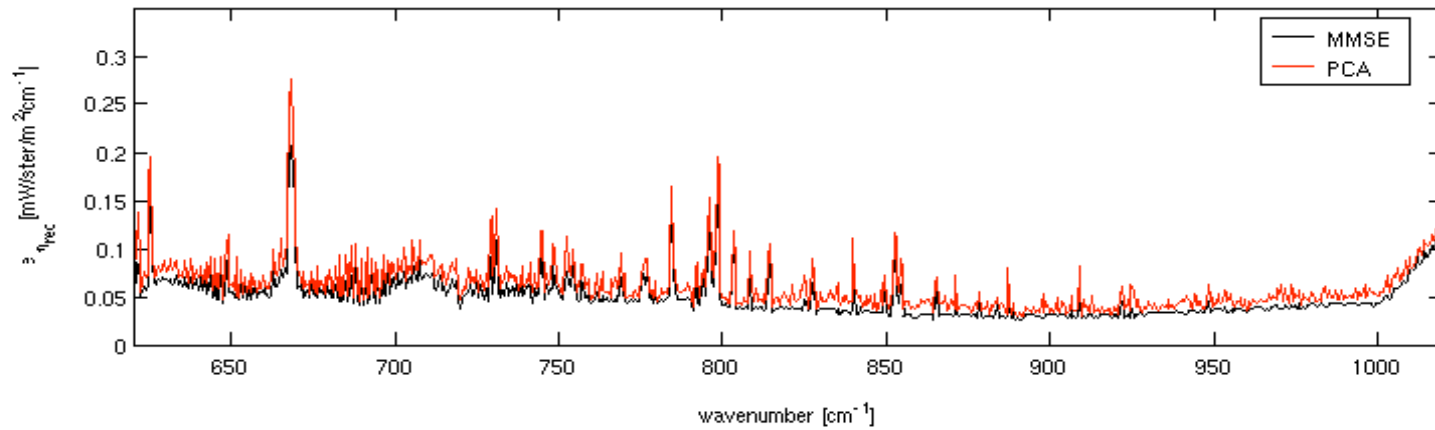
On simulated data



# Correlation in AIL

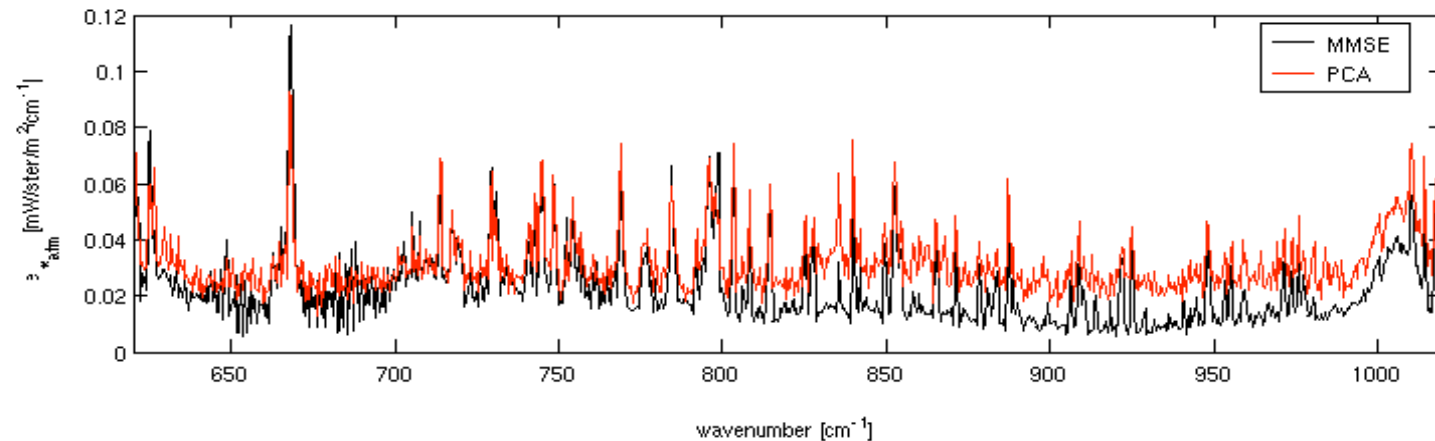


# On simulated data



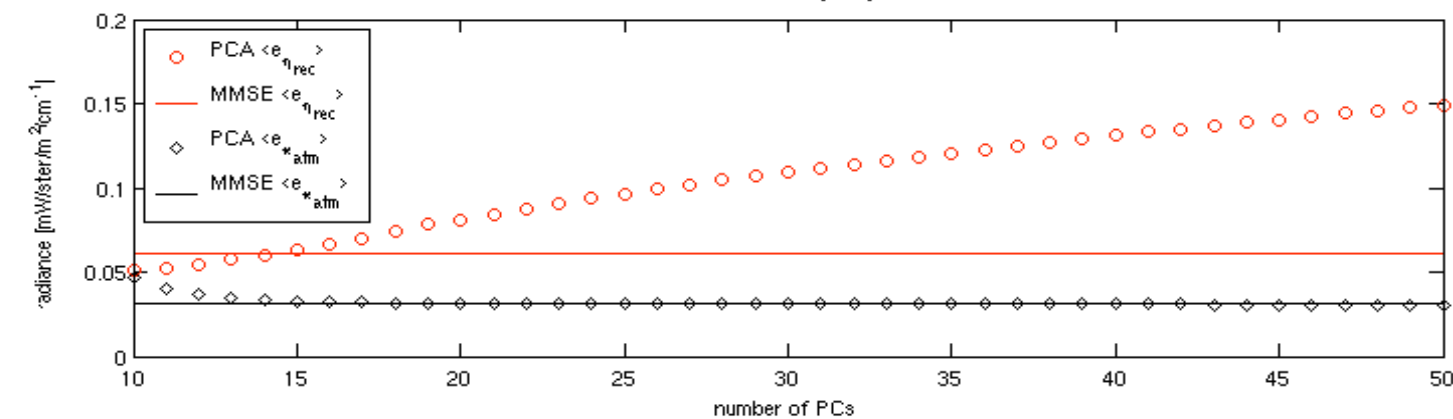
MMSE  
Rms(RN)

PCA  
Rms(RN)



MMSE  
Rms(AIL)

PCA  
Rms(AIL)



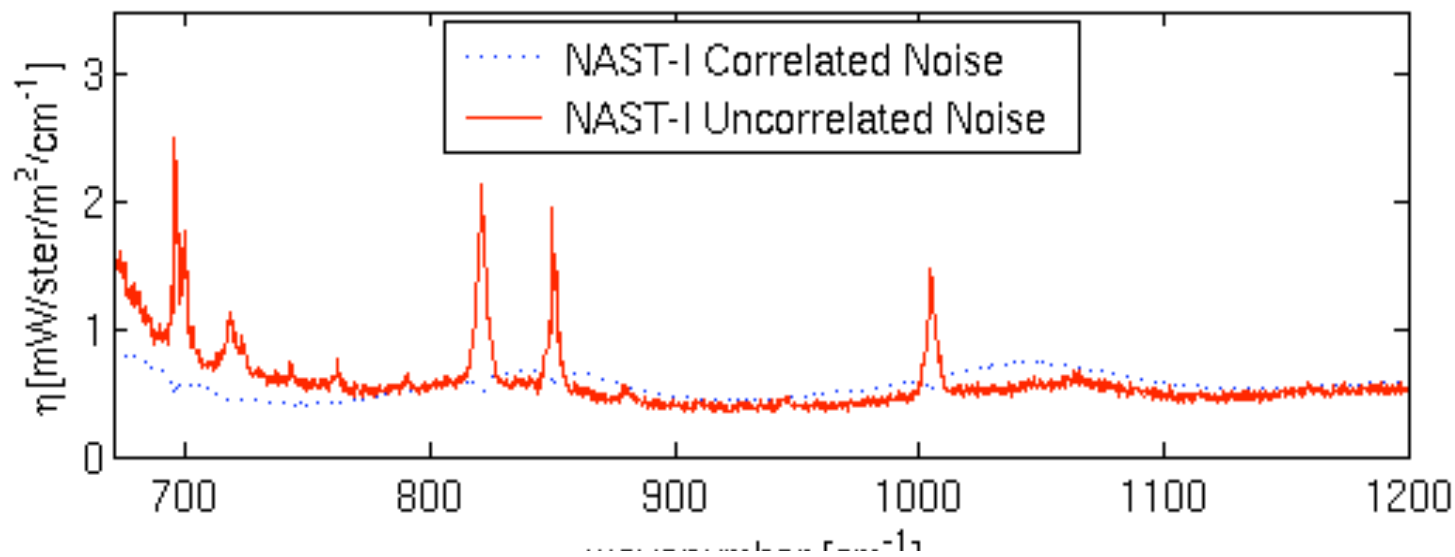
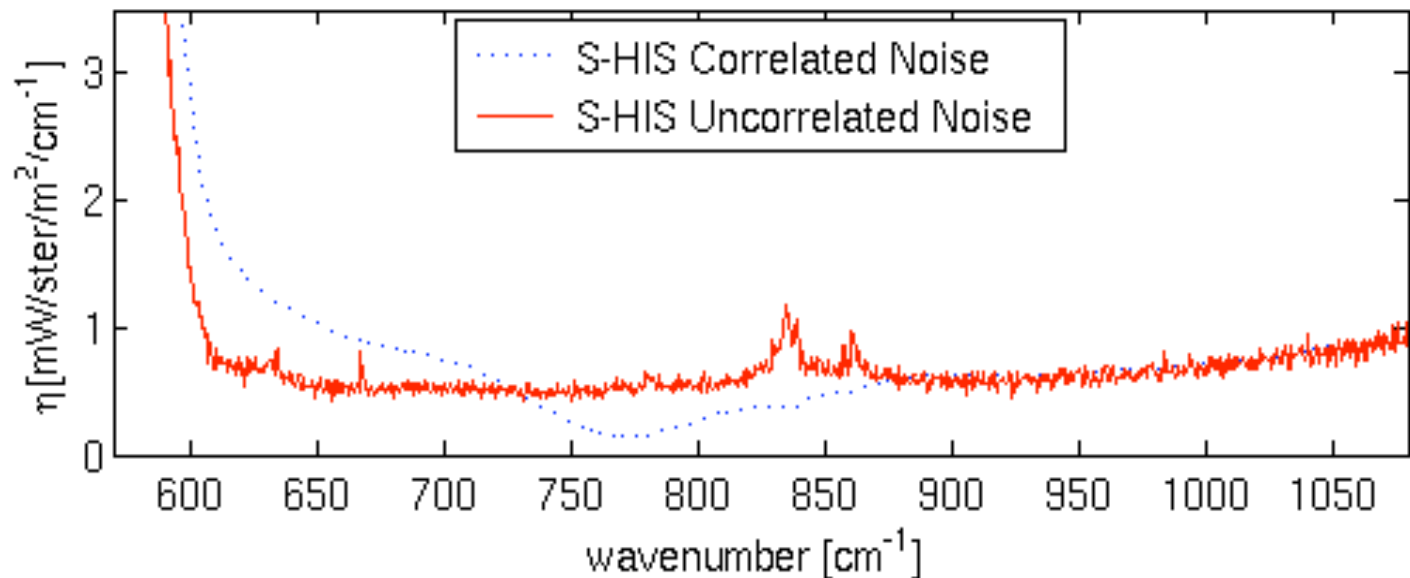
$\langle \text{Rms(AIL)} \rangle$

$\langle \text{Rms(RN)} \rangle$

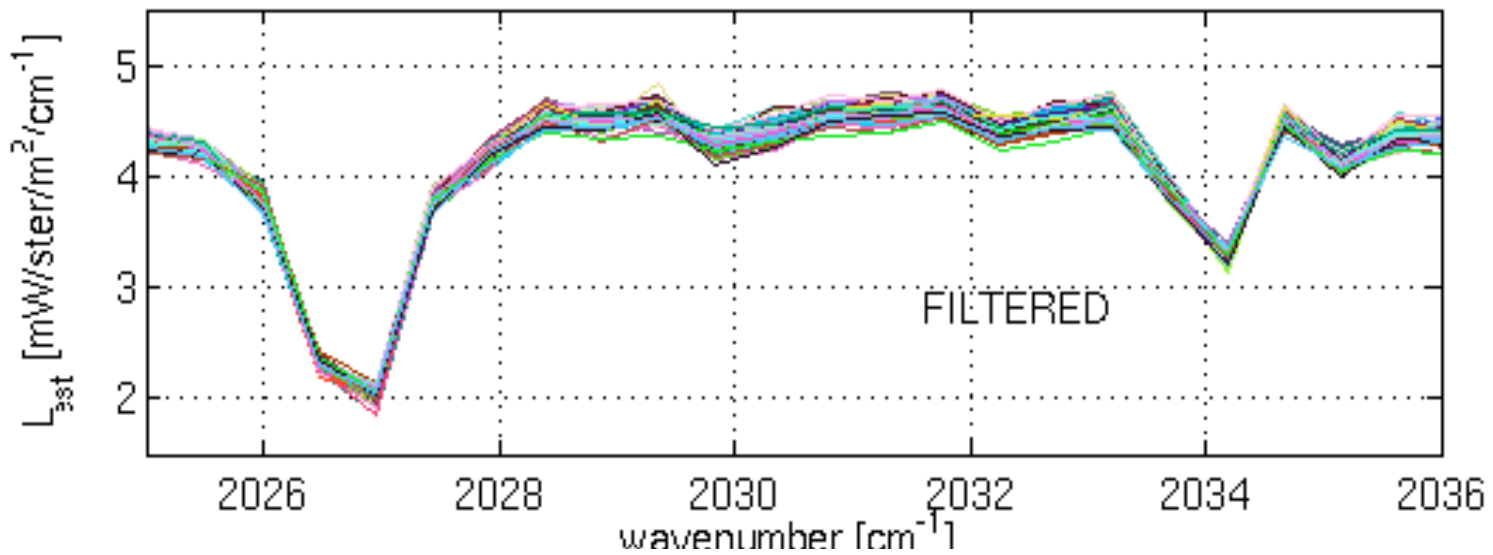
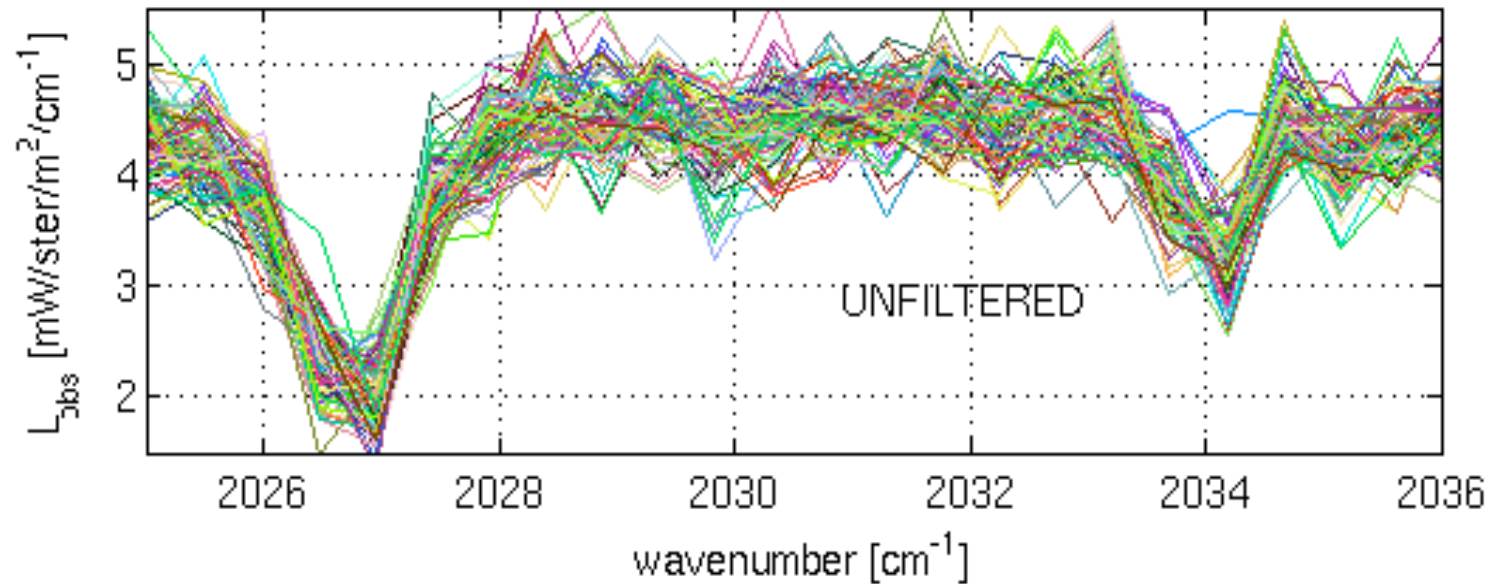




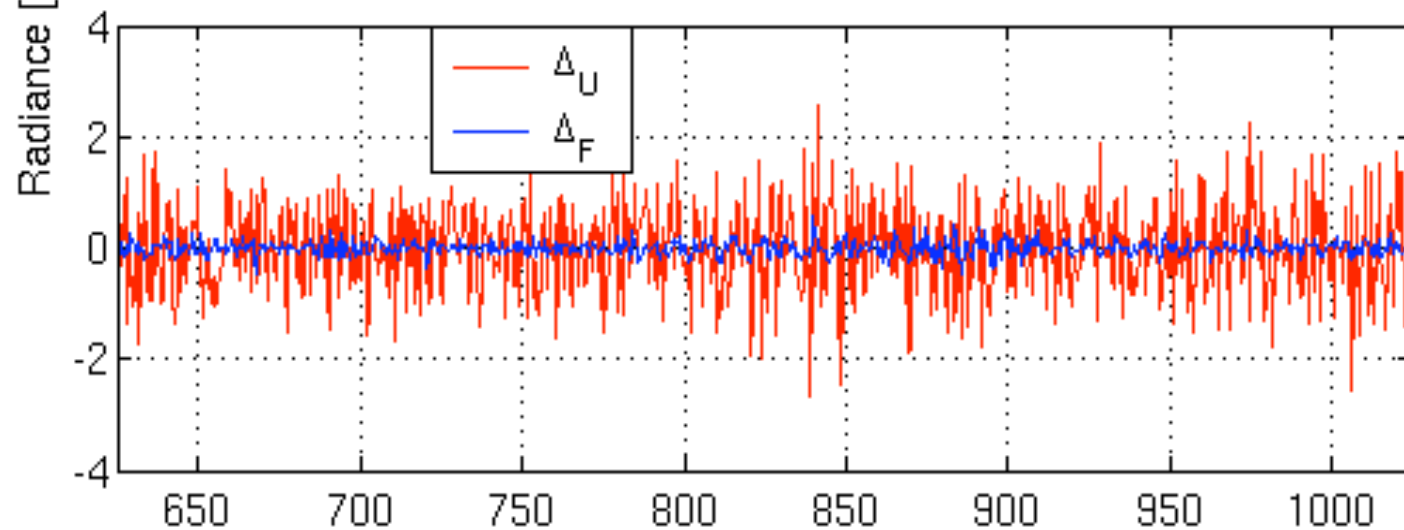
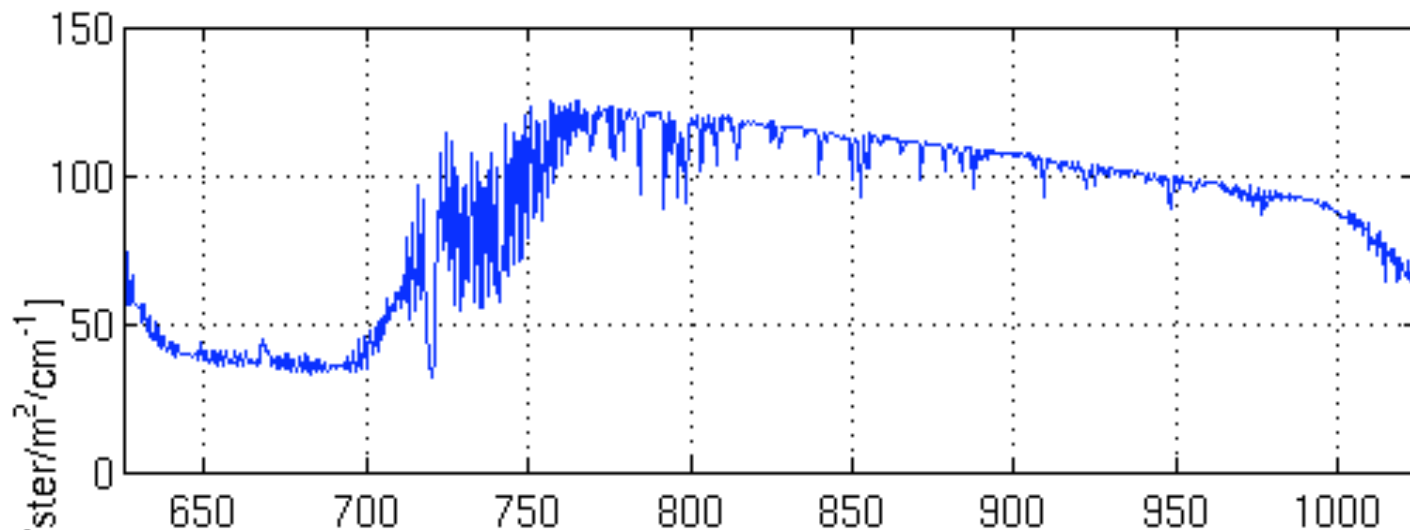
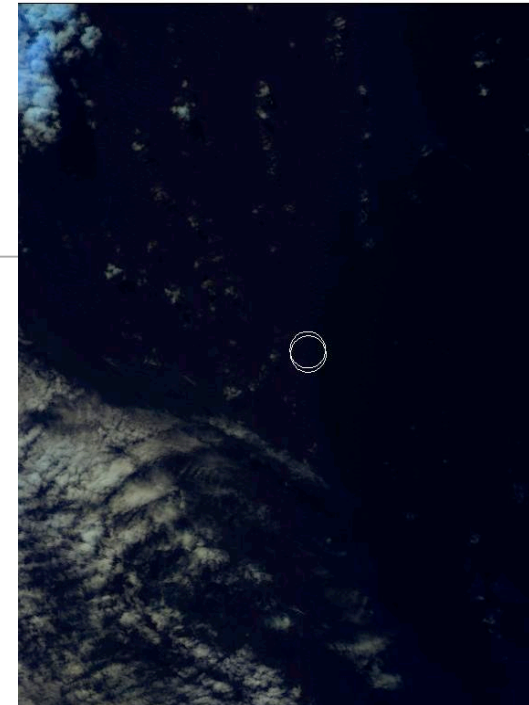
# Real data: S-HIS from SAFARI 2000



# The Noise Filter Effect of PCA



# Filtered-Unfiltered for almost overlapping FOVs over Ocean

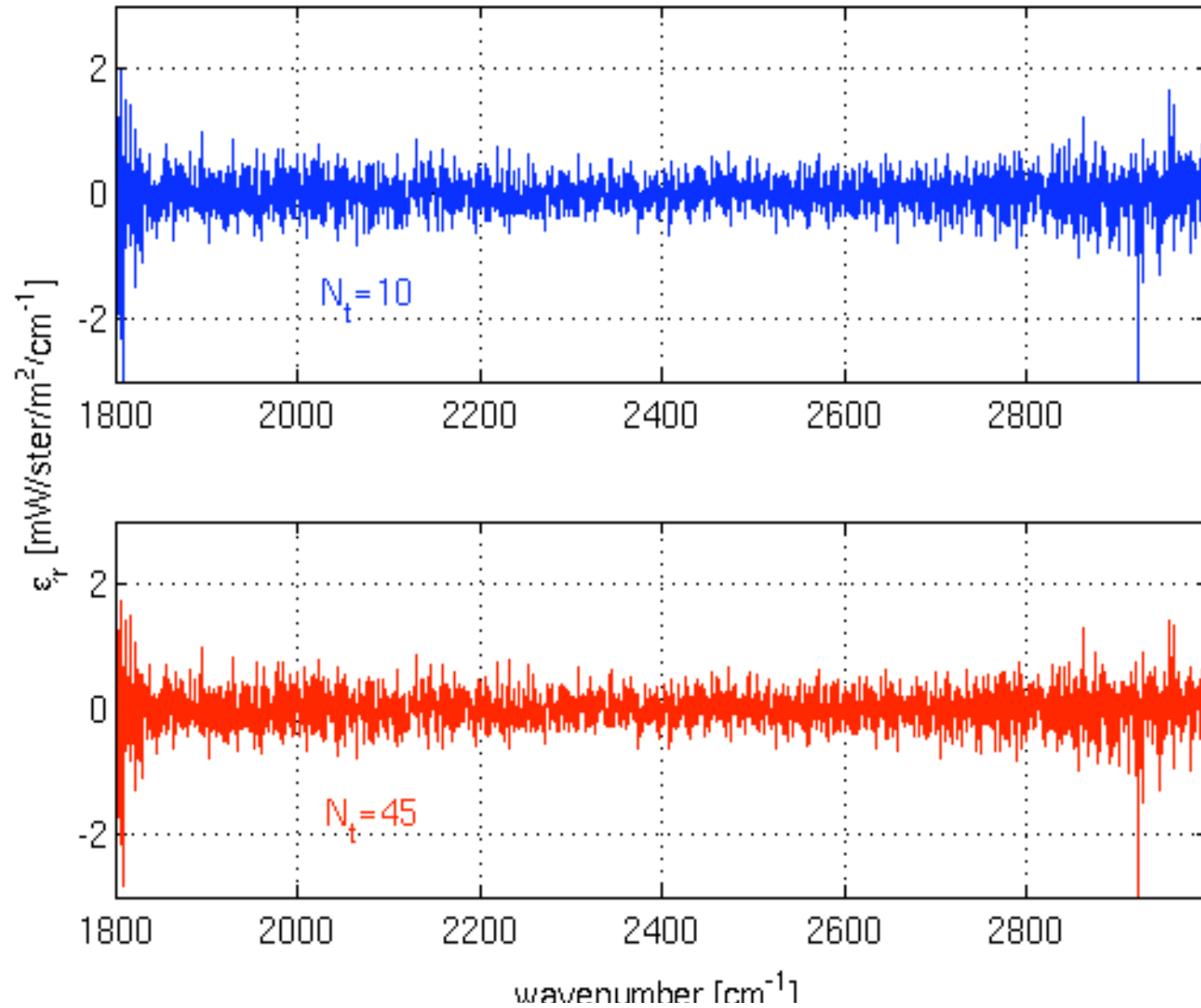


Unfiltered

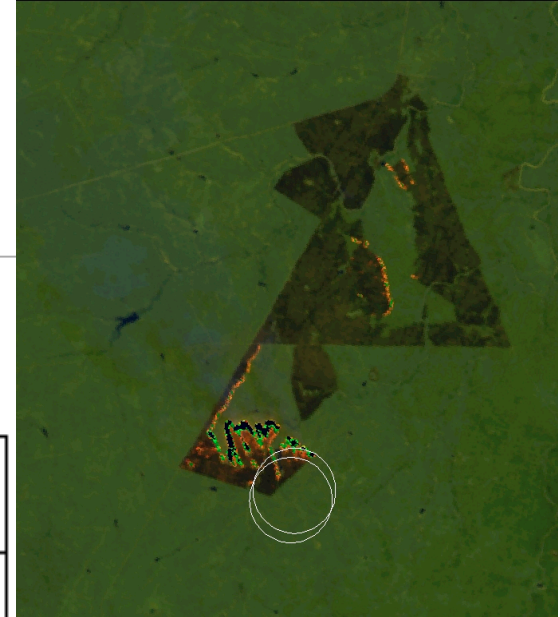
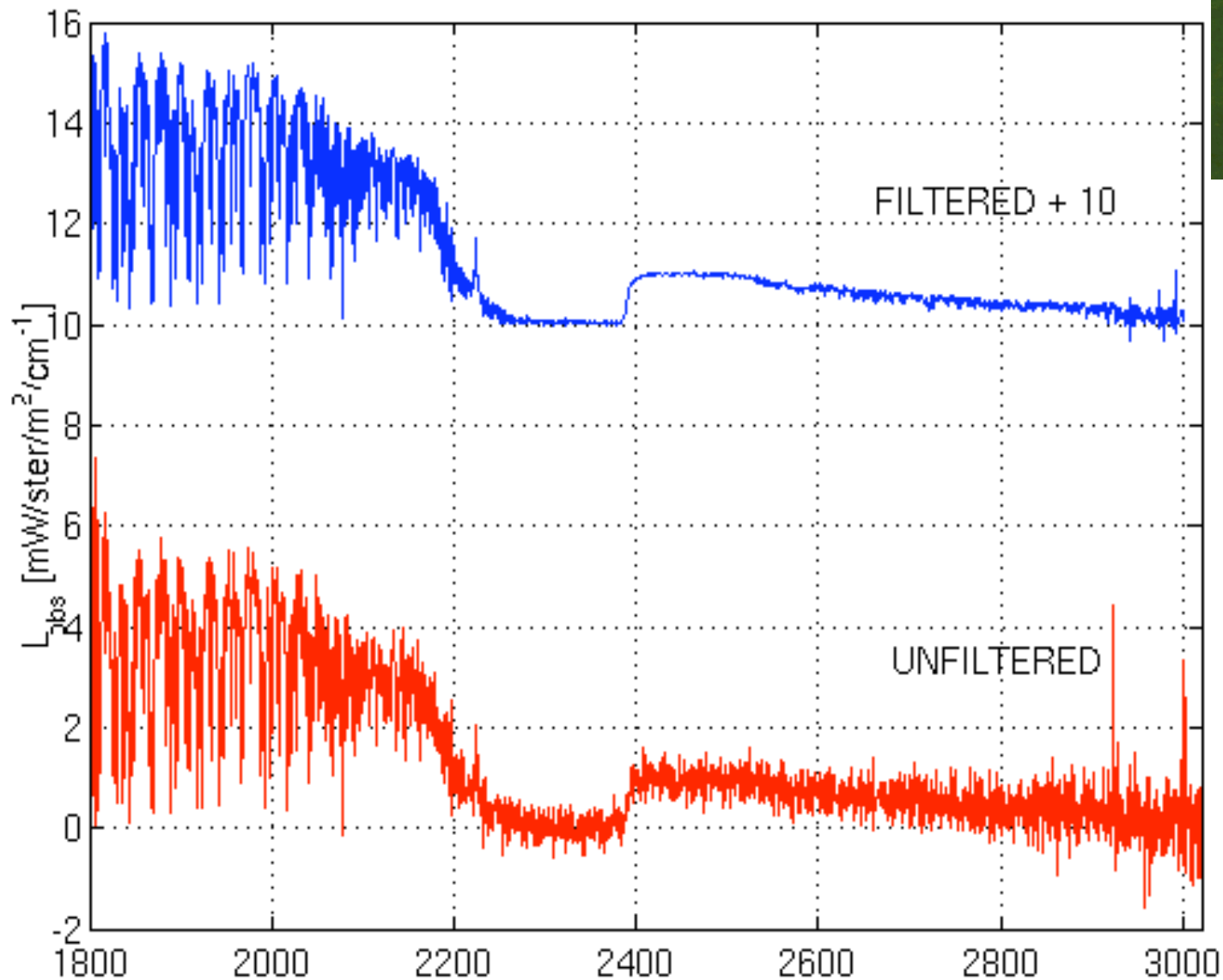
Filtered

# RR single FOV over Ocean

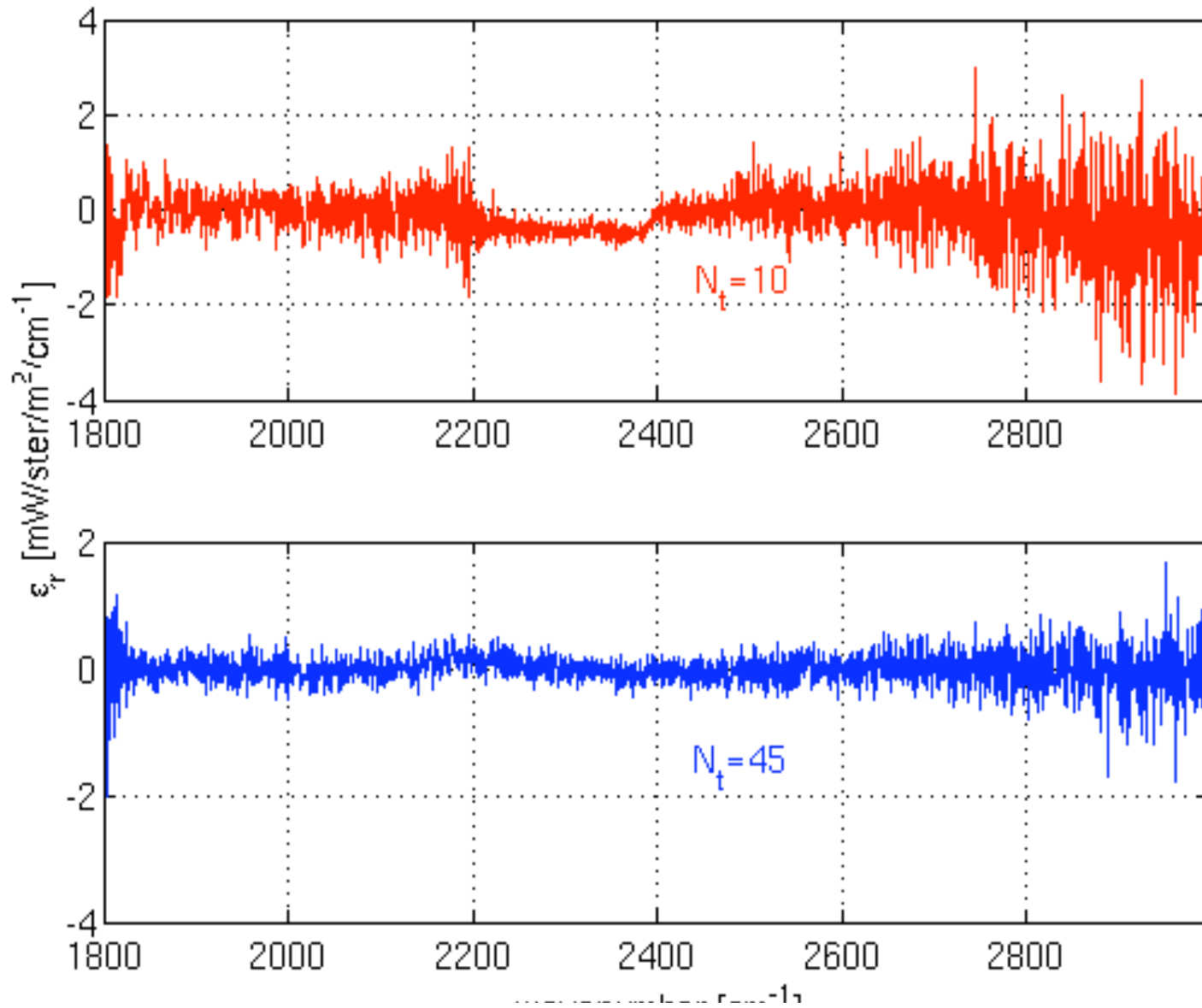
---



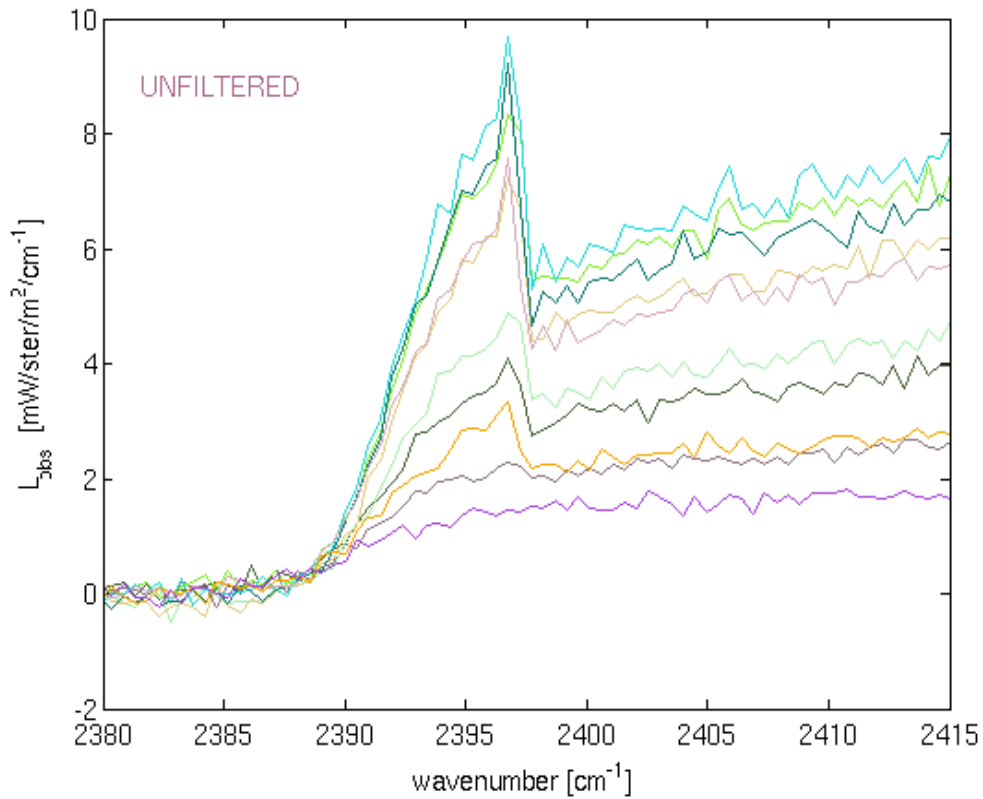
# RR for almost overlapping FOVs over Fire



# RR for almost overlapping FOVs over Fire

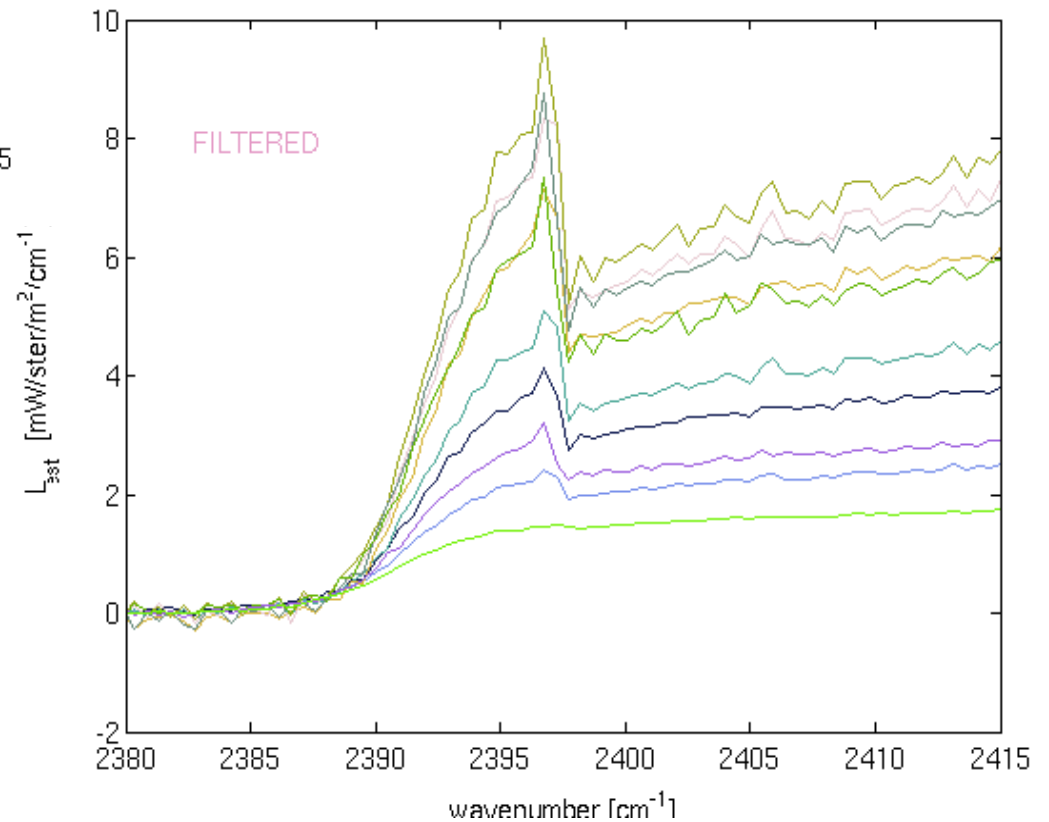


# PCA applied to strong Blue Spike

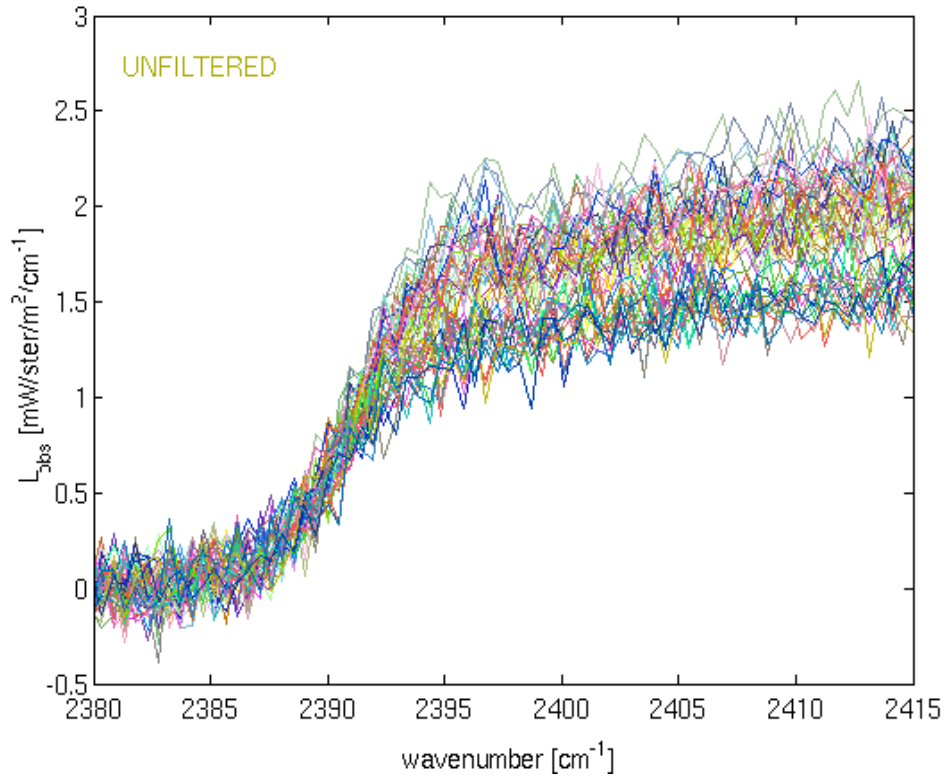


Unfiltered data for 10  
FOVs **over** Fire

Filtered data for 10  
FOVs **over** Fire

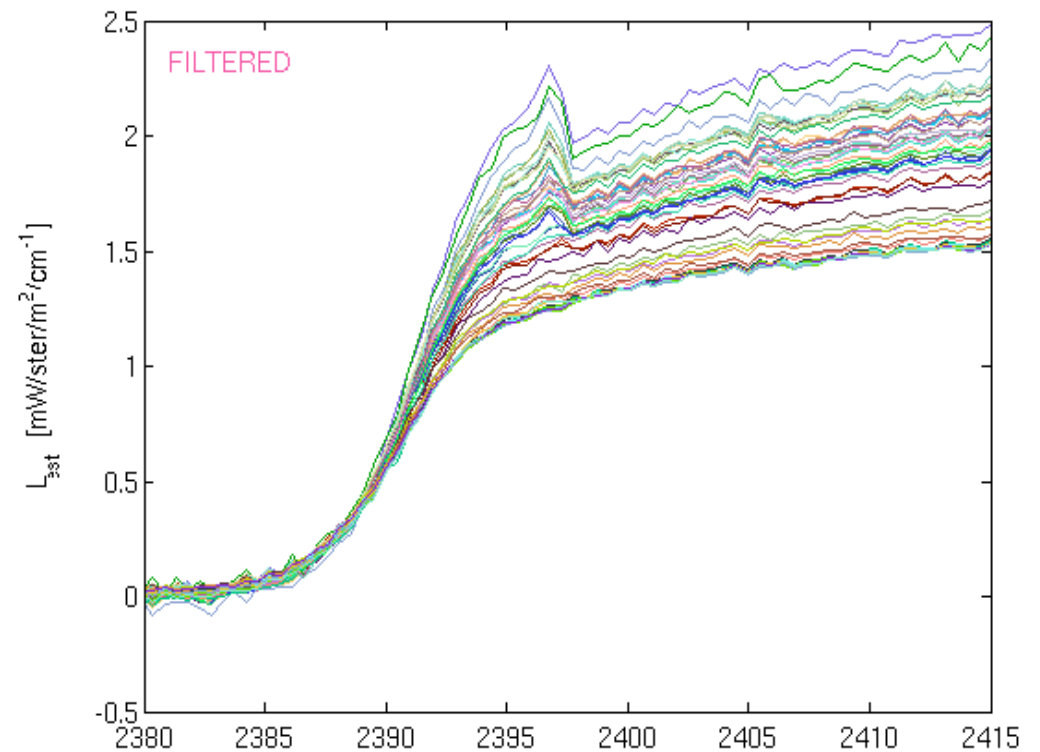


# PCA applied to weak Blue Spike



Unfiltered data for 10  
FOVs *after* Fire

Filtered data for 10  
FOVs *after* Fire





# General conclusions on PCA

---

- PCA by taking advantage of redundancy reduces random component of Instrument noise (PNF) and perform significant data compression;
- Both AIL and RN approach the optimal value defined by Linear Estimation Theory;
- For simulated data (presented case) AIL and RN are 7 times smaller than original noise, and compression ratio of about 50 is achieved;
- Both AIL and RN are correlated in wavenumber space;
- Most difficult cases, observation highly deviant from mean, are properly treated if PCs are derived in Dependent Mode

# PCA applied to Noise Estimation

---

- Dave Tobin, Hank Revercomb, Paolo Antonelli, Ken Vinson
- CIMSS/SSEC/UW-Madison

# Outline

---

- Introduction
  - Approach: Dependent set PCA of AIRS Earth scene data
  - Results with simulated data
- NeDT investigations
  - Comparisons to blackbody estimates
  - Signal dependence
  - Spectrally correlated
- Non-gaussian behavior
  - $N\sigma$  events, “popping”, “striping”
- Inspection of PCs and individual spectra, etc.
  - Array correlated noise
  - A/B state artifacts
- Summary, Conclusions

# Approach: Dependent Set PCA of AIRS L1B Earth Scene Data

---

Using an AIRS L1B granule (6 minutes of data, 90\*135 FOVs)

1) Exclude bad channels using the AIRS team prescription

- Typically retains ~2120 of 2378 channels

2) Noise normalize the radiance spectra using an initial noise estimate (divide by NeDN)

- This initial estimate can also come from non-noise-normalized PCA

3) Generate principle components (PCs) of the covariance matrix of the noise normalized spectra

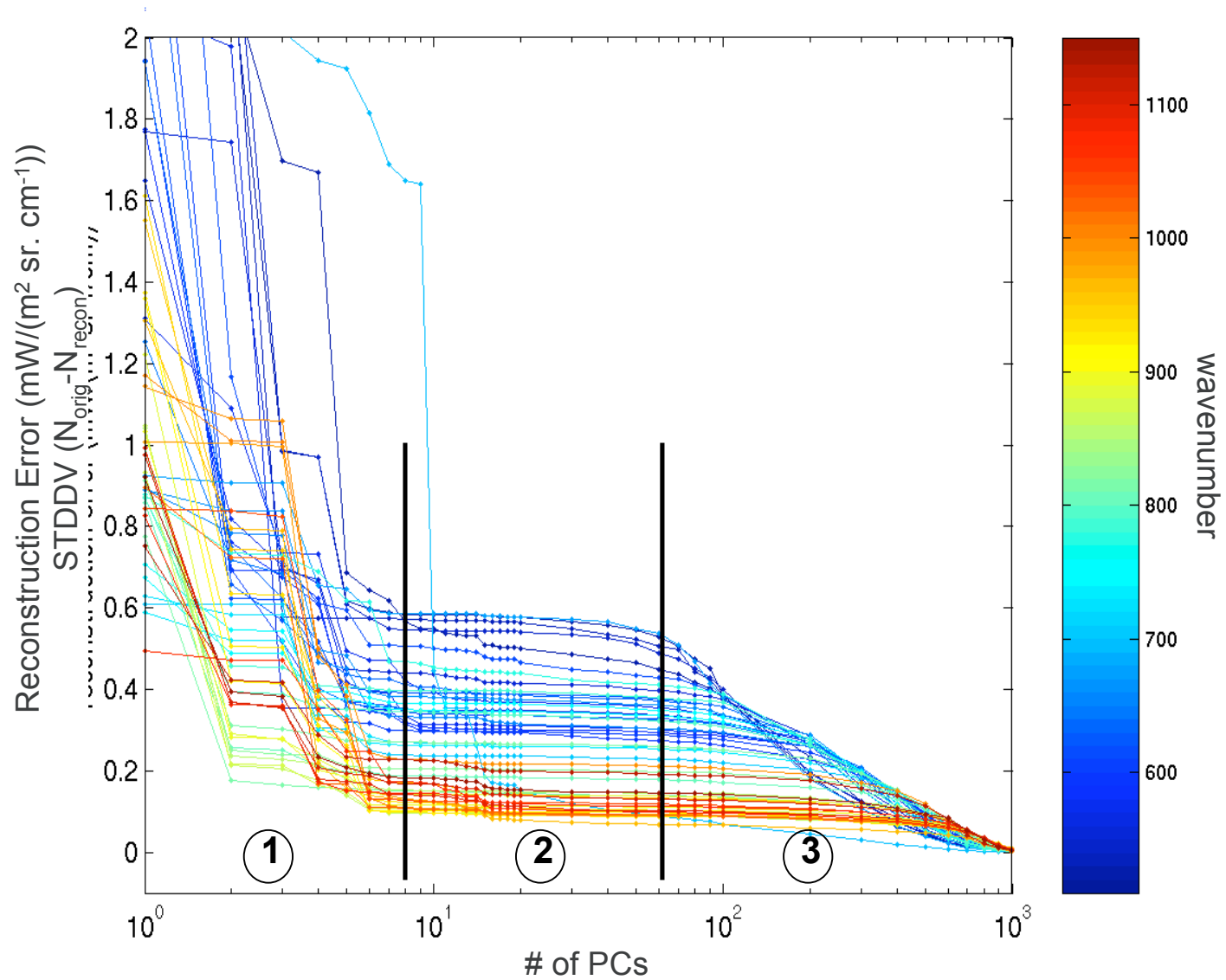
4) Reconstruct the spectra using a reduced number of PCs

- Using the method described in Turner et al. to determine this number

5) Remove the noise normalization (multiply the reconstructed spectra by the initial noise estimate) and perform analyses of the reconstruction error to characterize and derive noise estimates.

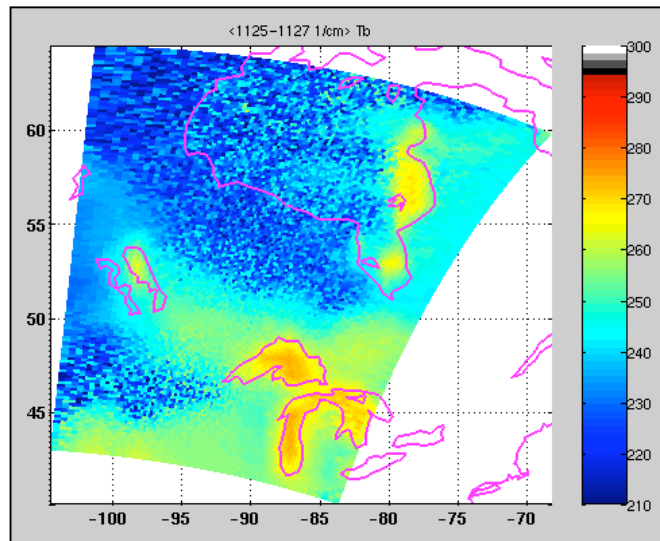
- e.g. NEDN = STDDEV(RR) is an estimate of the spectrally uncorrelated random noise

# Reconstruction Error versus #PCs

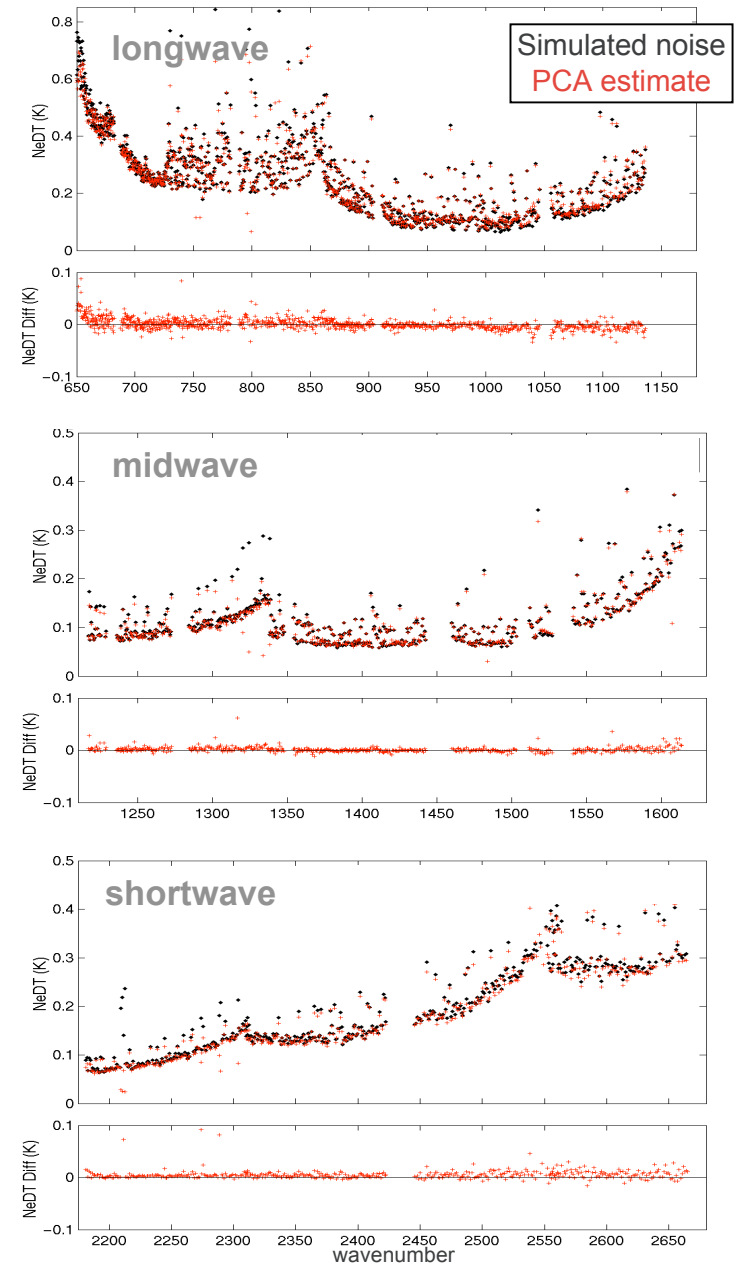
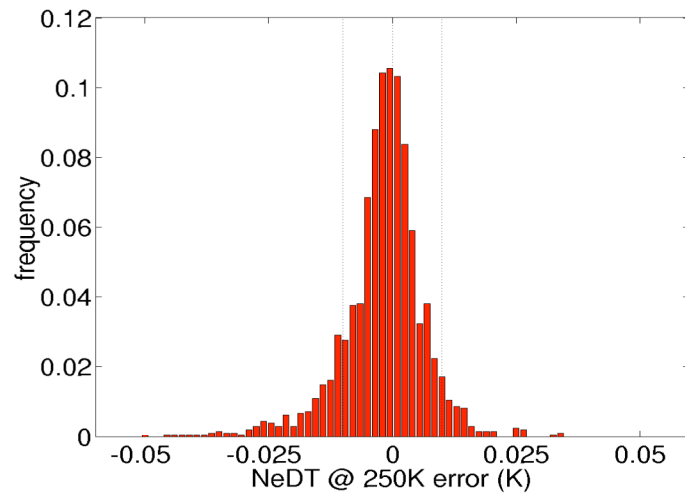


# Example results for simulated data (purely Gaussian random noise)

15-Dec-2000 granule 081

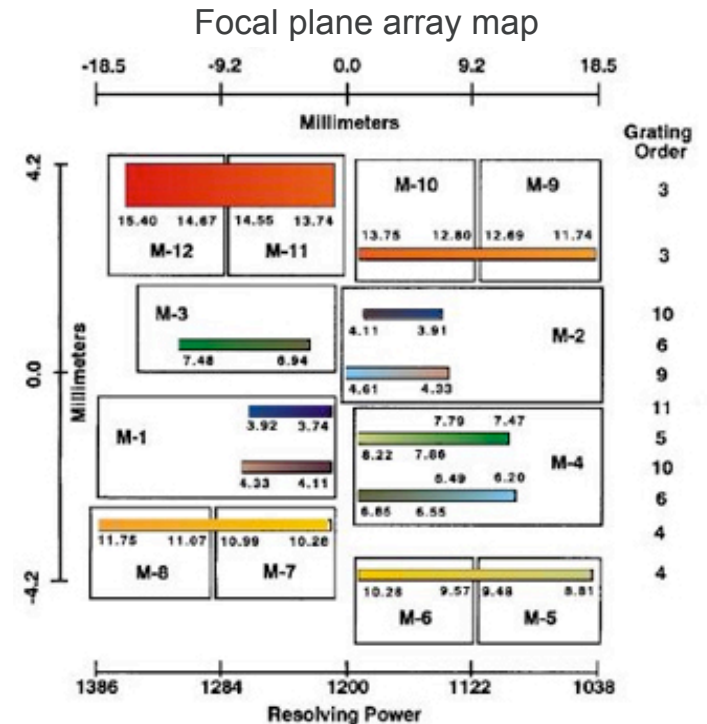
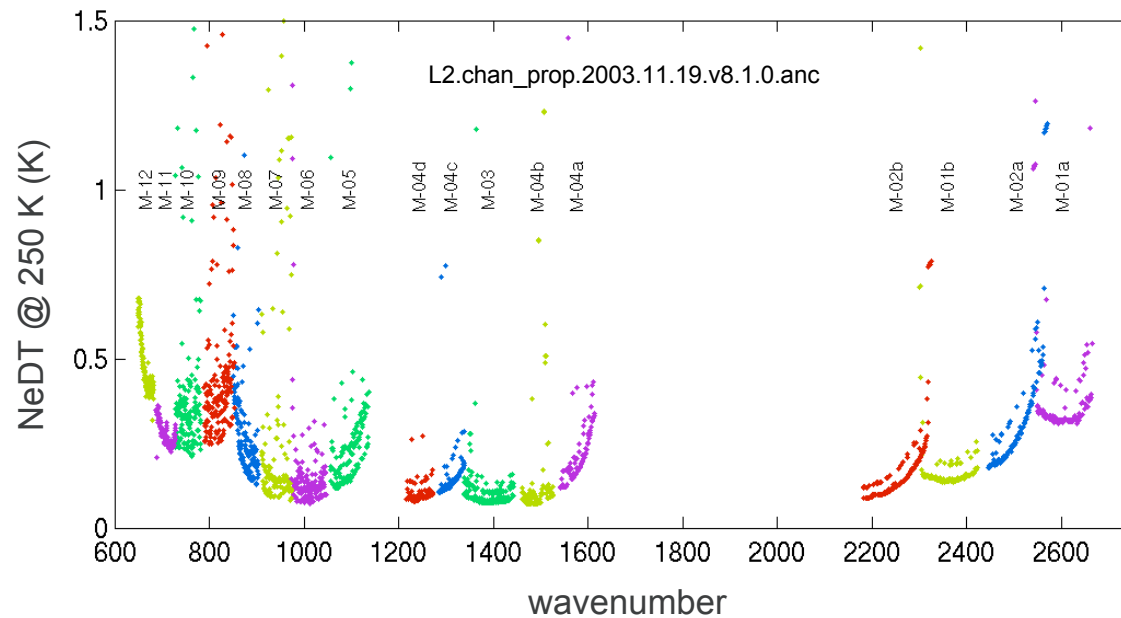


Distribution of differences



# AIRS Noise

- Total noise estimates (NEN, NEDT@250K) derived from on-board blackbody and space views
  - provided in 1) Channel properties files and 2) L1B granule files



- Signal dependence      AIRS L1B ATBD, l1bqa\_changes.pdf @ GDAAC
- Array correlated noise      Pagano, Weiler, AIRS Design Files #614, #620
- Striping      e.g. Gaiser, Dec 2004 AIRS STM
- “Popping”      M. Weiler, Nov 2002 AIRS TM; M. Weiler, SPIE Proc. 5882, 2005.

# NEDT investigations

---

- STDDEV(RR)

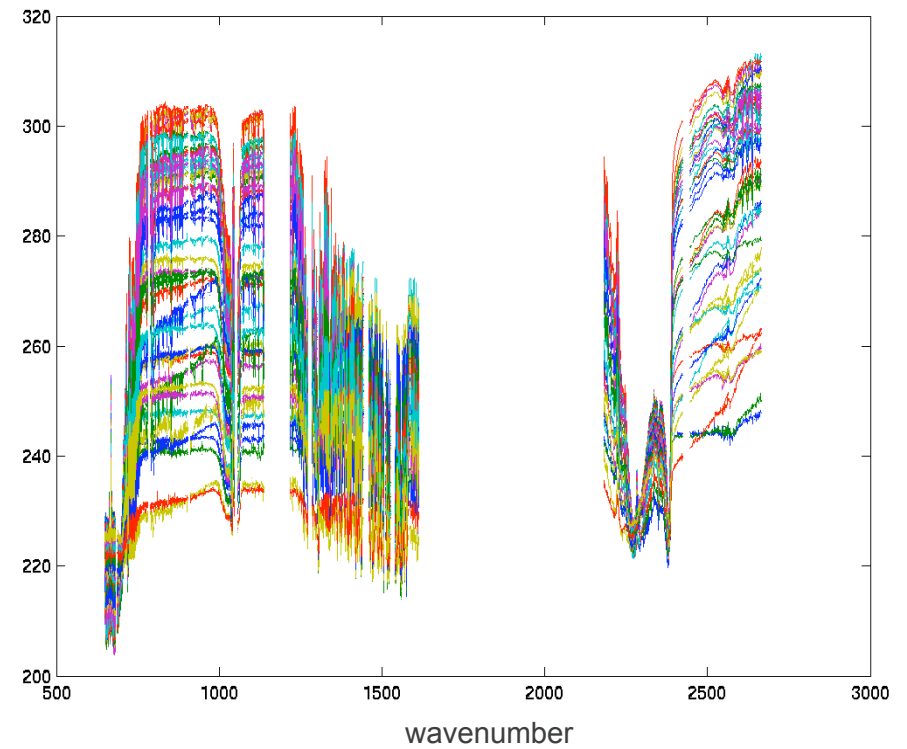
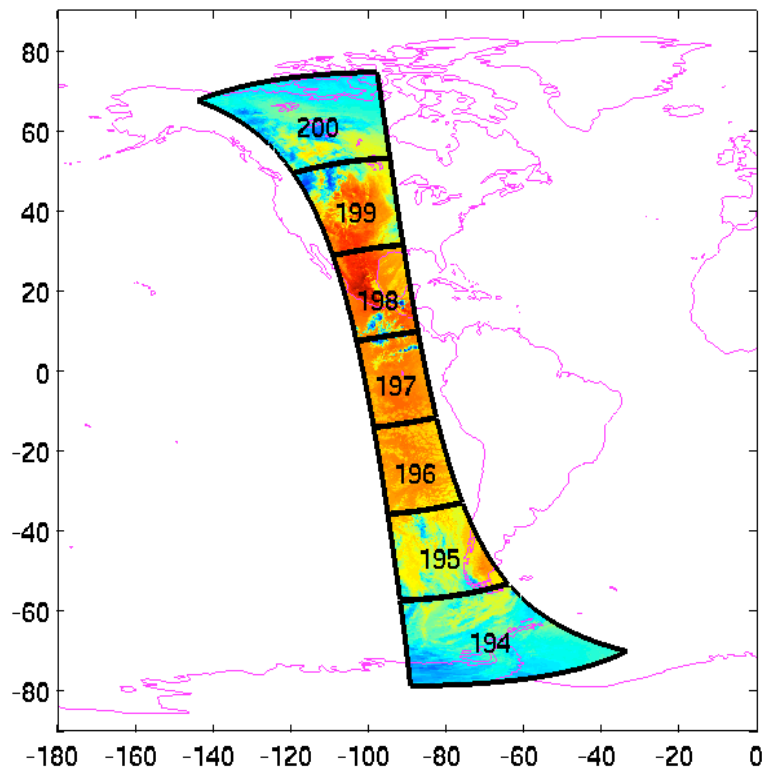


# Analysis of 01 April 2005 data (v4.0.9 L1B)

7 ascending (daytime) granules

1000  $\text{cm}^{-1}$  brightness temperatures

sample spectra



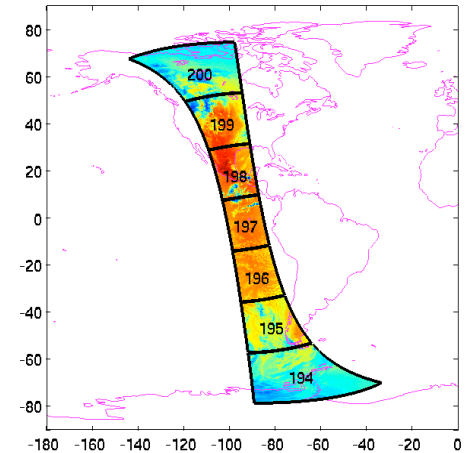
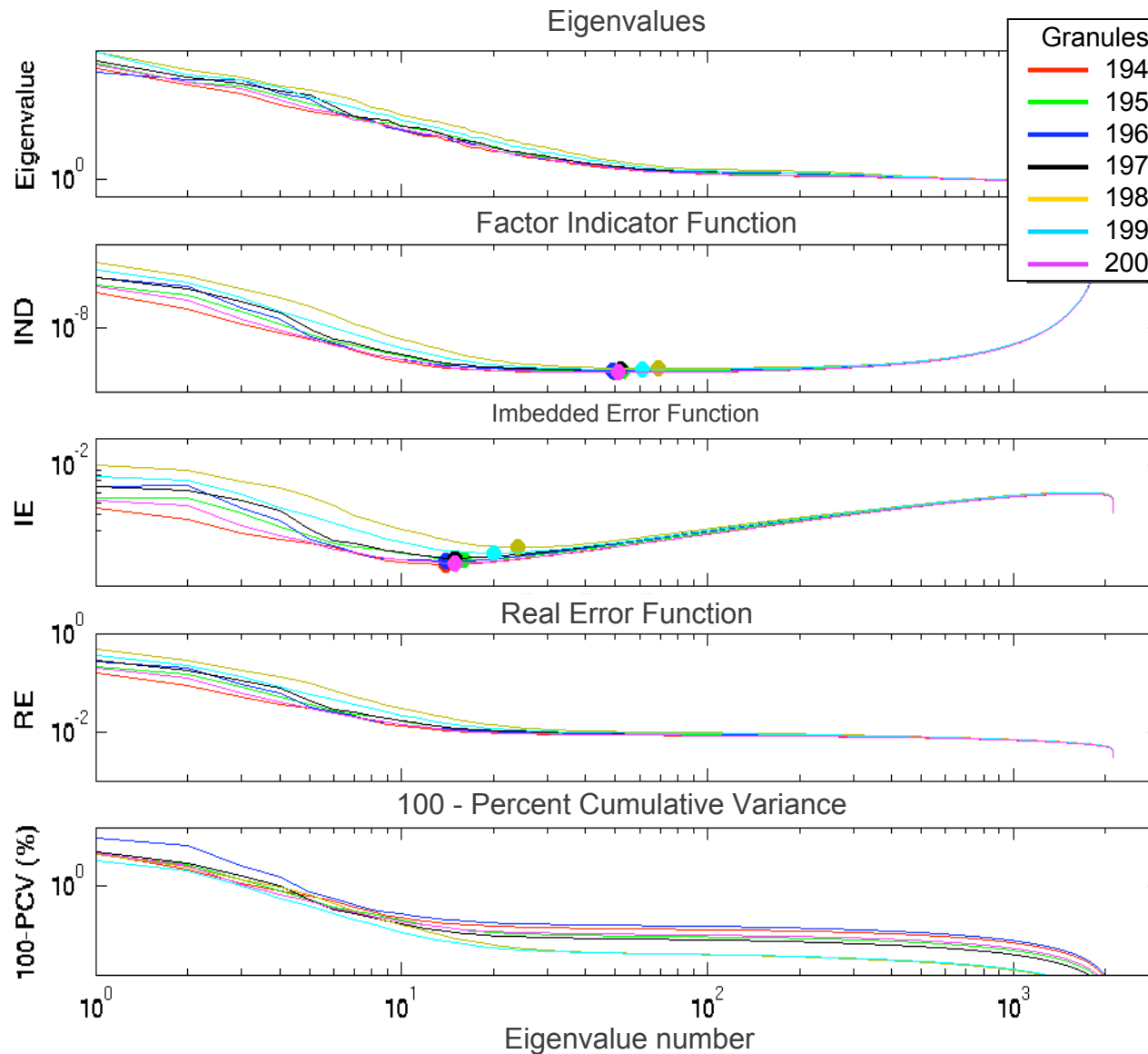
# Channel Selection

---

Follows the guidelines provided by the AIRS project:

1. AB\_State (in channel properties file)  $\leq 2$ . (If AB\_State  $> 2$ , the channel has known radiometric problems.)
2. NEDT@250K (computed from NeN in L1B granule file)  $\leq 2K$
3. Bits 6 (Anomaly in offset calculation), 5 (Anomaly in gain calculation), 4 (Pop detected), 3 (High Noise) of CalChanSummary (in L1B granule file) are not set.

# Variance Metrics, following Turner et al.



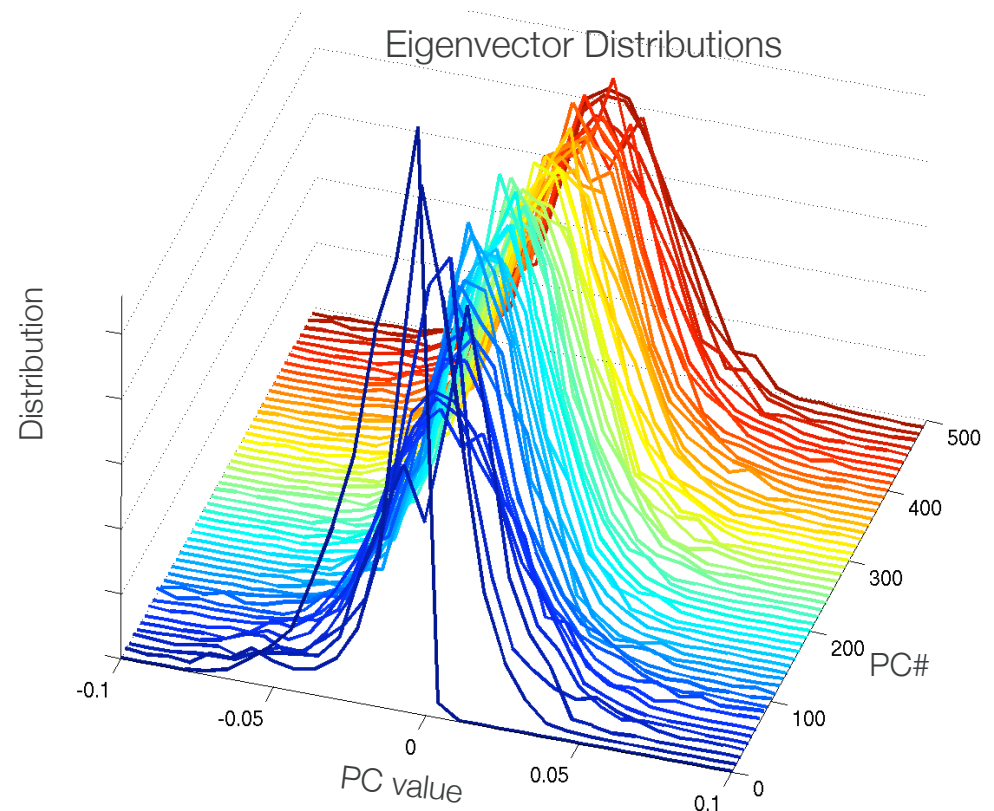
Gran.	IND	IE
194	50	14
195	53	16
196	49	14
197	52	15
198	69	24
199	61	20
200	51	15

↑  
# of PCs  
used in the  
reconstructions

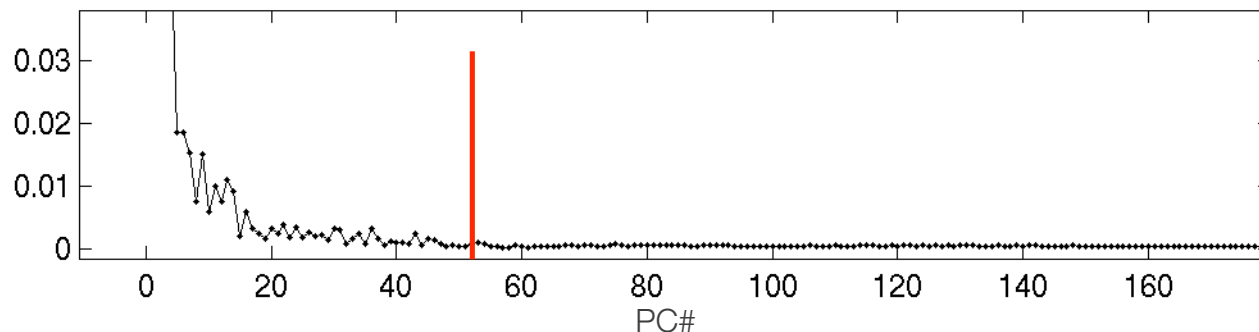
# Variance Metrics: “brute force” determinations

The high order (least significant) PCs should represent random white noise. Various normality tests performed on the PCs suggest that the number PCs used in the reconstructions (determined with the IND method) are reasonable.

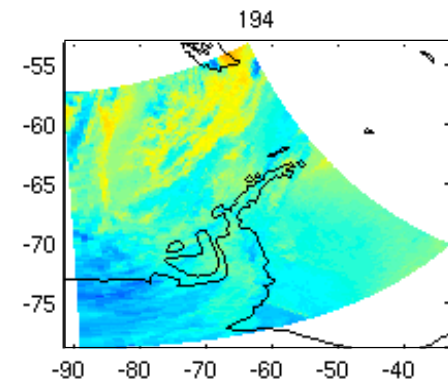
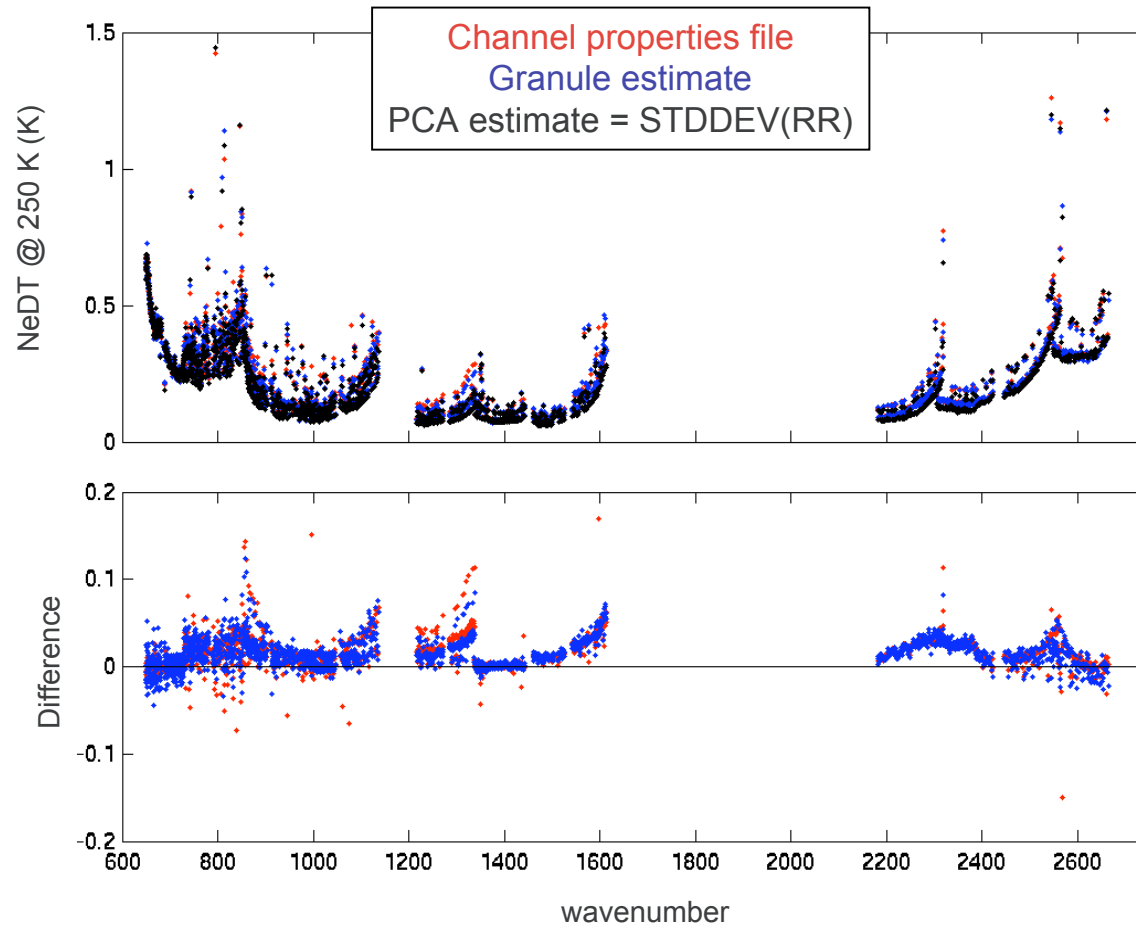
Example for granule 195 PCs:



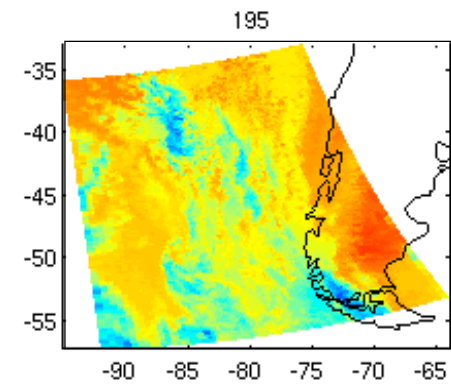
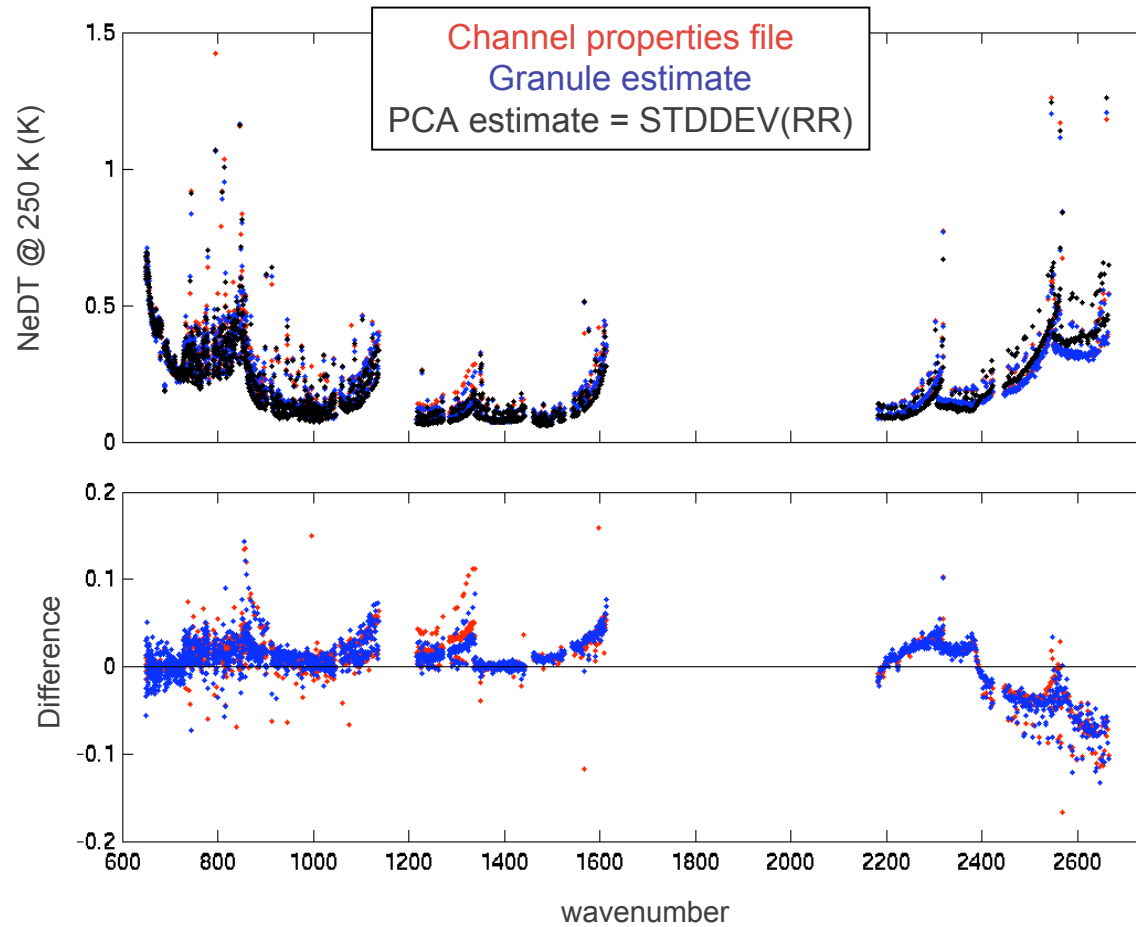
Gaussian distribution test statistic (largest deviation from Gaussian CDF)



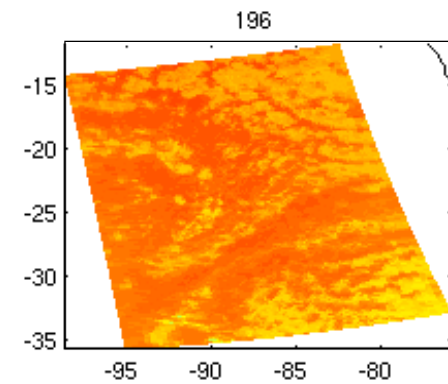
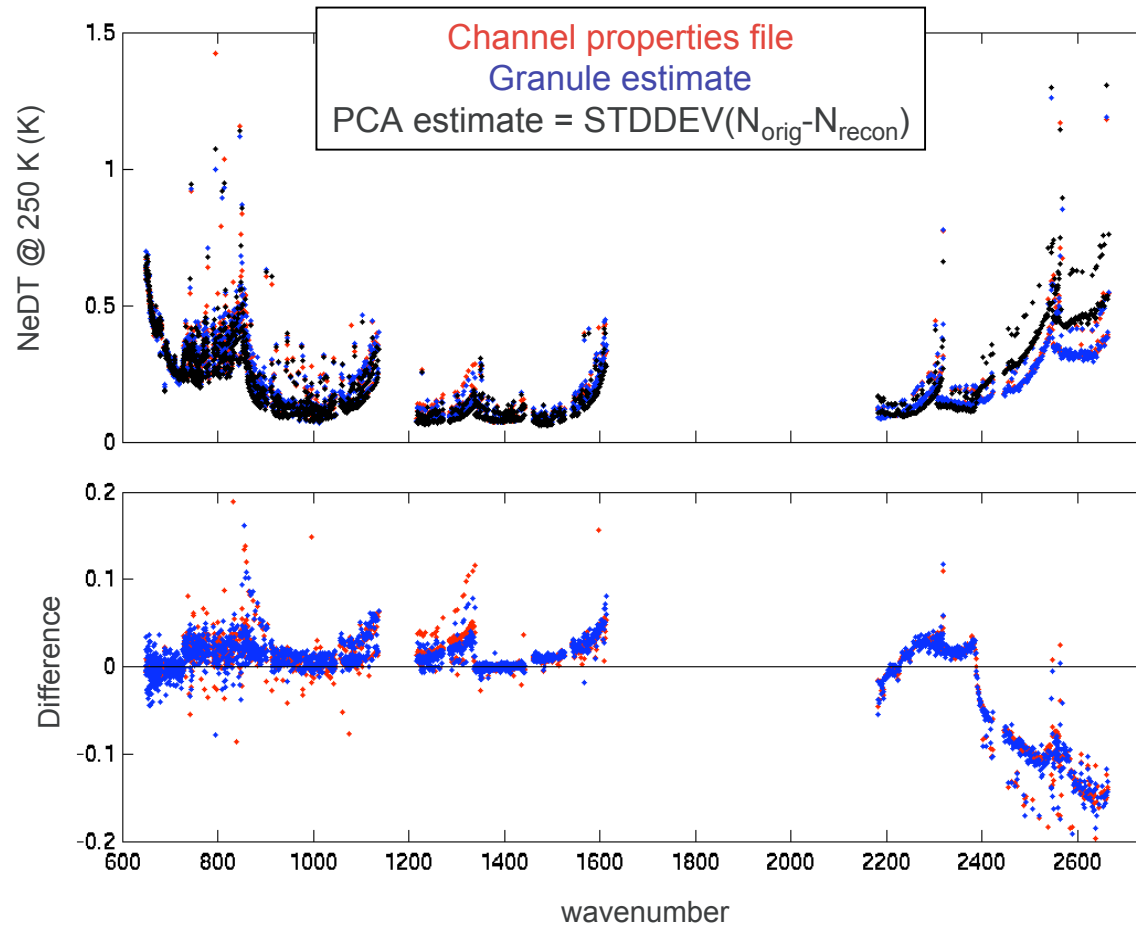
# NeDT comparisons, granule 194



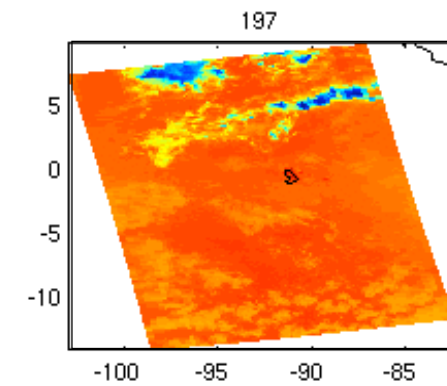
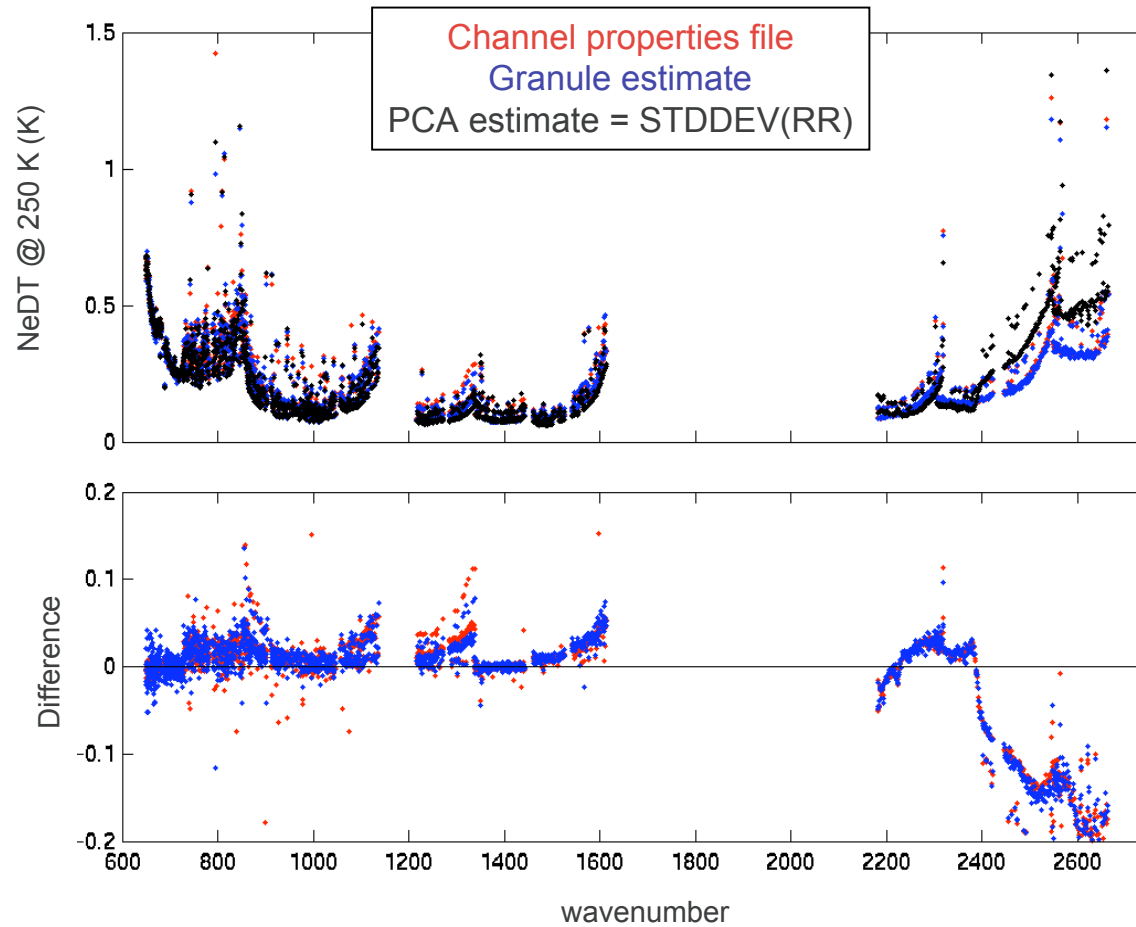
# NeDT comparisons, granule 195



# NeDT comparisons, granule 196

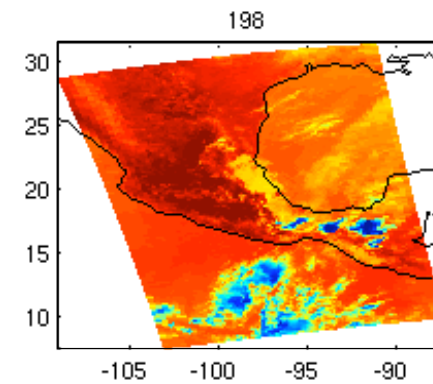
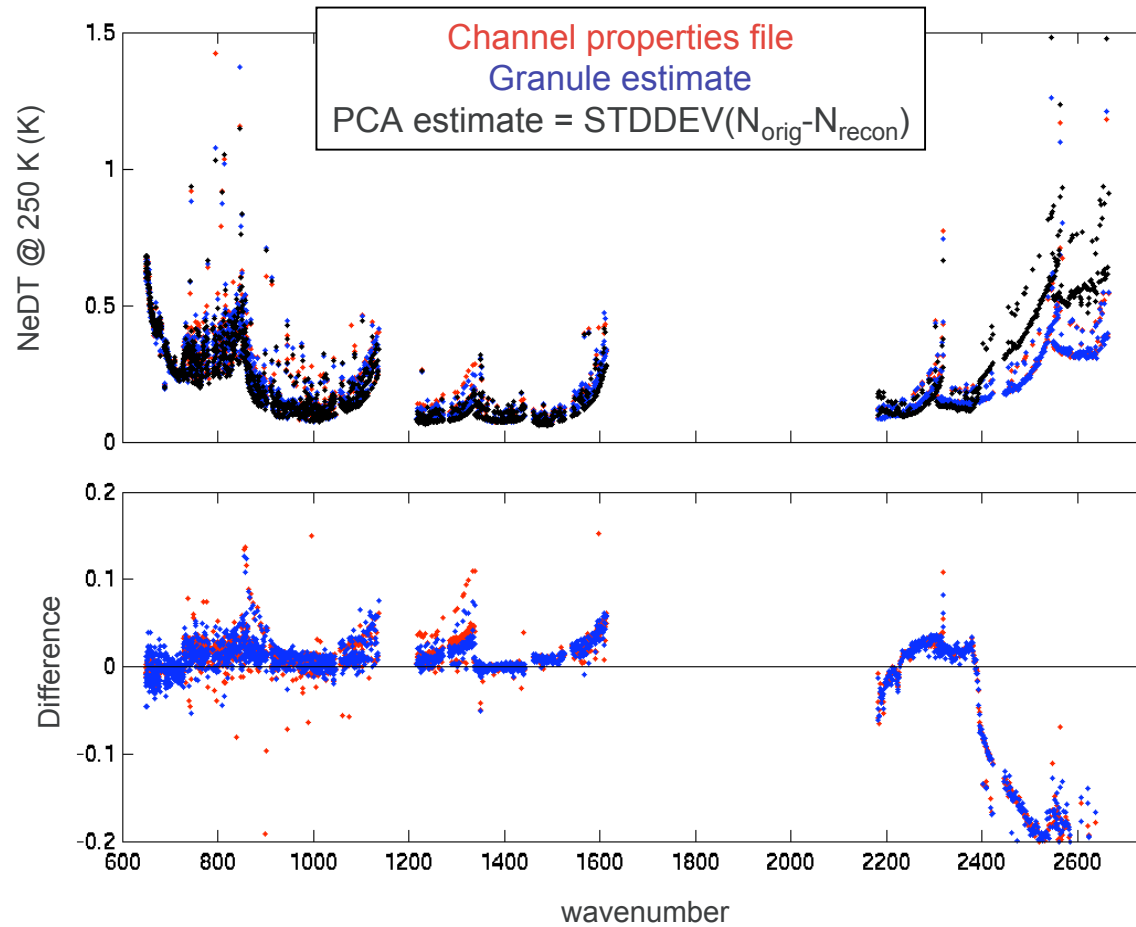


# NeDT comparisons, granule 197

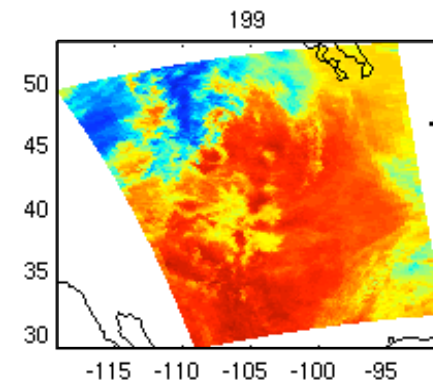
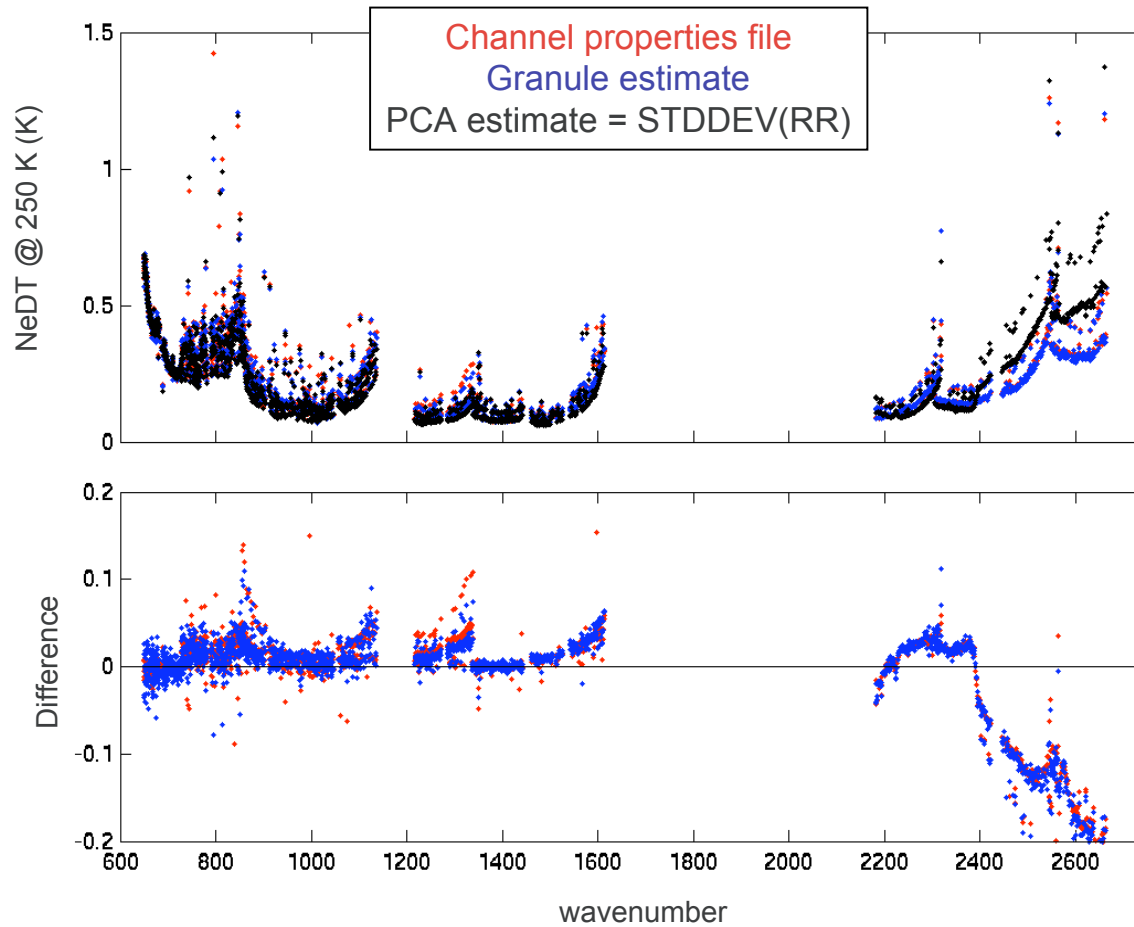




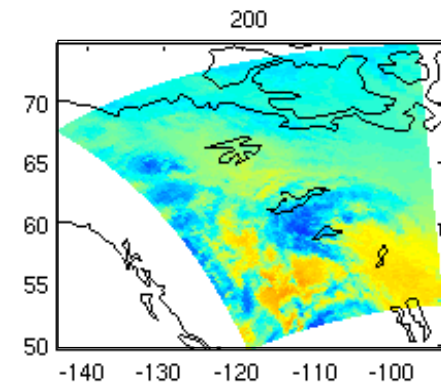
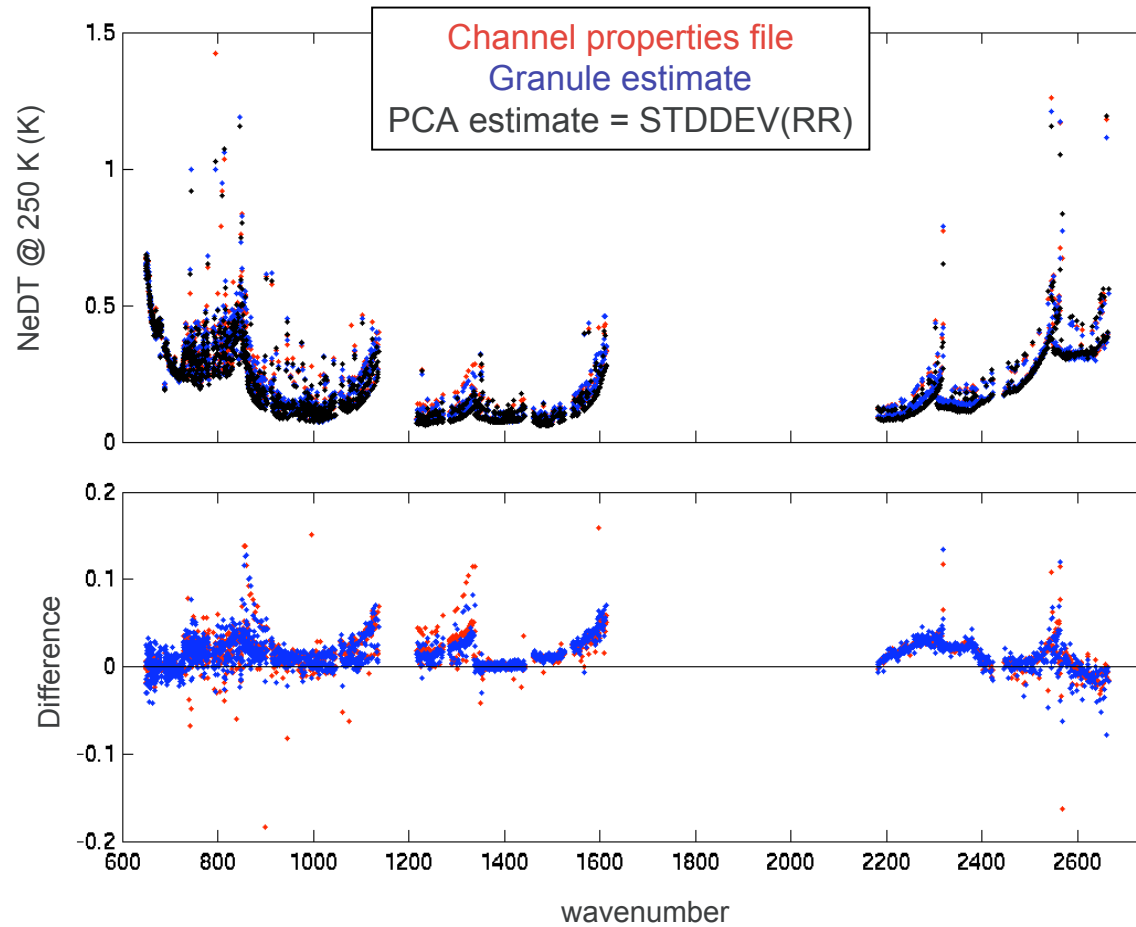
# NeDT comparisons, granule 198



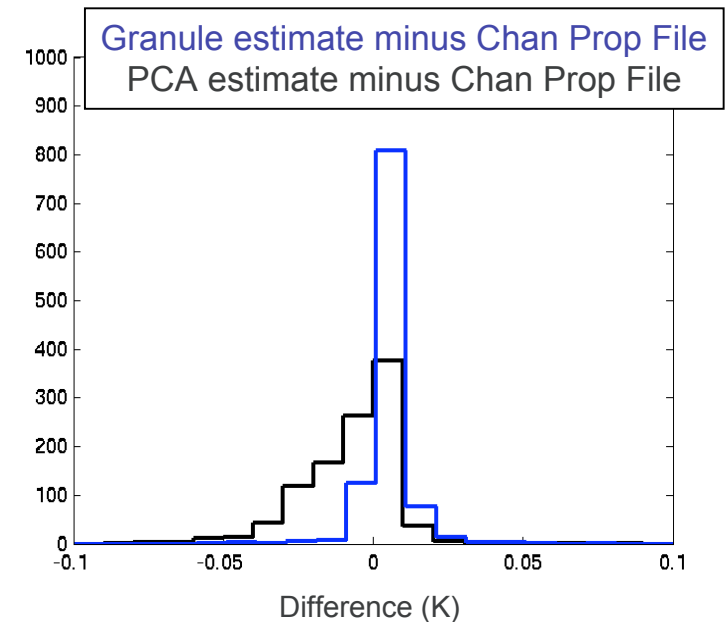
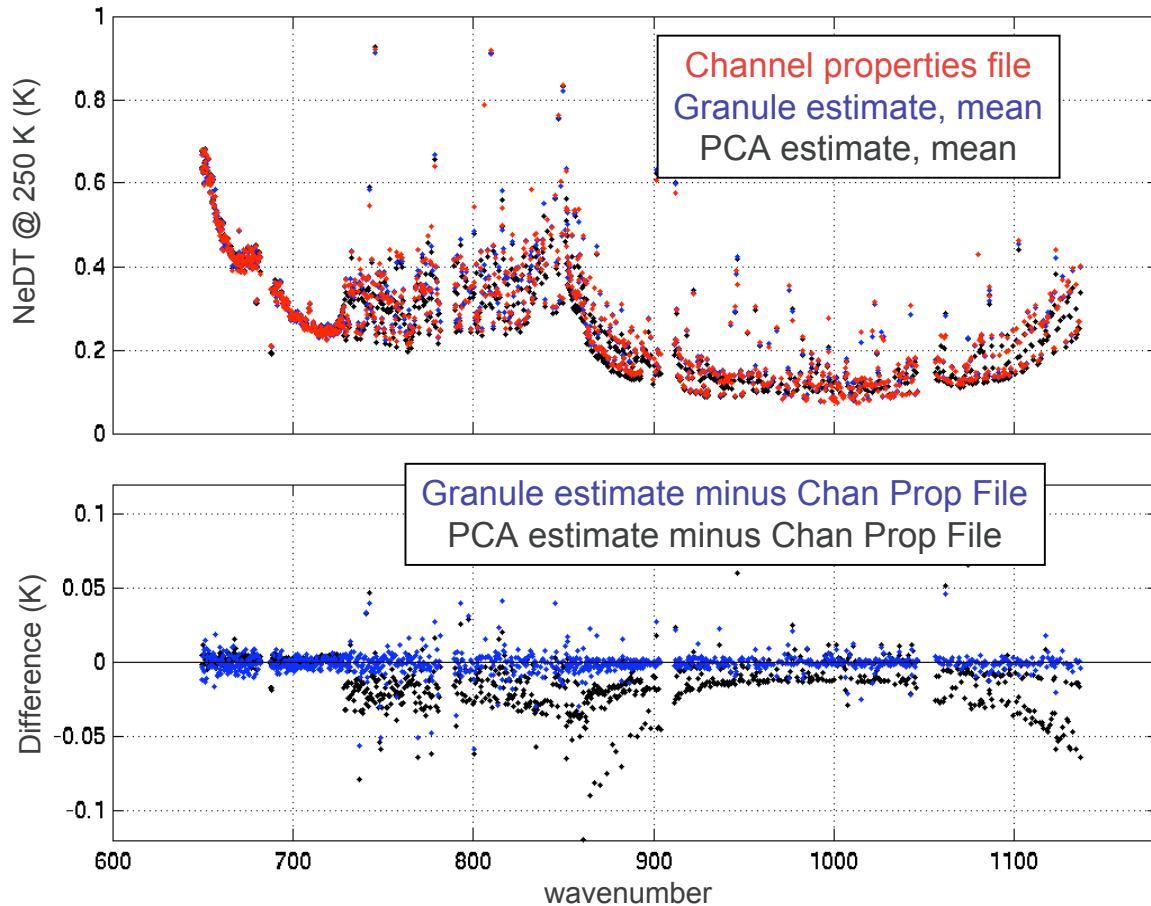
# NeDT comparisons, granule 199



# NeDT comparisons, granule 200

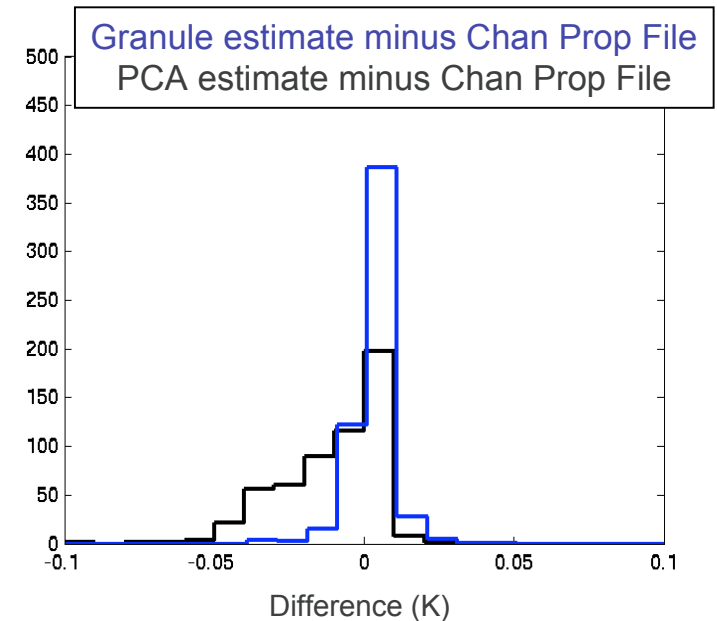
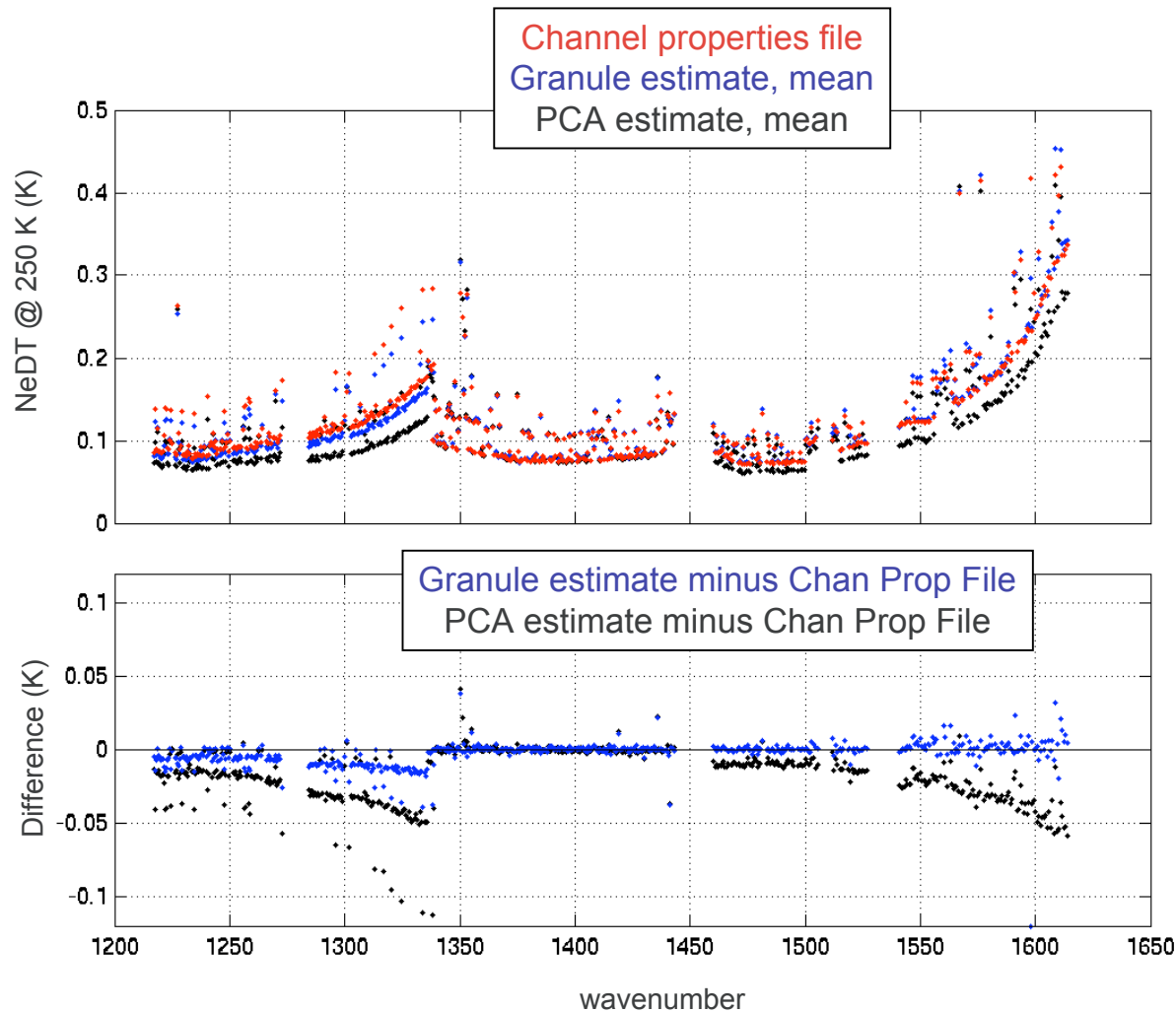


# NeDT comparison summary, longwave



- Good agreement for the longwave PC arrays M-11 and M-12
- PCA estimates are slightly, but consistently, lower for the other arrays

# NeDT comparison summary, midwave

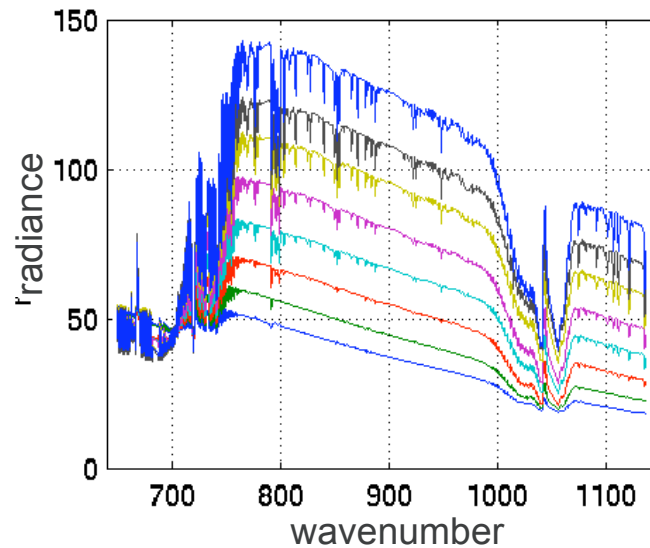


- Good agreement for array M-03. PCA estimates are slightly, but consistently, lower for the other arrays
- The granule-based estimate is also slightly lower than the channel properties estimate for arrays M-04c and M-04d

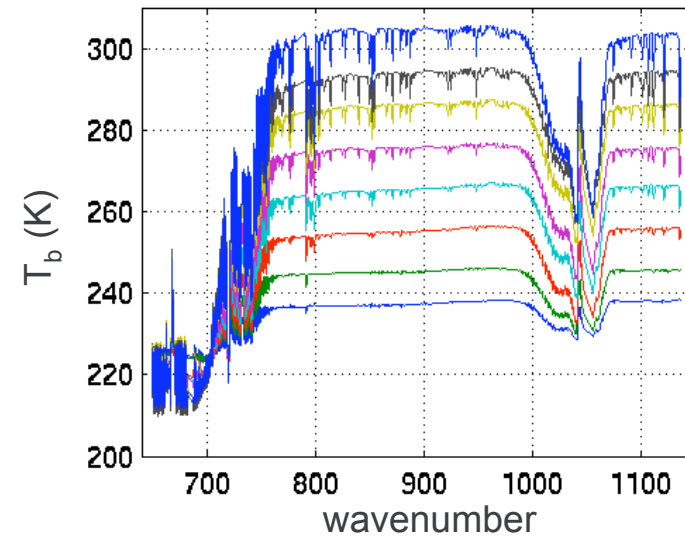
# Scene dependence of NEN, longwave

The data from all 7 granules is binned according to the SW window region signal levels. PCA is then performed for each bin and NEDN is reported as a function of signal level.

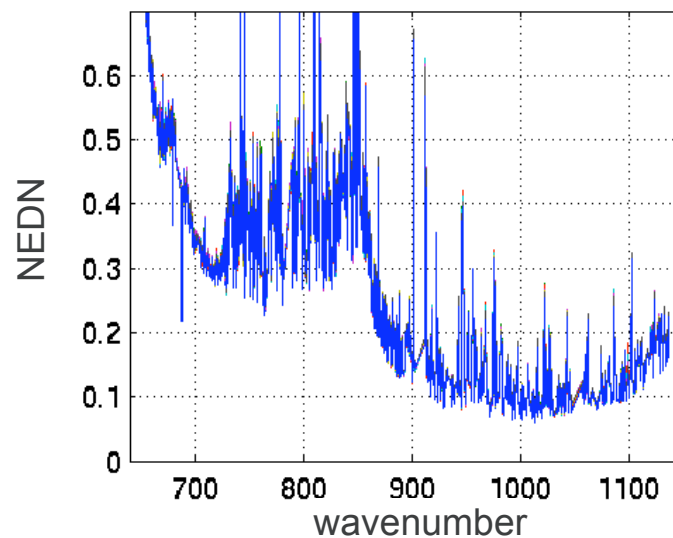
Mean radiance spectrum for each bin



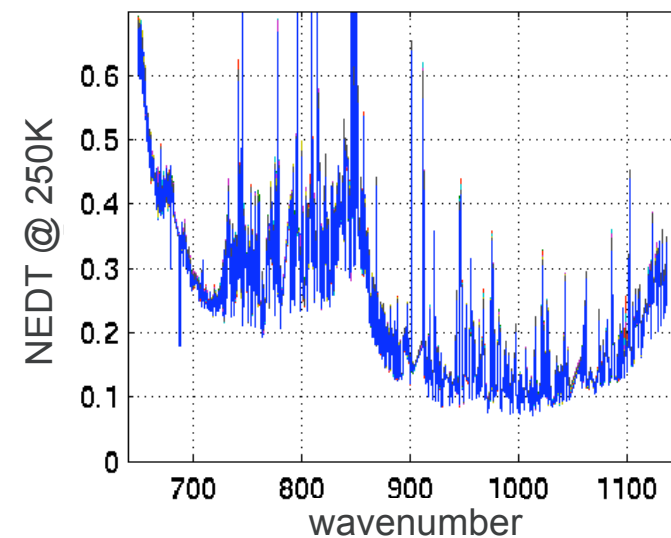
→ converted to BT



NEDN for each bin



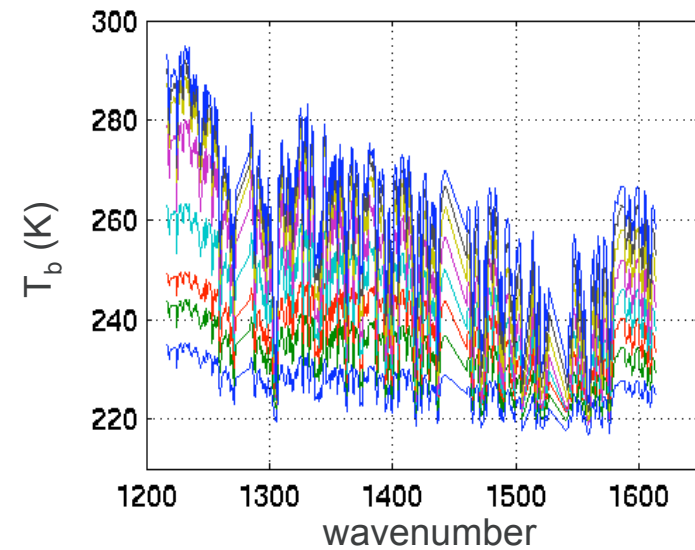
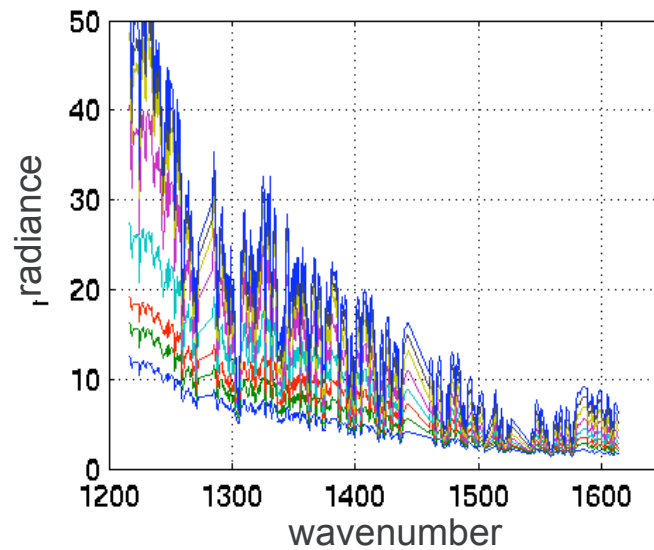
→ converted to NEDT@250K



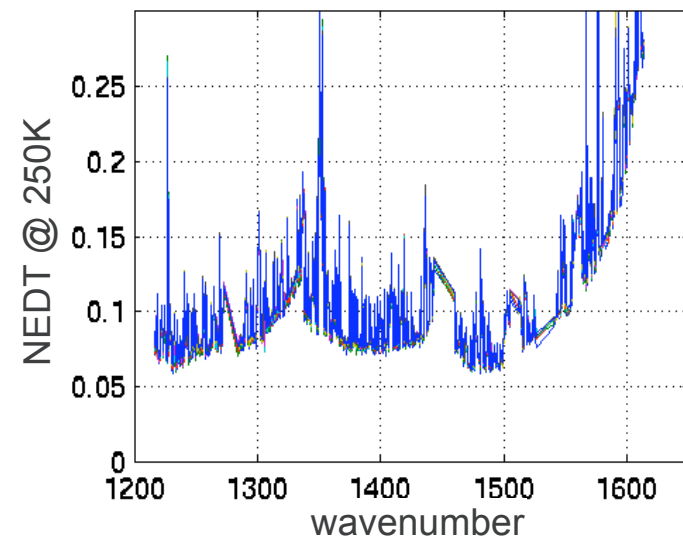
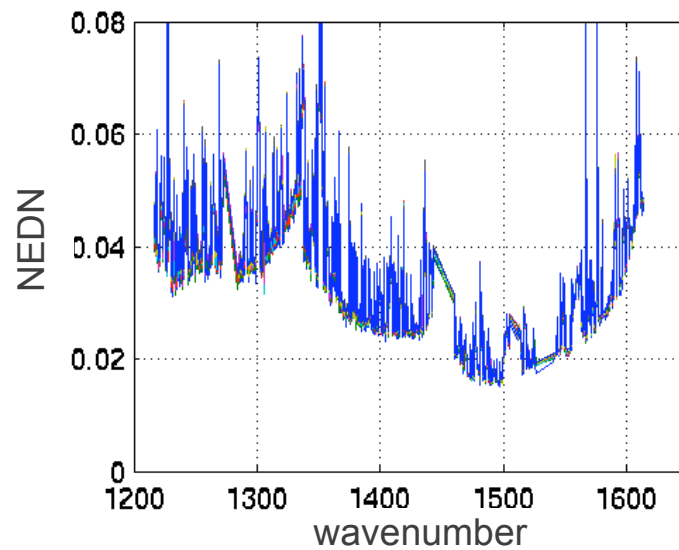
## Bins:

- 245-255 K
- 255-265 K
- 265-275 K
- 275-285 K
- 285-295 K
- 295-305 K
- 305-315 K
- 315-325 K

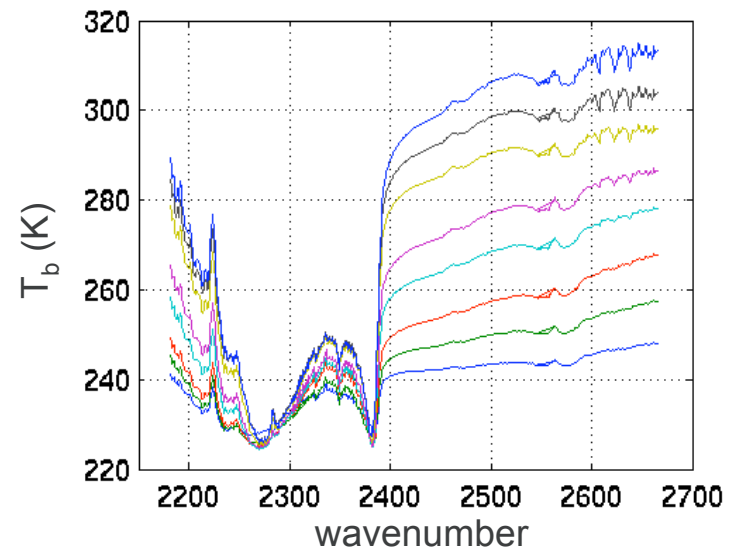
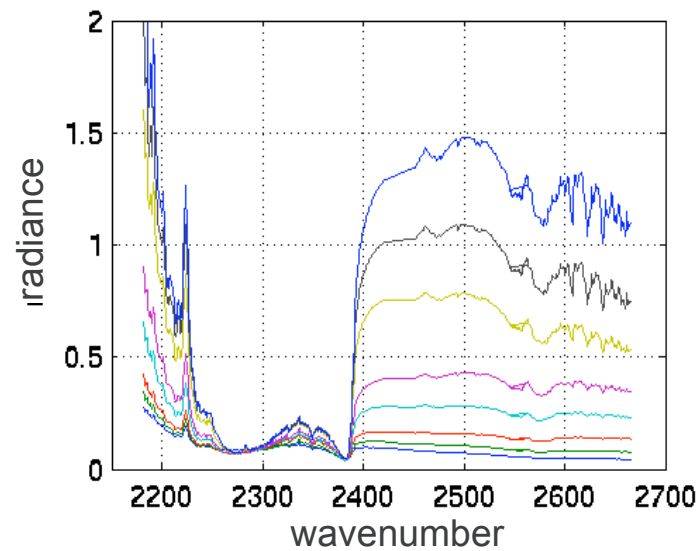
# Scene dependence of NEN, midwave



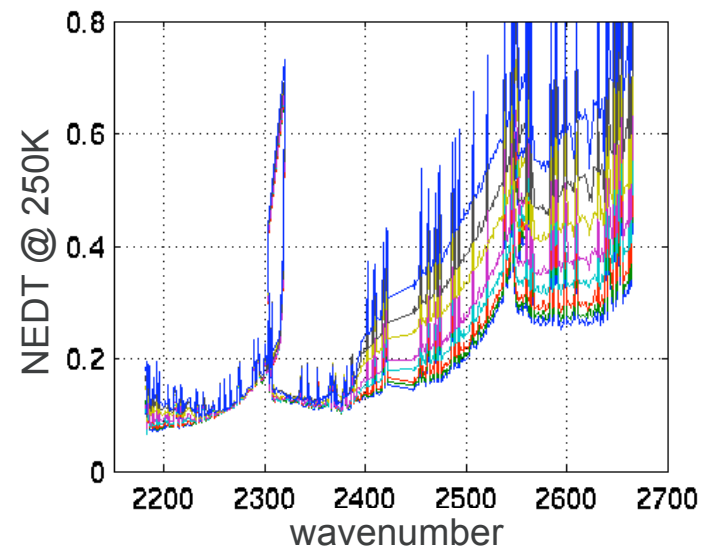
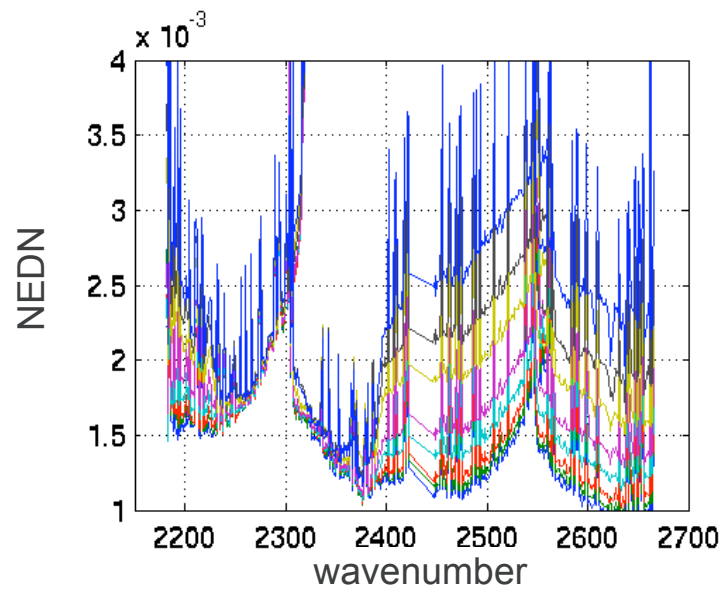
- Bins:
- 245-255 K
  - 255-265 K
  - 265-275 K
  - 275-285 K
  - 285-295 K
  - 295-305 K
  - 305-315 K
  - 315-325 K



# Scene dependence of NEN, shortwave



- Bins:
- 245-255 K
  - 255-265 K
  - 265-275 K
  - 275-285 K
  - 285-295 K
  - 295-305 K
  - 305-315 K
  - 315-325 K



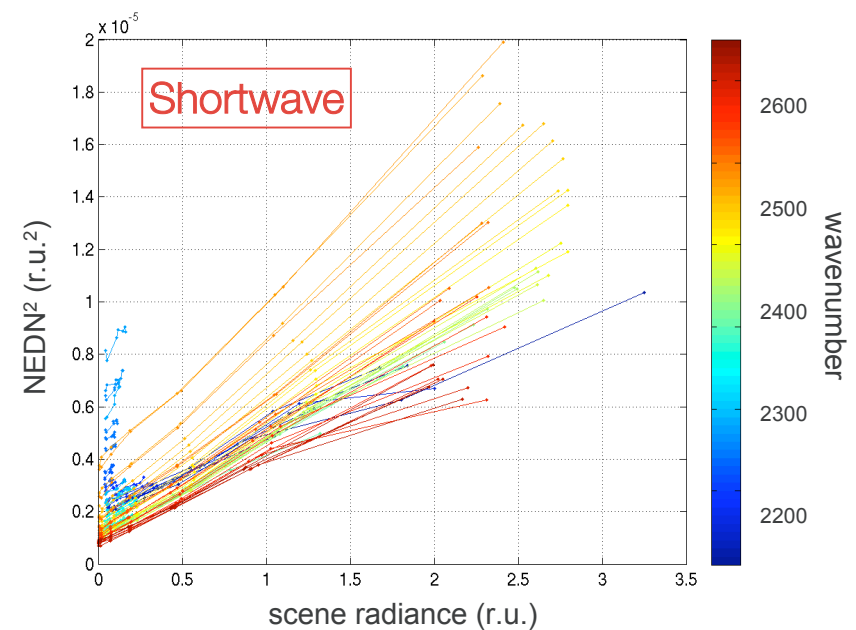
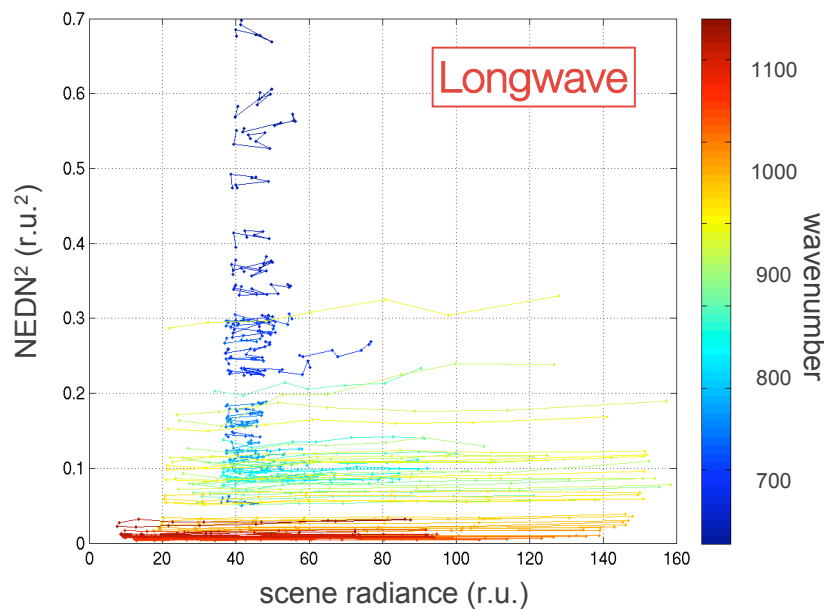
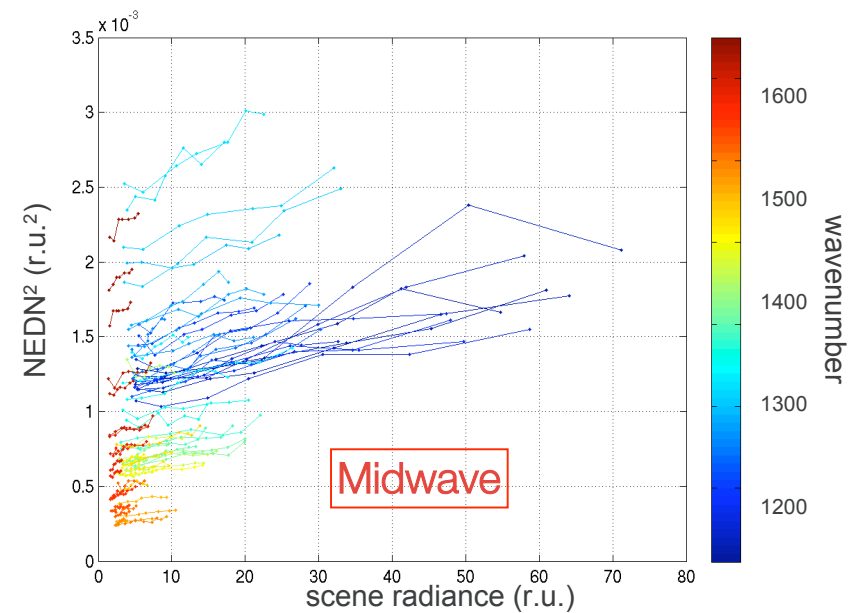


# NEDN versus scene radiance

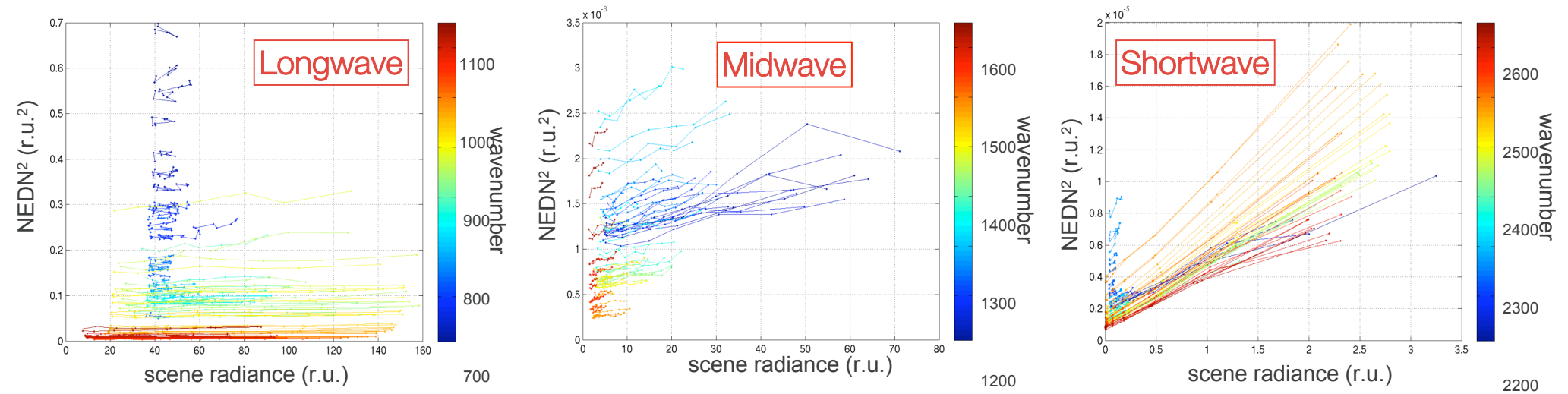
NEDN increases with  $\sqrt{\text{scene radiance}}$ , consistent with photon noise. The total noise at scene temperature  $T$  is parameterized as

$$\text{NEDN}(T) = [N(T) \gamma_{\text{photon}} + \text{NEDN}_{\text{thermal}}^2]^{1/2}$$

where  $\text{NEDN}_{\text{thermal}}^2$  (the y-intercepts) and  $\gamma_{\text{photon}}$  (the slopes) are determined for each channel.

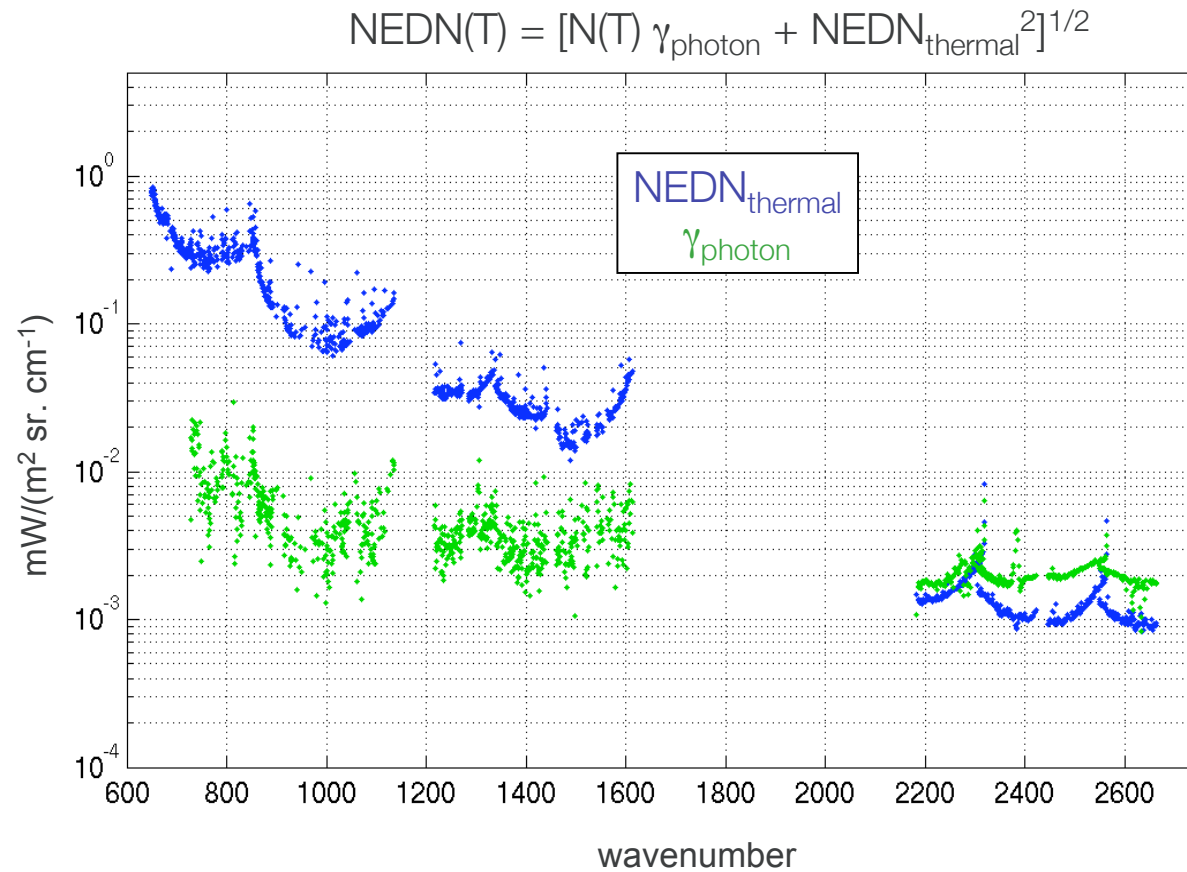


# NEDN versus scene radiance



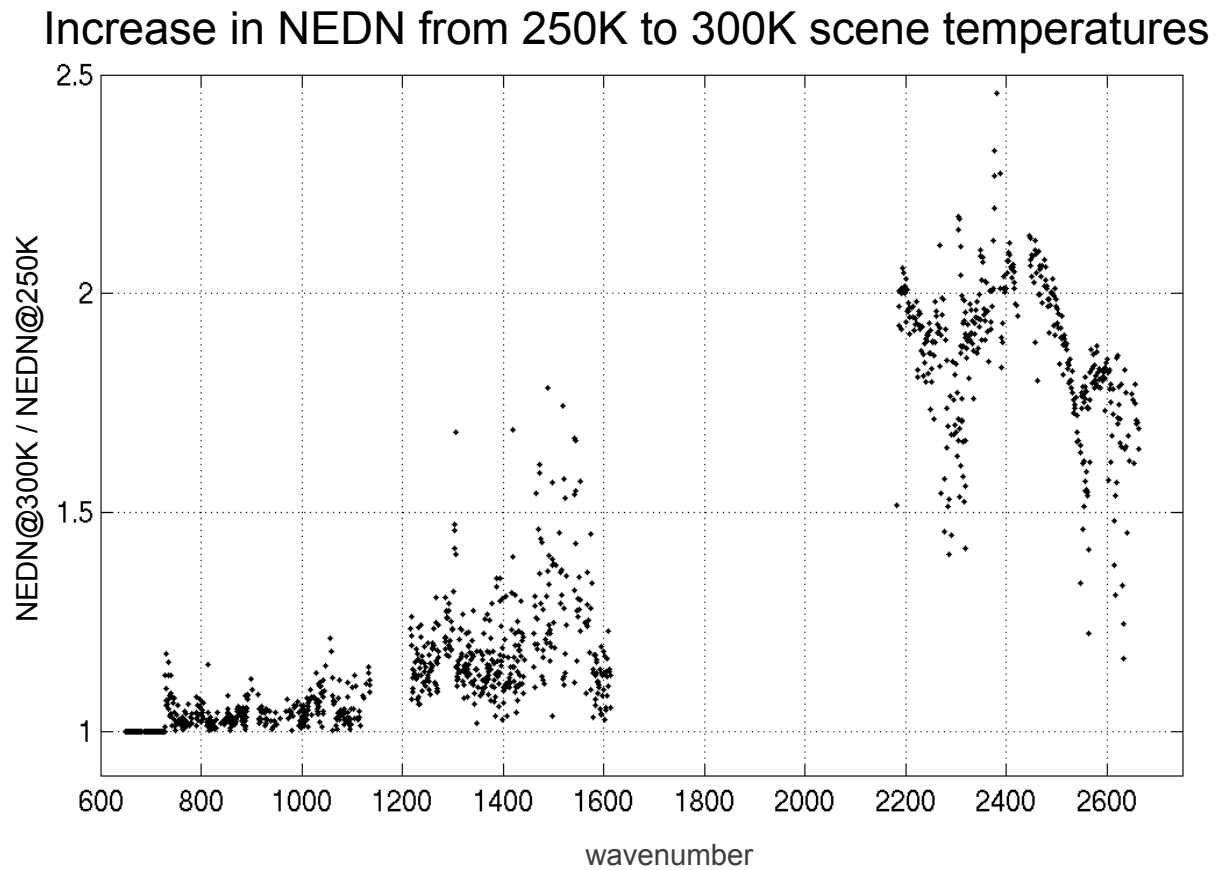
# NEDN versus scene radiance parameterization

---

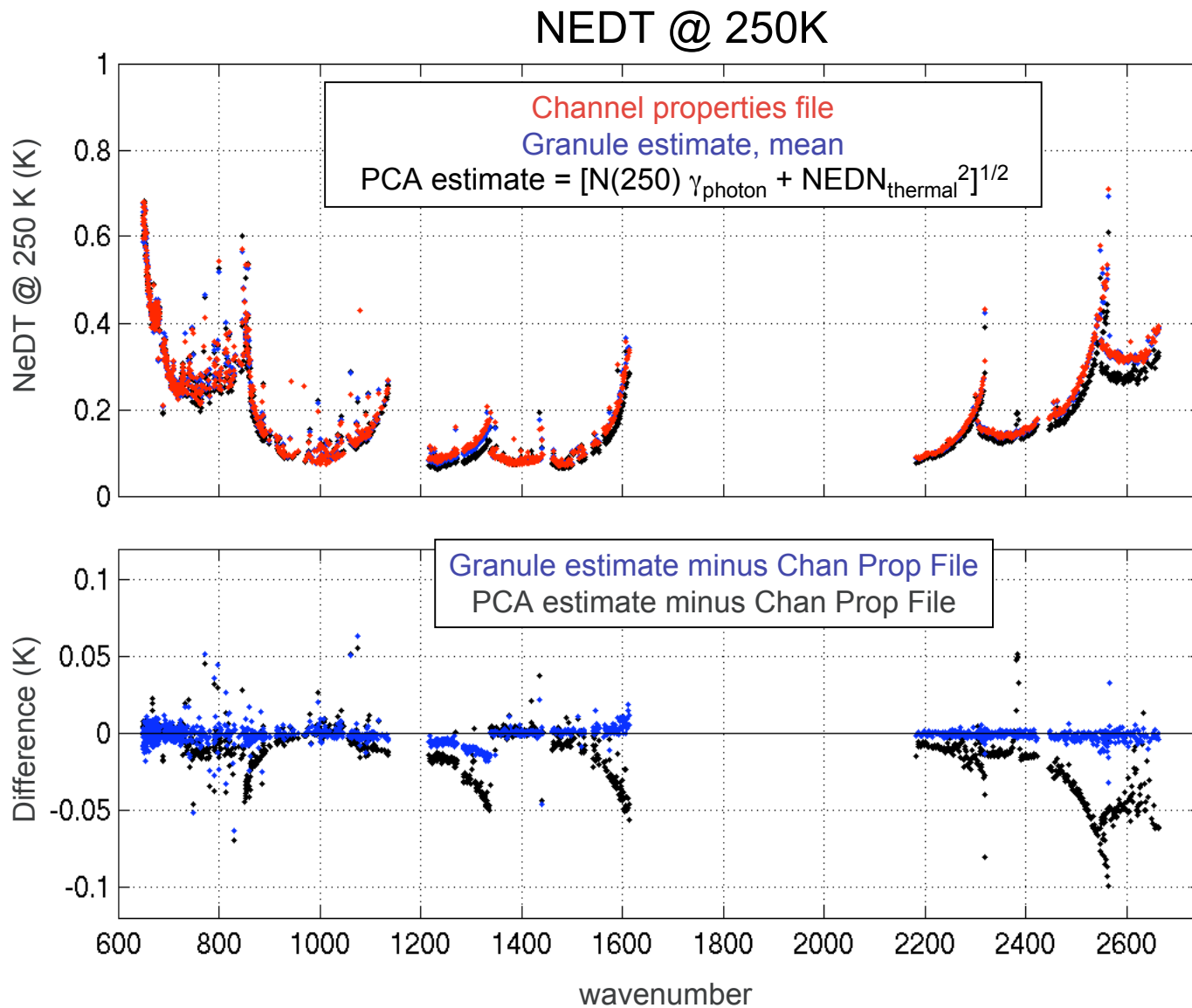


# NEDN versus scene radiance

---

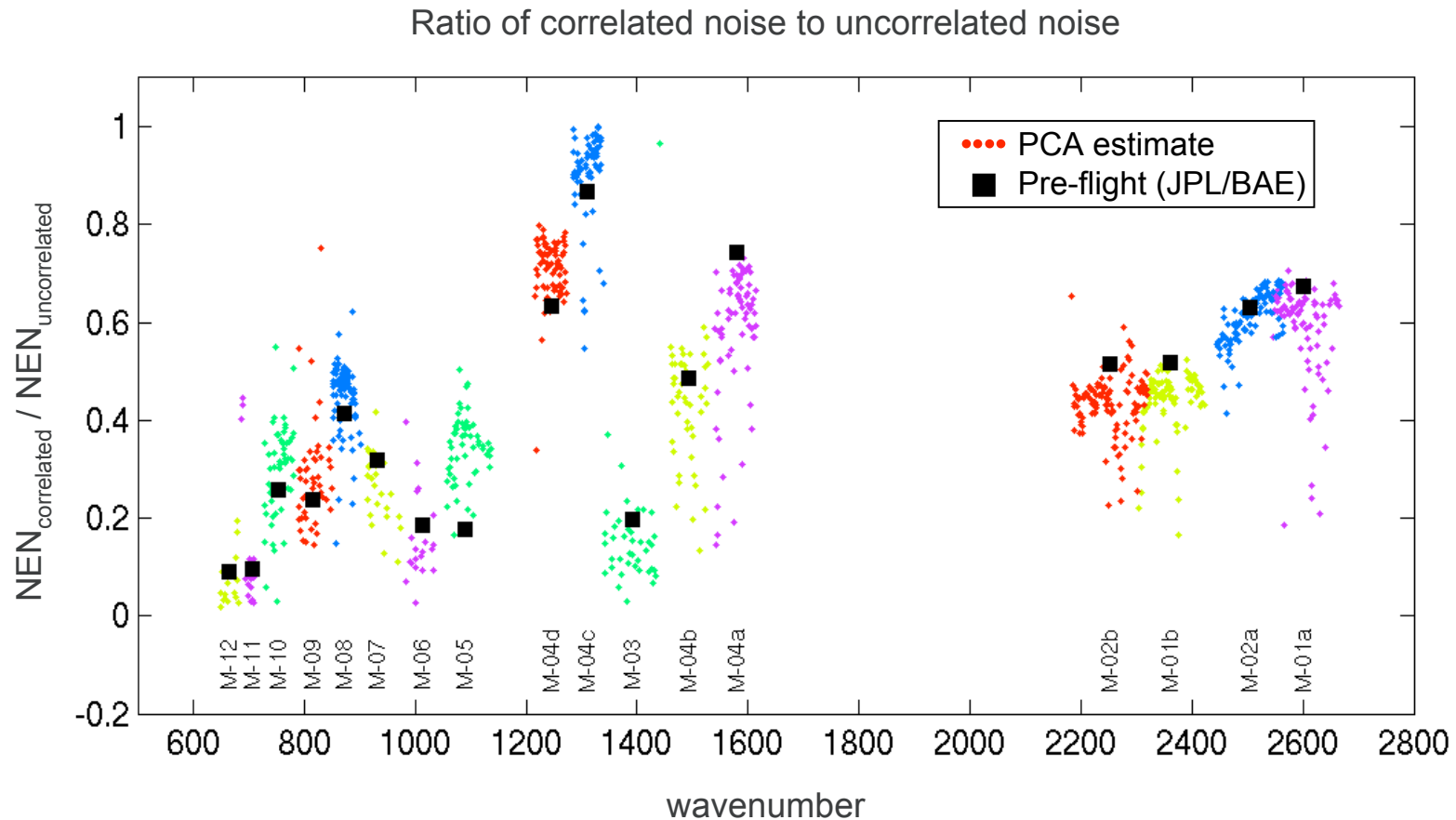


# NeDT comparison summary, all bands



# Spectrally Correlated Noise

The PCA estimate is of the spectrally uncorrelated noise; the spectrally correlated noise is computed as  $[\text{total\_noise}^2 - \text{pca\_noise}^2]^{1/2}$  and compared to pre-flight determinations performed by JPL/BAE:



- Very good agreement between two very different and independent analyses.
- The correlated noise is a large fraction of the total noise for several arrays.

# Two caveats re: this presentation

---

- Correction factor to PCA NEDN estimates to account for the random noise included in the  $n_T$  retained PCs
  - Not included in plots shown here
  - But the effect is small.  $[n/(n-n_T)]^{1/2}$ , e.g.  $(2120/2060)^{1/2} = 1.015$
- Reconstruction with a reduced number of PCs introduces spectral correlation
  - This effect is also small, perhaps negligible (see Antonelli 2004, Turner 2006), but I have not quantified it here.

NOTE: Reconstructed spectra are derived using a reduced number of PCs

According to the method described in Turner et al. to determine this number

# Non-Gaussian behavior

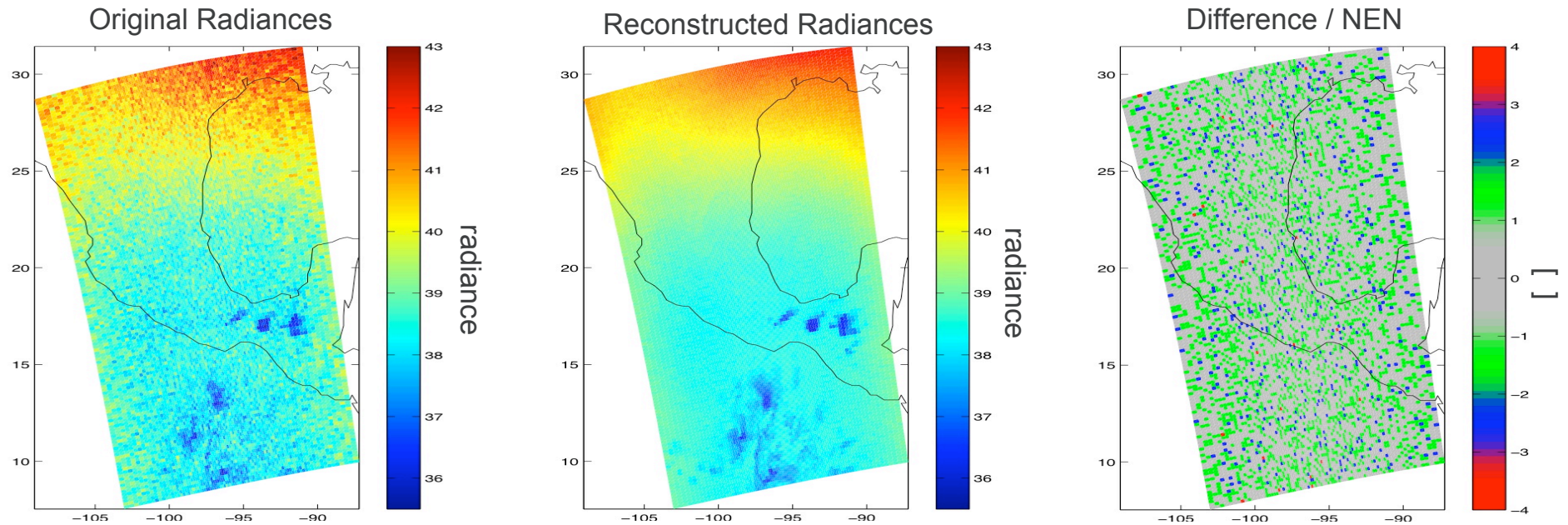
---

- Further investigation of RR

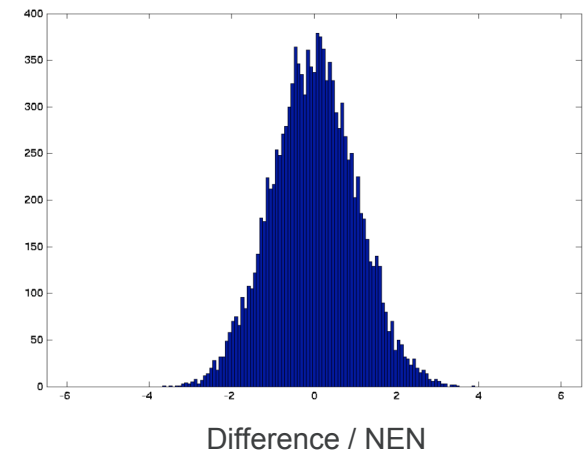
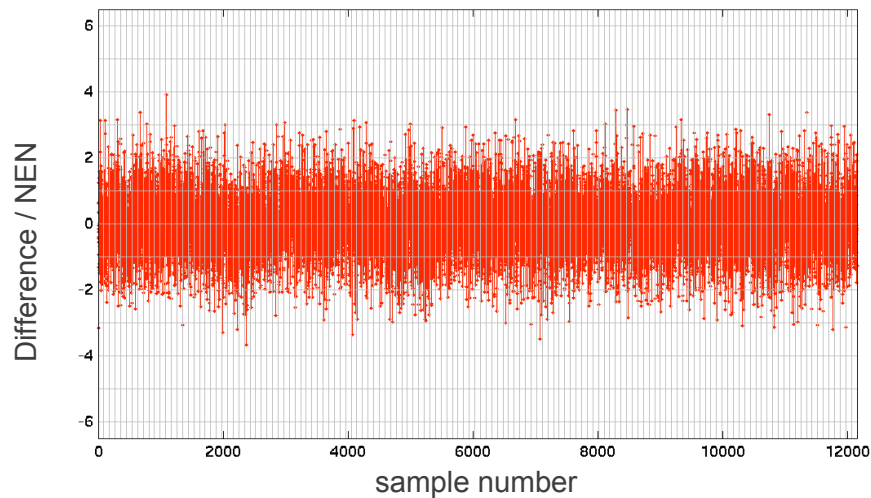


# Gaussian channel example

Granule 198, Array M-11, Channel 171 @ 698.545 cm<sup>-1</sup>



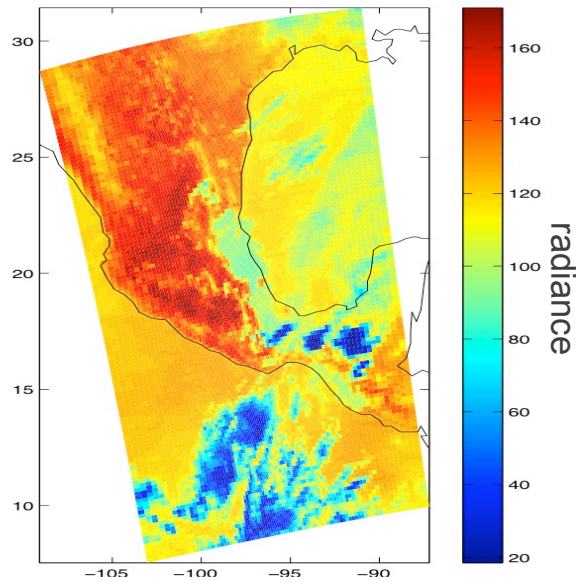
- # 1 $\sigma$  events = 3897
- # 2 $\sigma$  events = 566
- # 3 $\sigma$  events = 23
- # 1 $\sigma$  pops = 17
- # 2 $\sigma$  pops = 0
- # 3 $\sigma$  pops = 0
- # stripes = 0



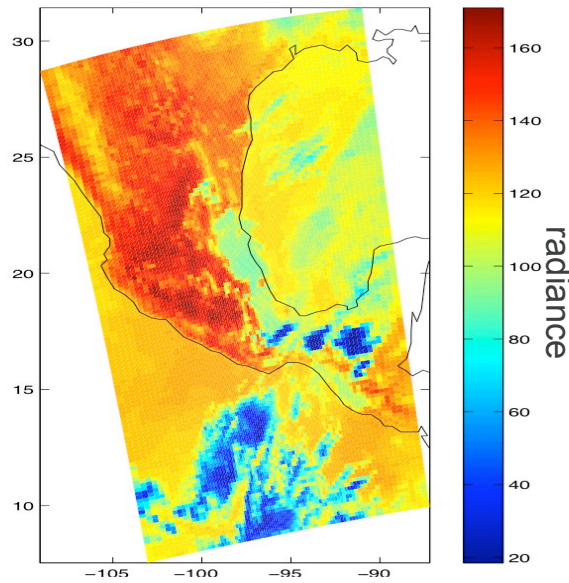
# “Popping” channel example

Granule 198, Array M-09, Channel 530 @ 821.597 cm<sup>-1</sup>

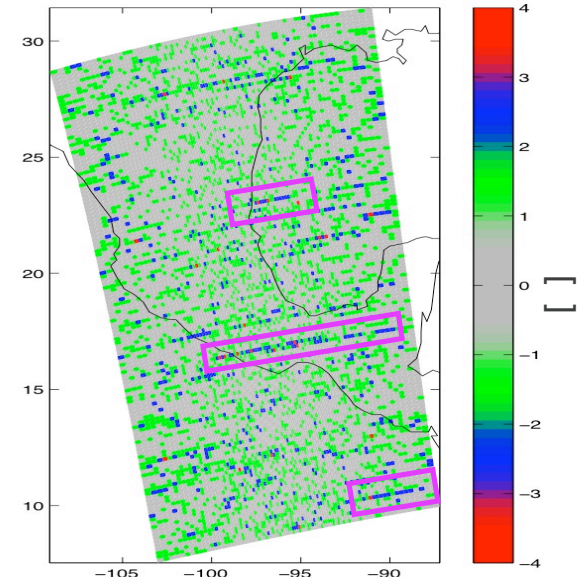
Original Radiances



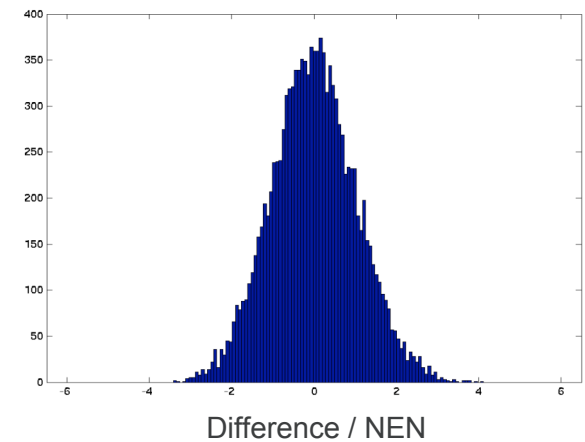
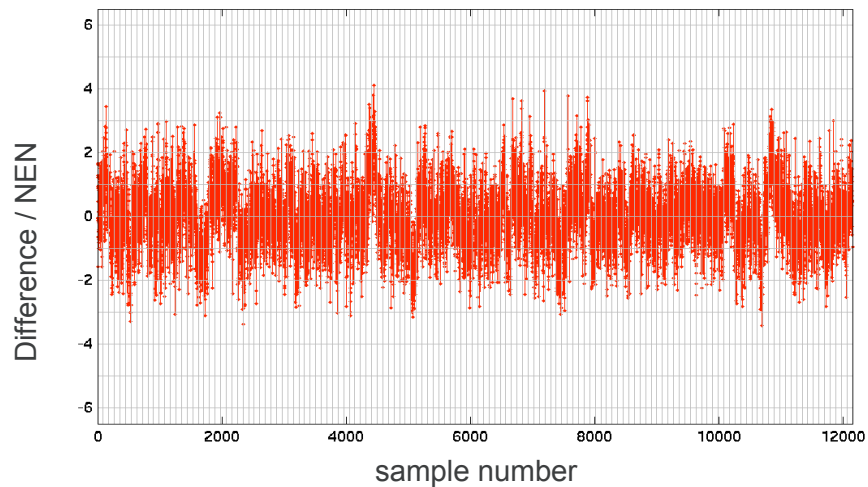
Reconstructed Radiances



Difference / NEN



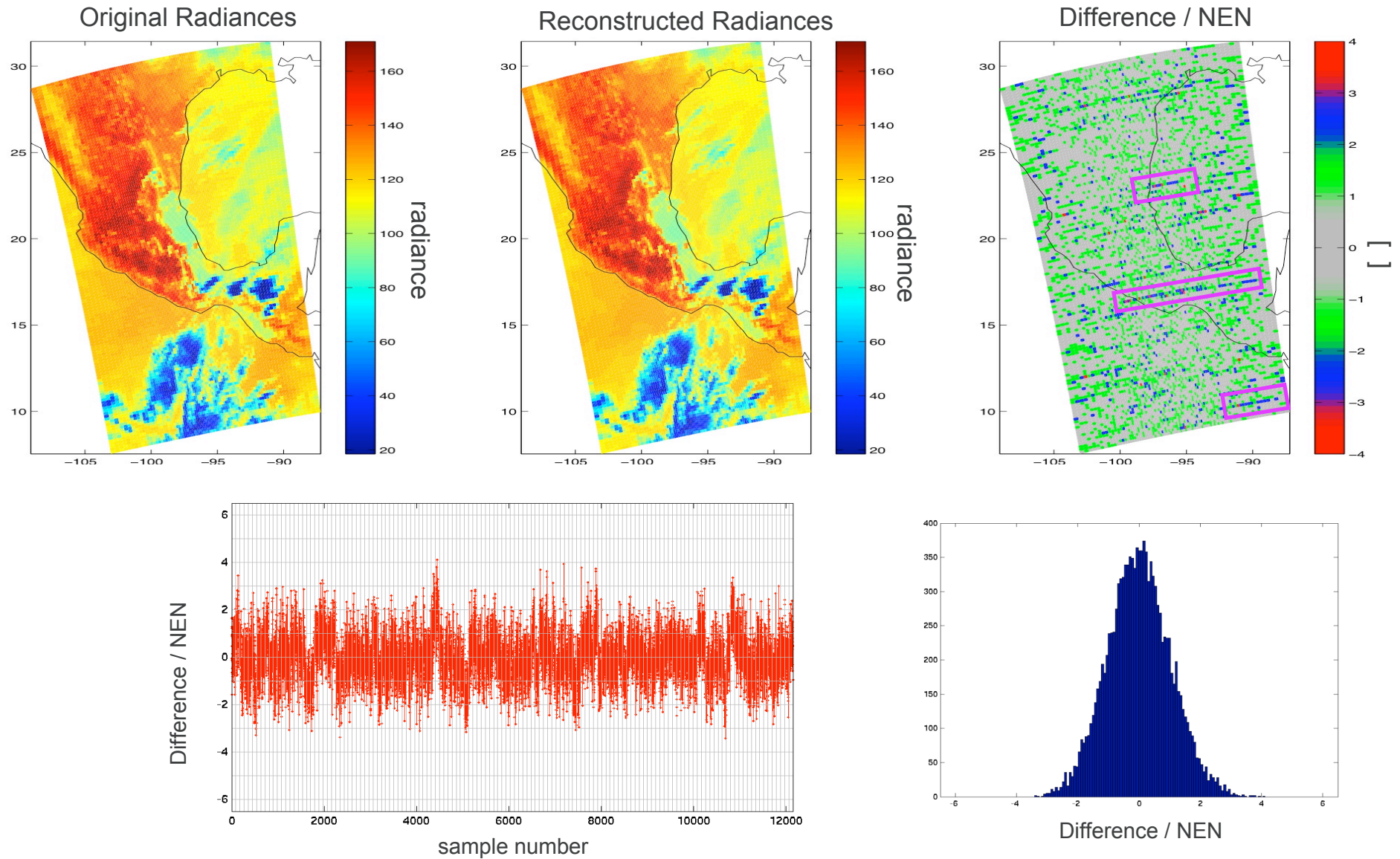
- # 1 $\sigma$  events = 3825
- # 2 $\sigma$  events = 563
- # 3 $\sigma$  events = 26
- # 1 $\sigma$  pops = 187
- # 2 $\sigma$  pops = 15
- # 3 $\sigma$  pops = 0
- # stripes = 0





# “Popping” channel example

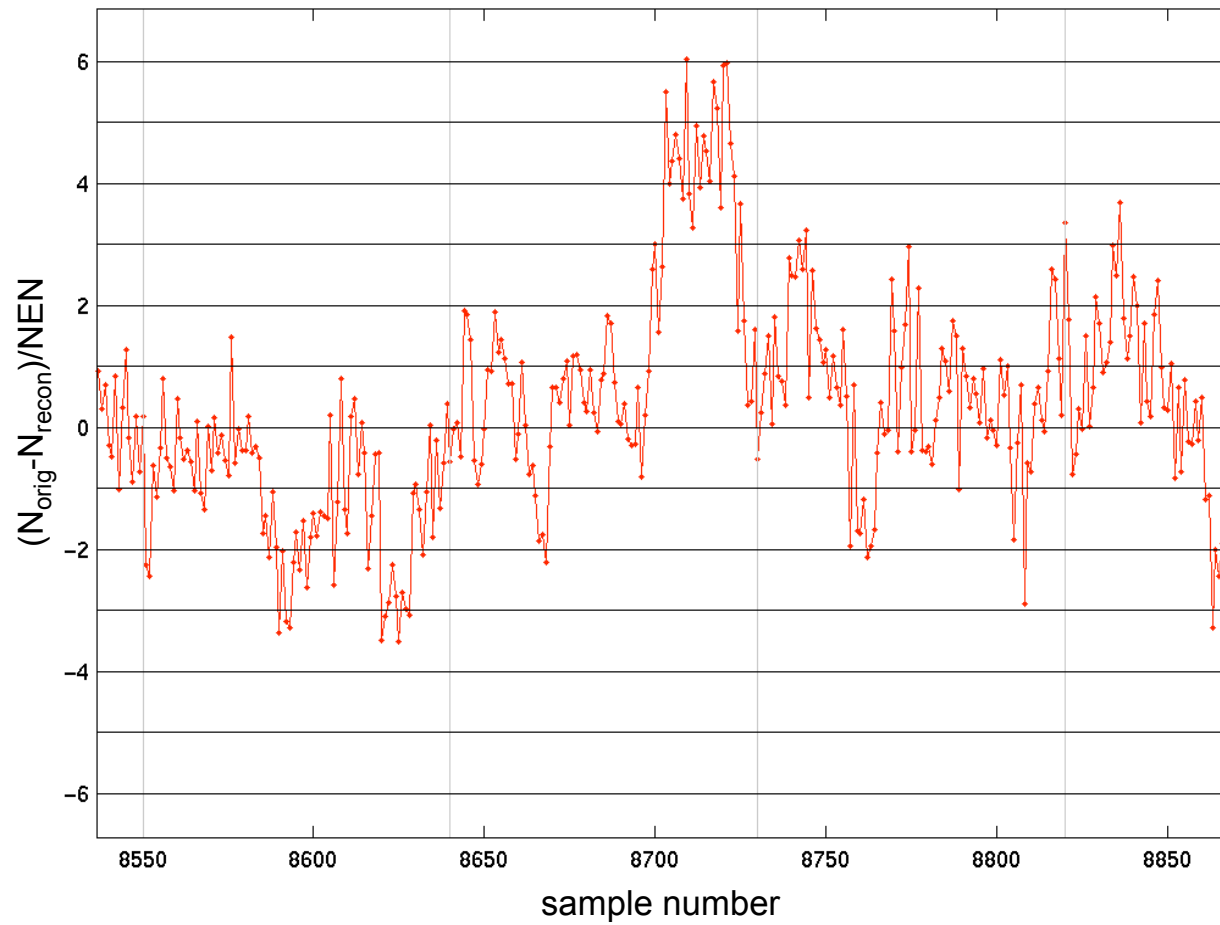
Granule 198, Array M-09, Channel 530 @ 821.597 cm<sup>-1</sup>



# “Popping” channel example

---

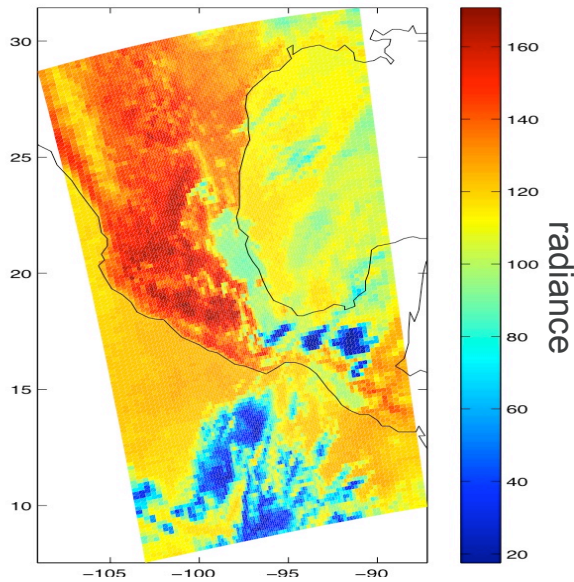
Granule 198, Array M-09, Channel 573 @ 838.106 cm<sup>-1</sup>



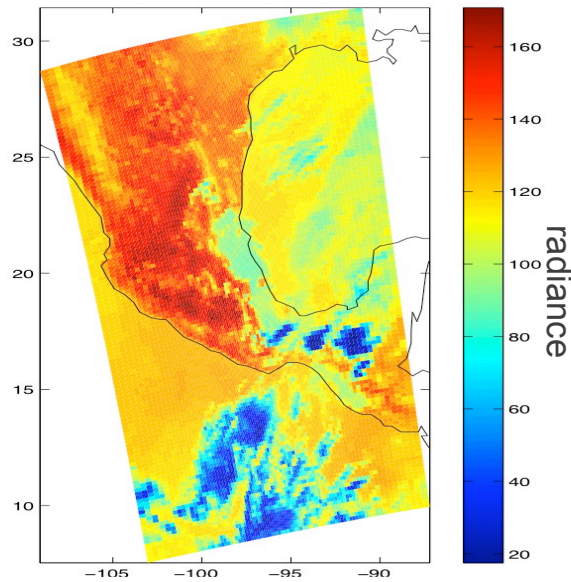
# “Striping” channel example

Granule 198, Array M-09, Channel 564 @ 834.772 cm<sup>-1</sup>

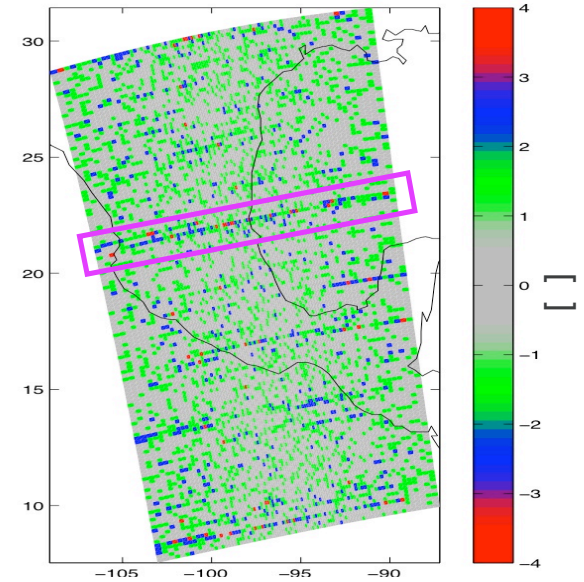
Original Radiances



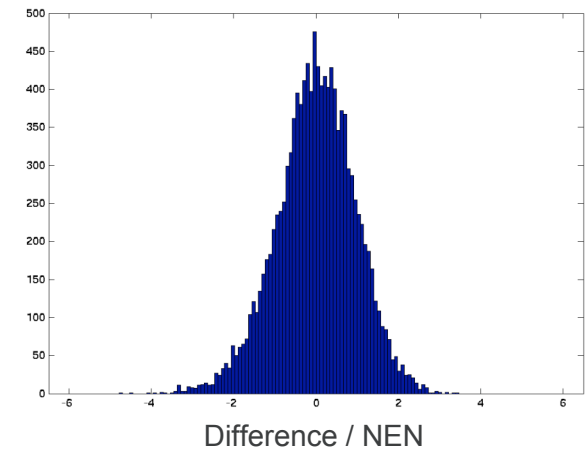
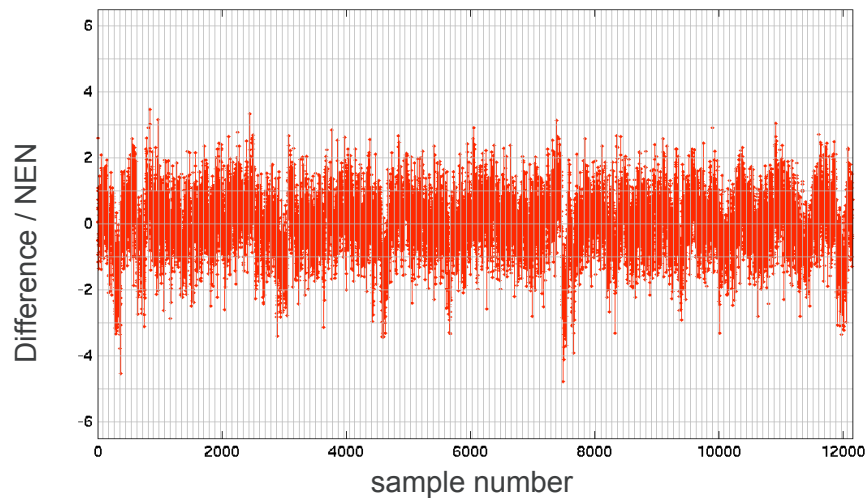
Reconstructed Radiances



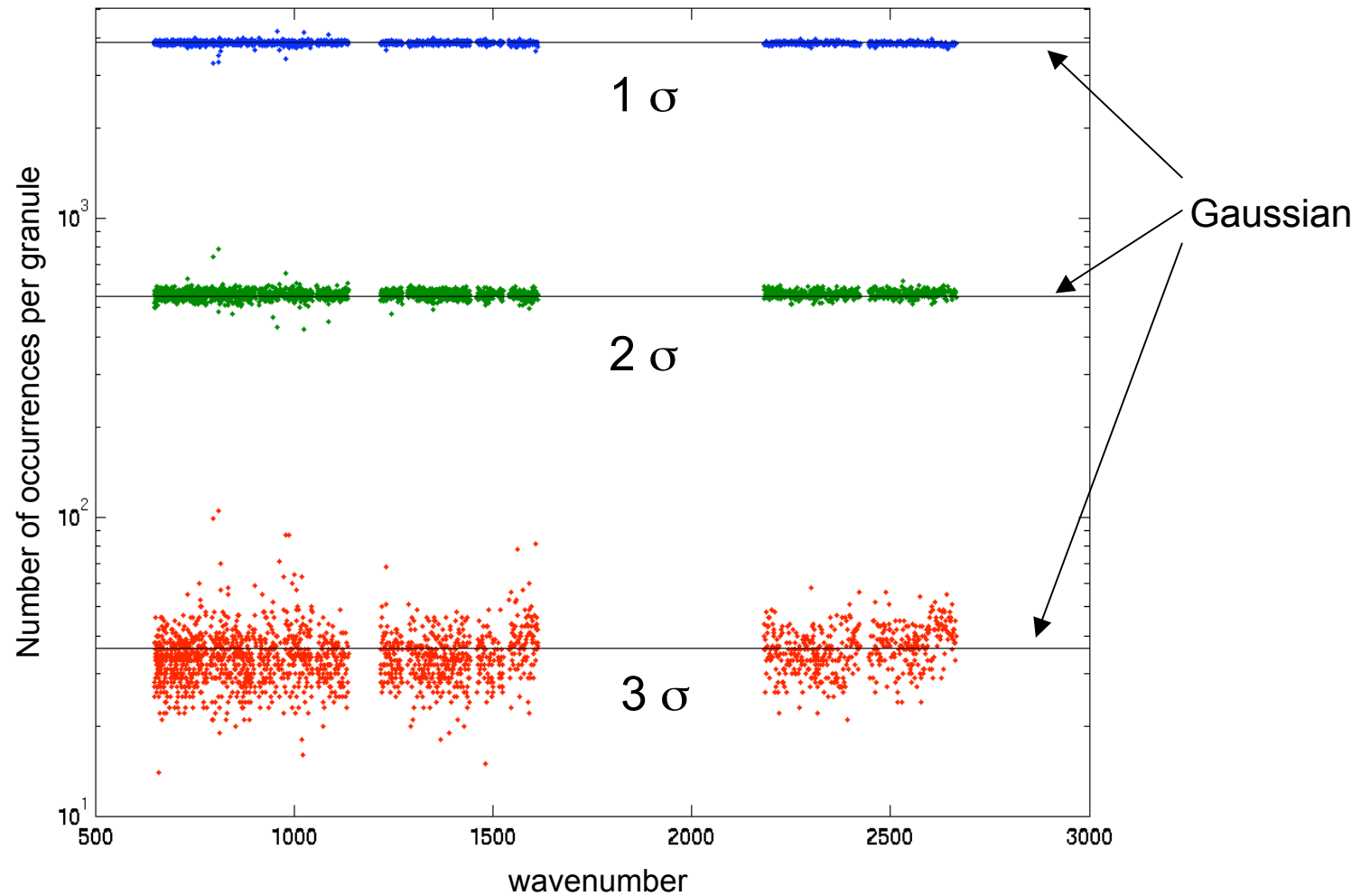
Difference / NEN



- # 1 $\sigma$  events = 3713
- # 2 $\sigma$  events = 593
- # 3 $\sigma$  events = 61
- # 1 $\sigma$  pops = 118
- # 2 $\sigma$  pops = 12
- # 3 $\sigma$  pops = 0
- # stripes = 1



# Number of $N\sigma$ events detected



Number of events for pure Gaussian behavior:

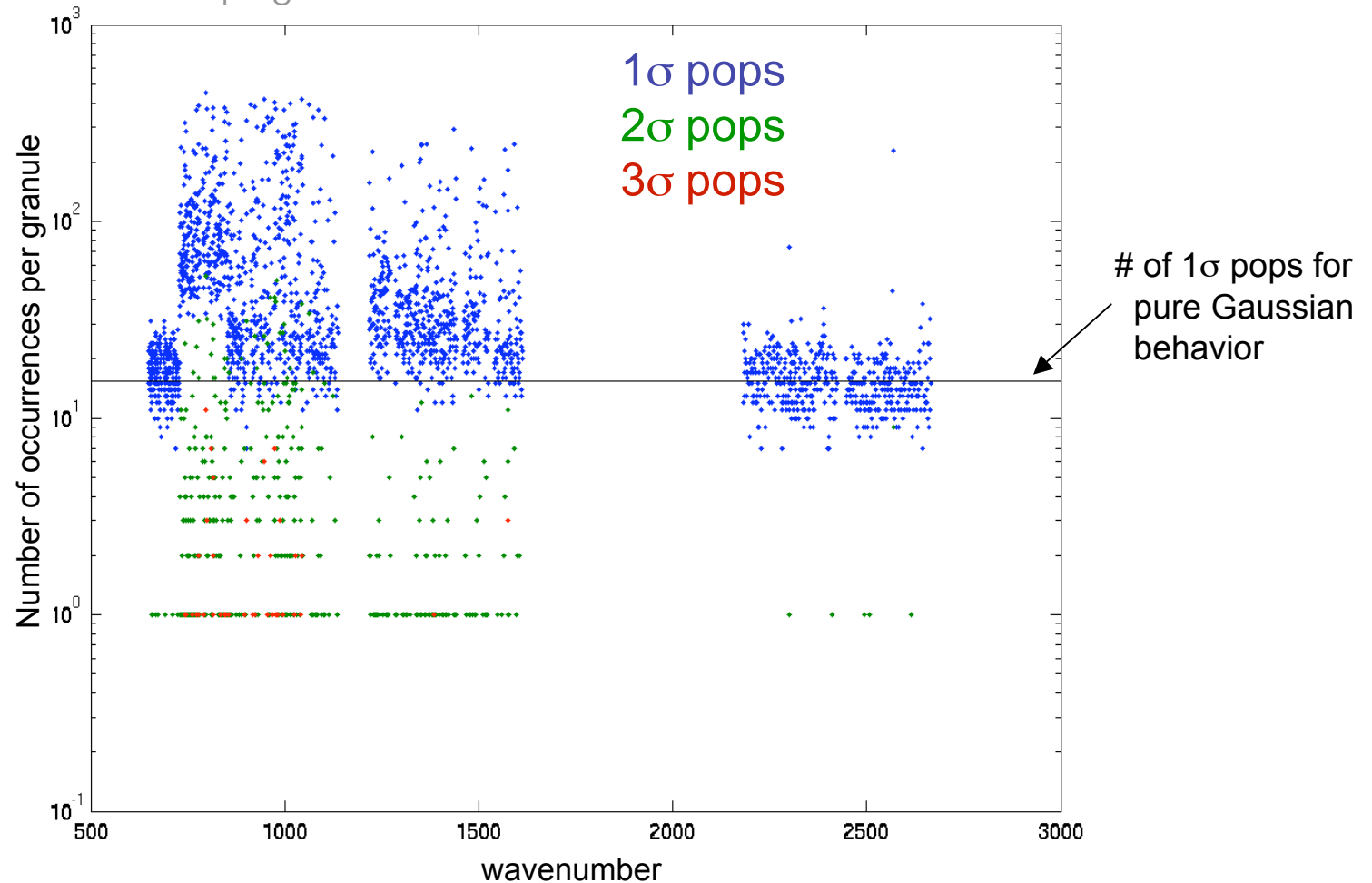
# 1 $\sigma$  events per granule =  $90 \cdot 135 \cdot (1 - 0.683) = 3852$

# 2 $\sigma$  events per granule =  $90 \cdot 135 \cdot (1 - 0.955) = 547$

# 3 $\sigma$  events per granule =  $90 \cdot 135 \cdot (1 - 0.997) = 36$

# Number of $N\sigma$ Pops detected

- $N\sigma$  pop defined here as 4 or more consecutive  $N\sigma$  events of same sign
- 875 / 482 / 42 channels exhibit  $1\sigma$  /  $2\sigma$  /  $3\sigma$  popping significantly above Gaussian behavior
- 14 channels found to exhibit “striping”



Number of pops for pure Gaussian behavior:

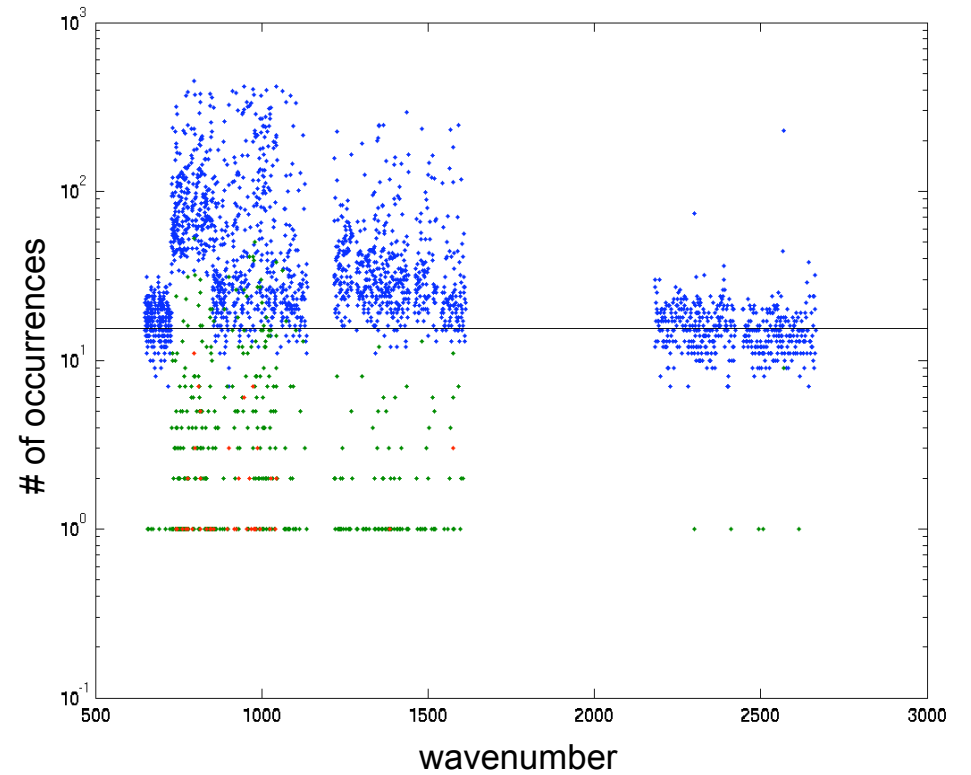
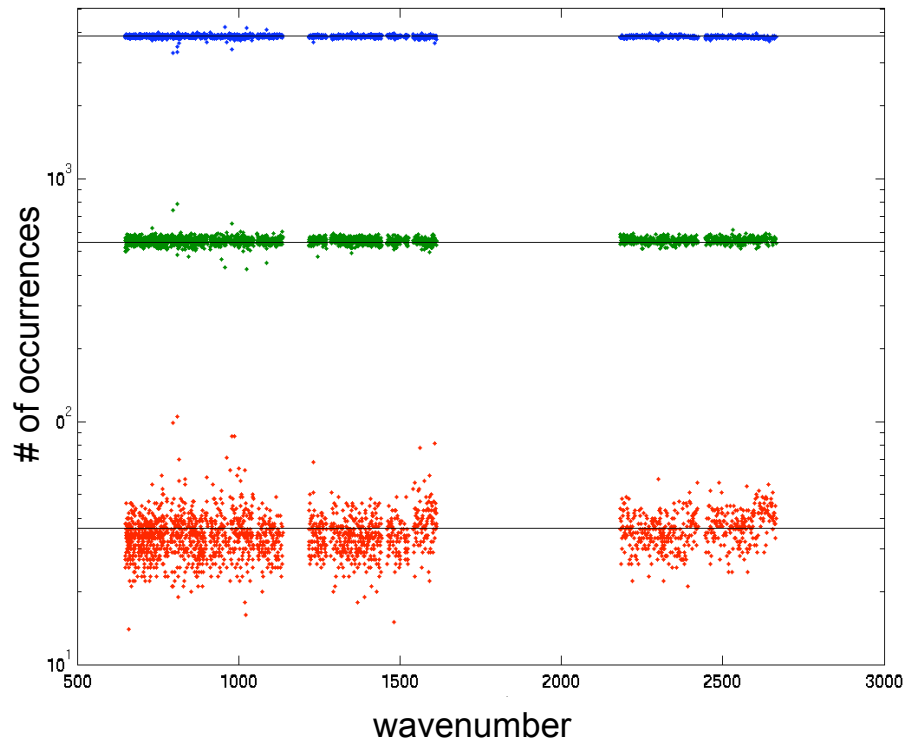
$$\# \text{ } 1\sigma \text{ pops per granule} = 2 \cdot 90 \cdot 135 \cdot (0.5 \cdot (1 - 0.683))^4 = 15$$

$$\# \text{ } 2\sigma \text{ pops per granule} = 2 \cdot 90 \cdot 135 \cdot (0.5 \cdot (1 - 0.955))^4 = 0$$

$$\# \text{ } 3\sigma \text{ pops per granule} = 2 \cdot 90 \cdot 135 \cdot (0.5 \cdot (1 - 0.997))^4 = 0$$

# Number of $N\sigma$ Pops detected

---





# Inspection of PCs and individual spectra

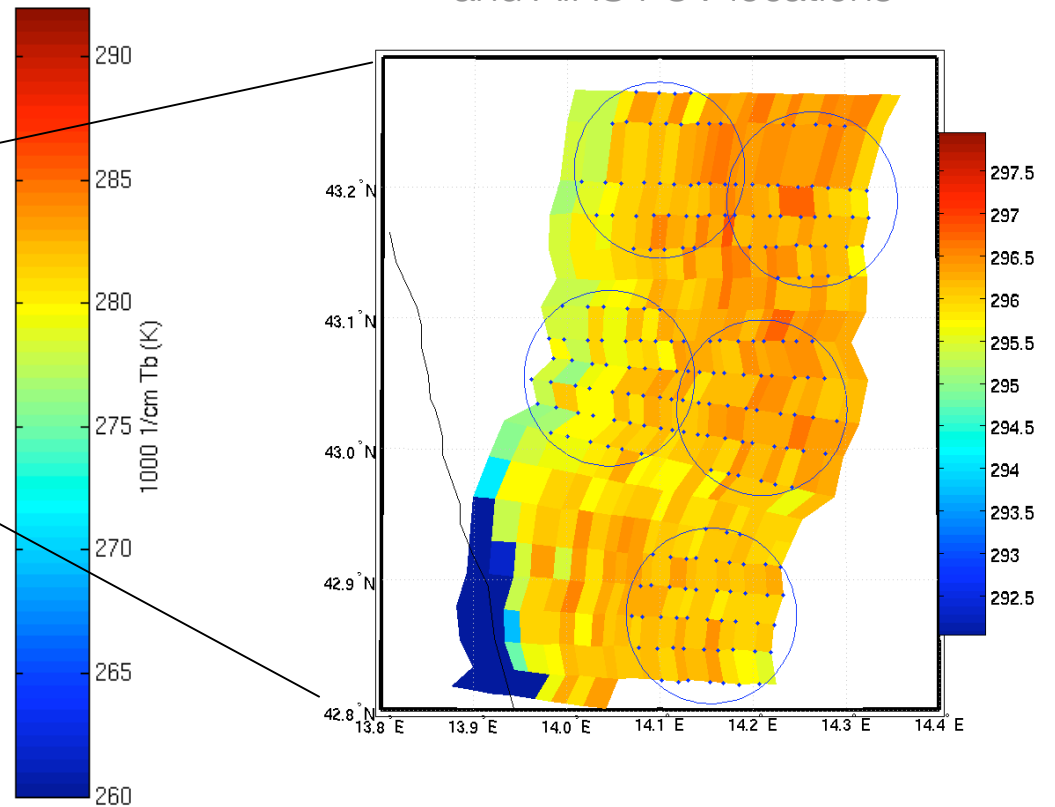
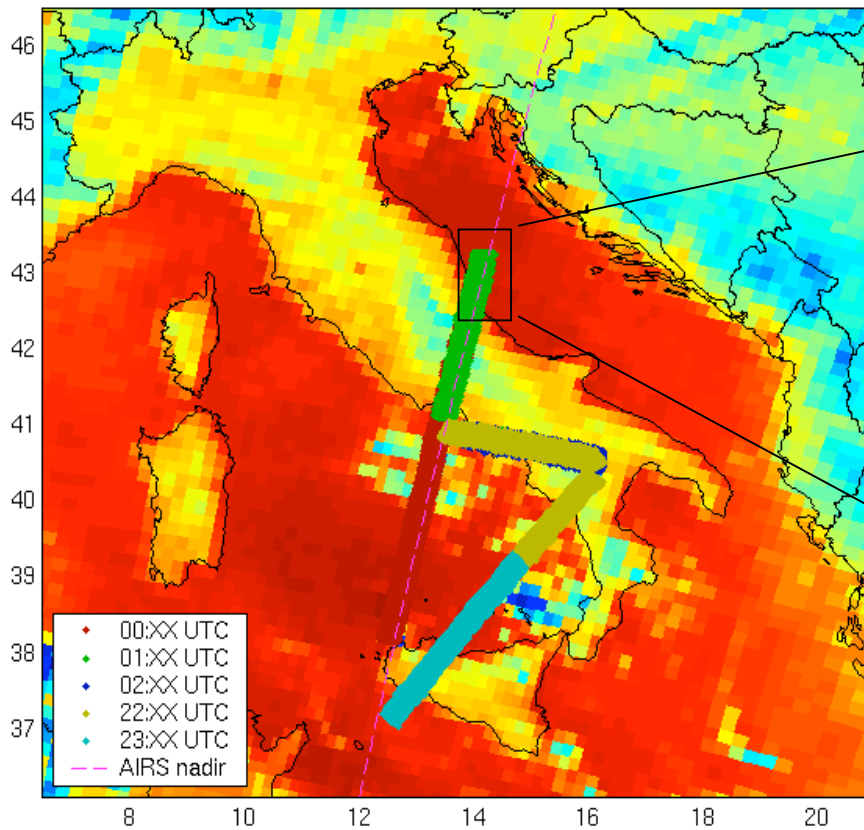
---

- Effects that lie in the less understood domain between calibration (long average) and spectrally random, repeatable noise.

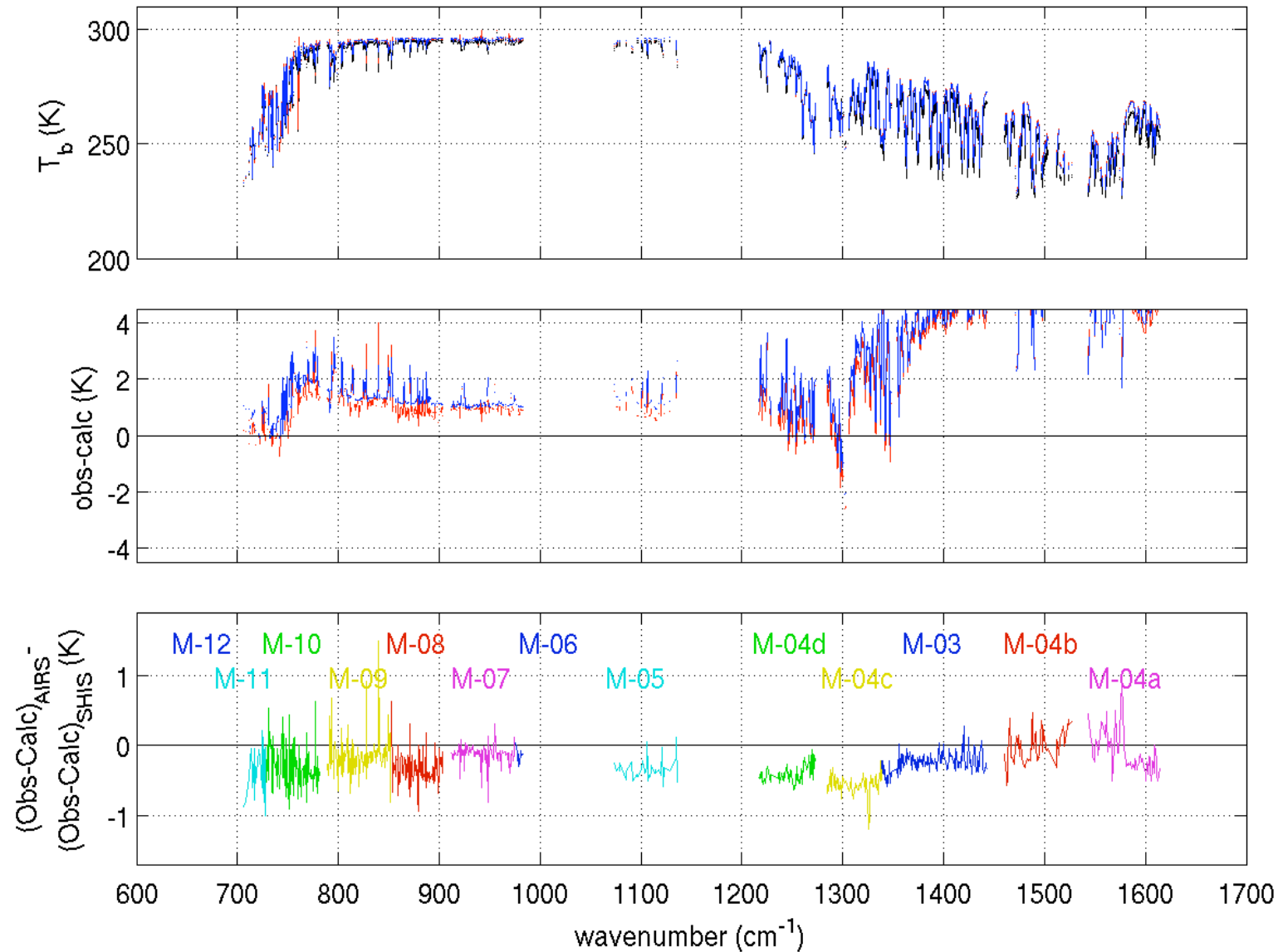
# AIRS underflight with the Scanning-HIS

ADRIEX (EAQUATE) Campaign  
S-HIS on Proteus aircraft @ 16km over Adriatic Sea  
2004.09.08, 01:10 UTC

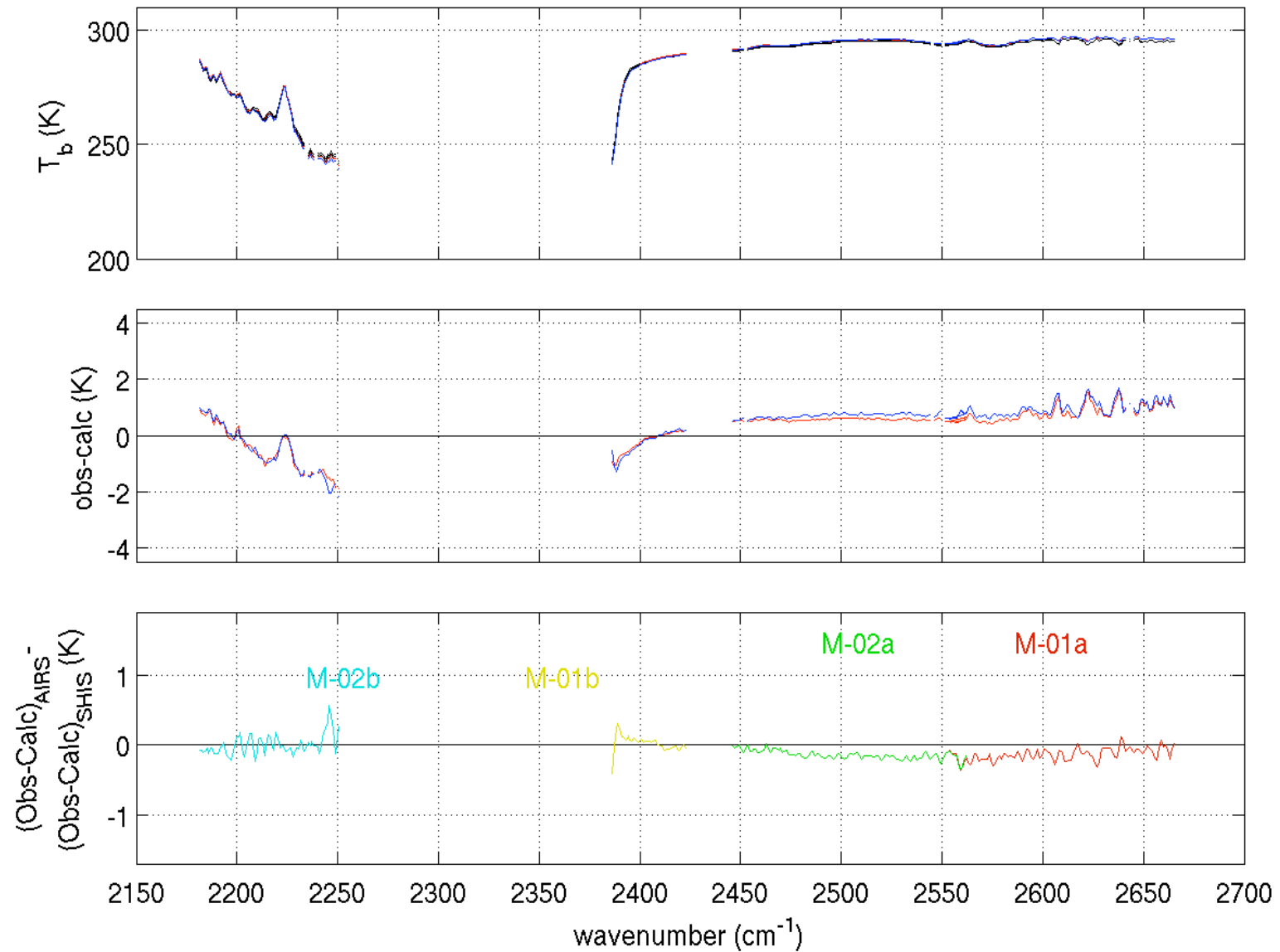
S-HIS 12  $\mu\text{m}$  brightness temperatures  
and AIRS FOV locations



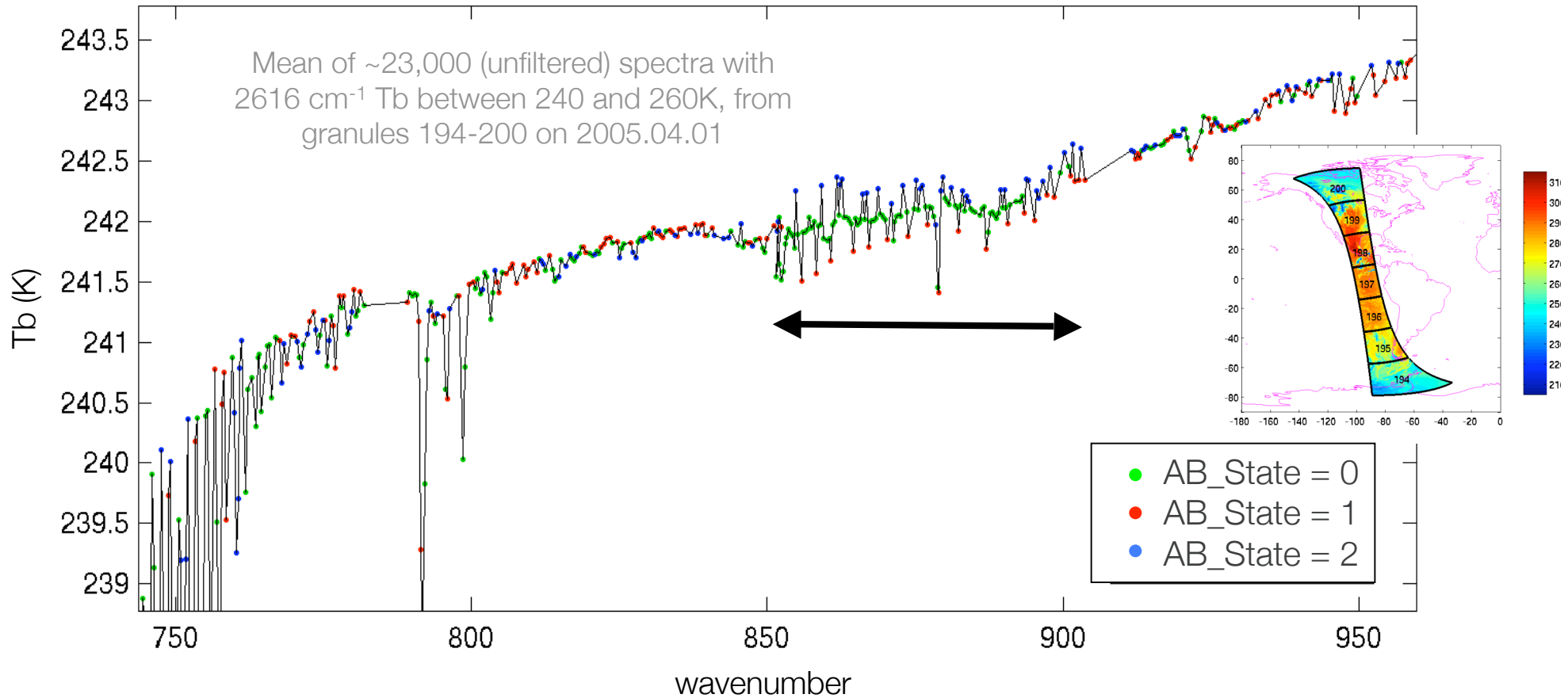
# AIRS radiance validation, longwave and midwave



# AIRS radiance validation, shortwave

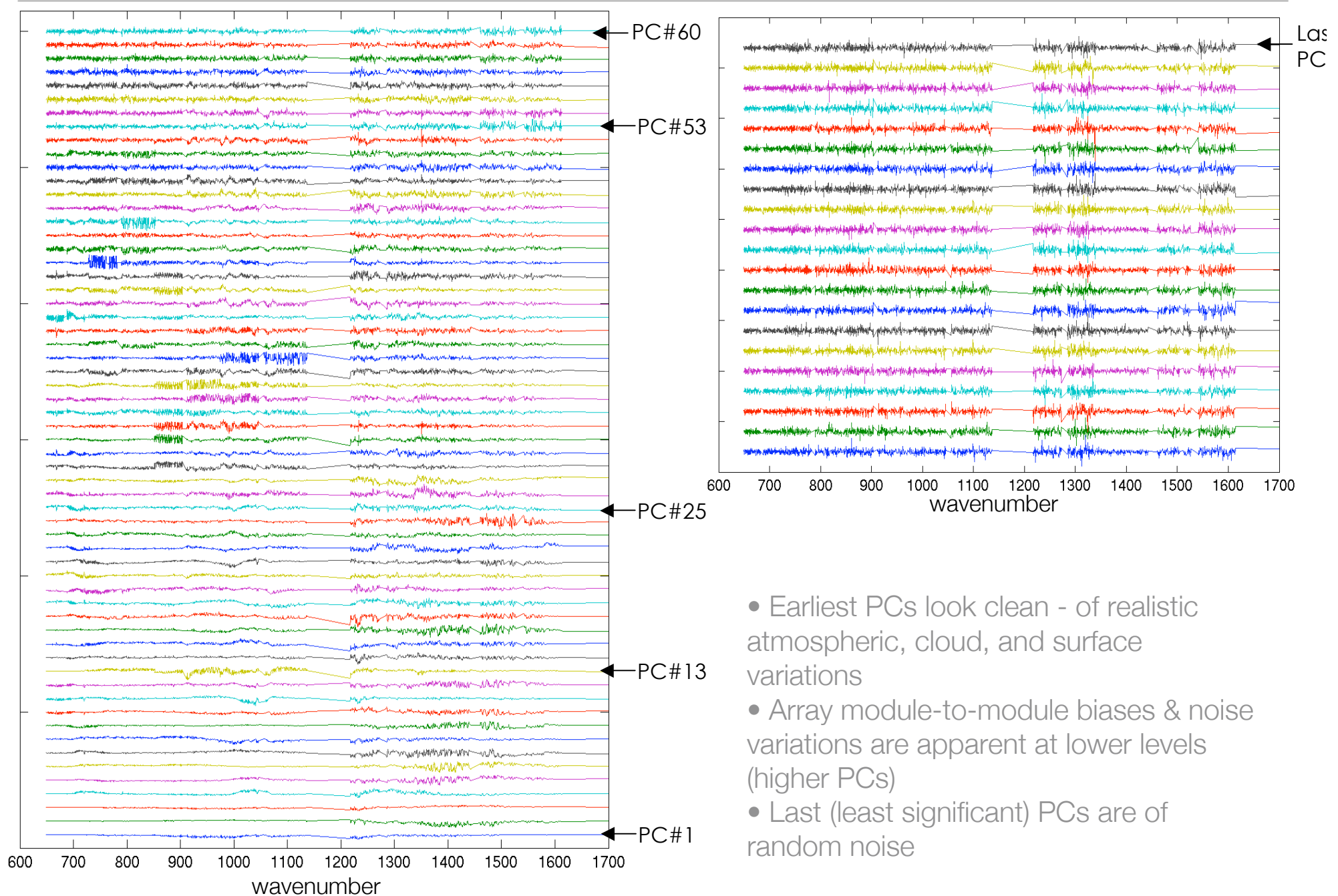


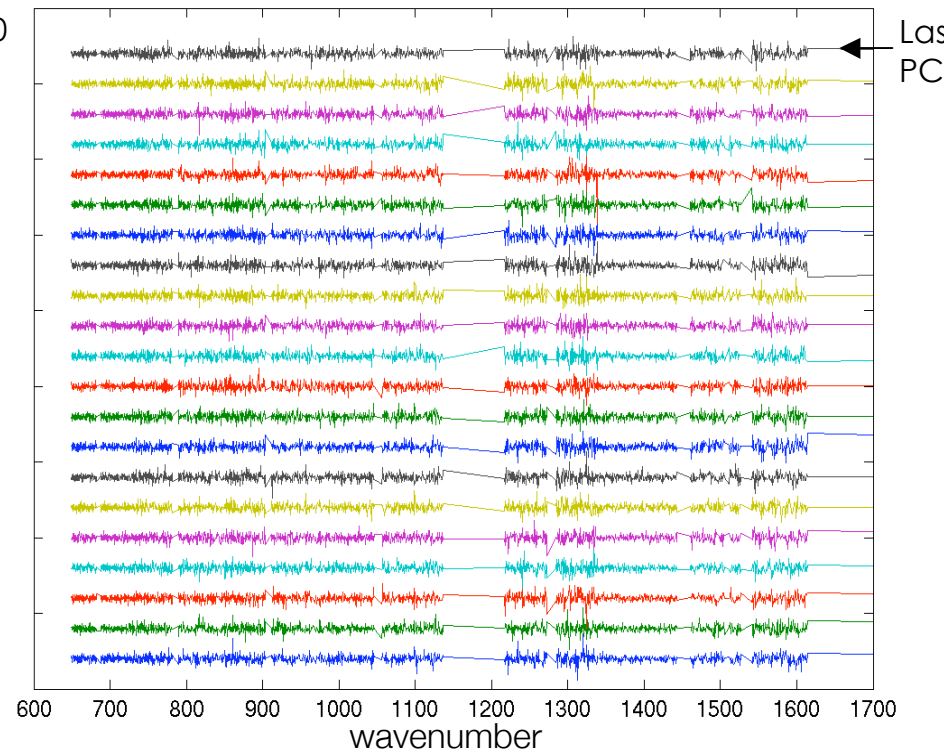
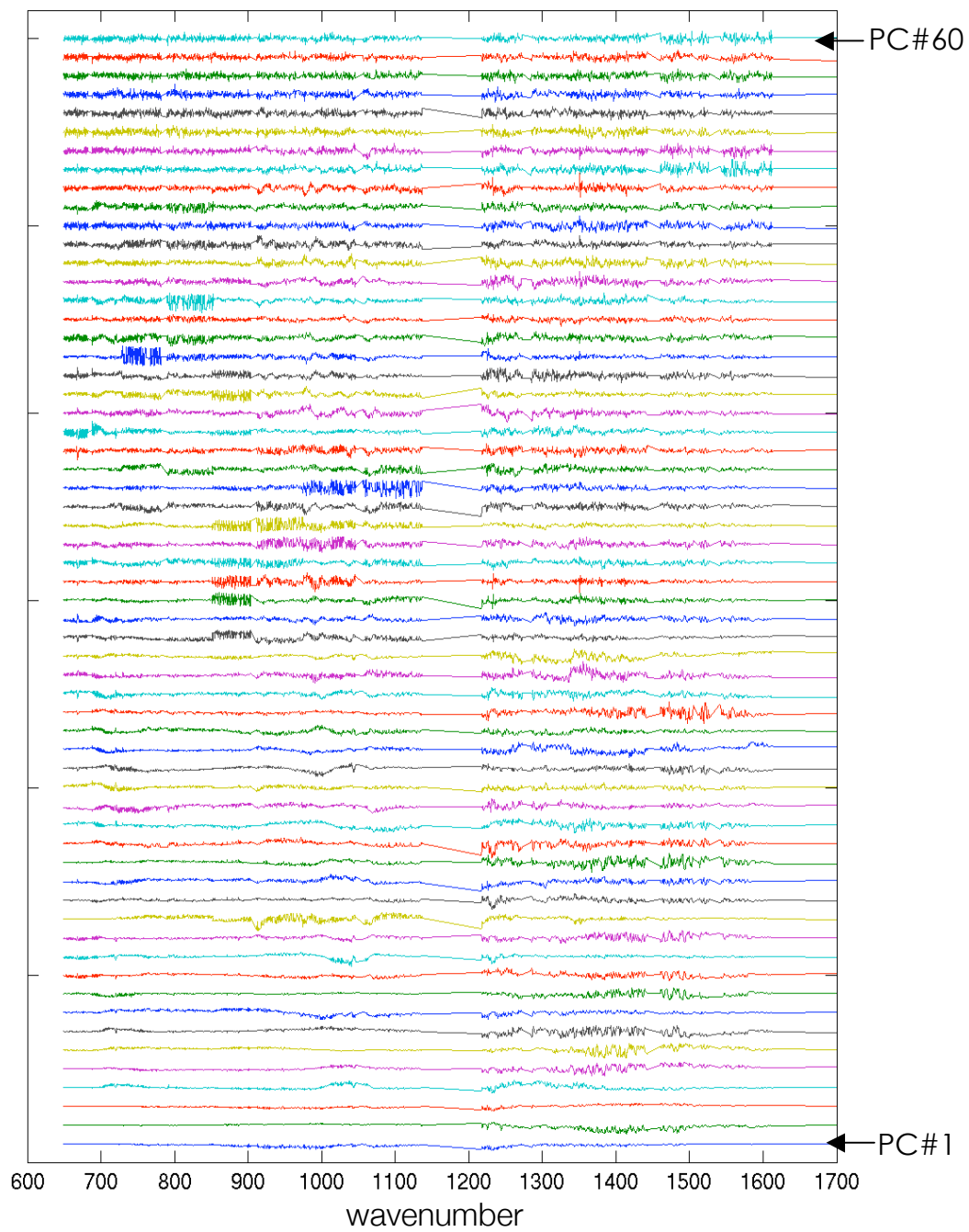
# A / B State dependent calibration in M-08



- Similar behavior observed for similar scenes throughout the mission
- Less evident in mean spectra at colder (e.g. Antarctica) and warmer (e.g. clear ocean) scenes.

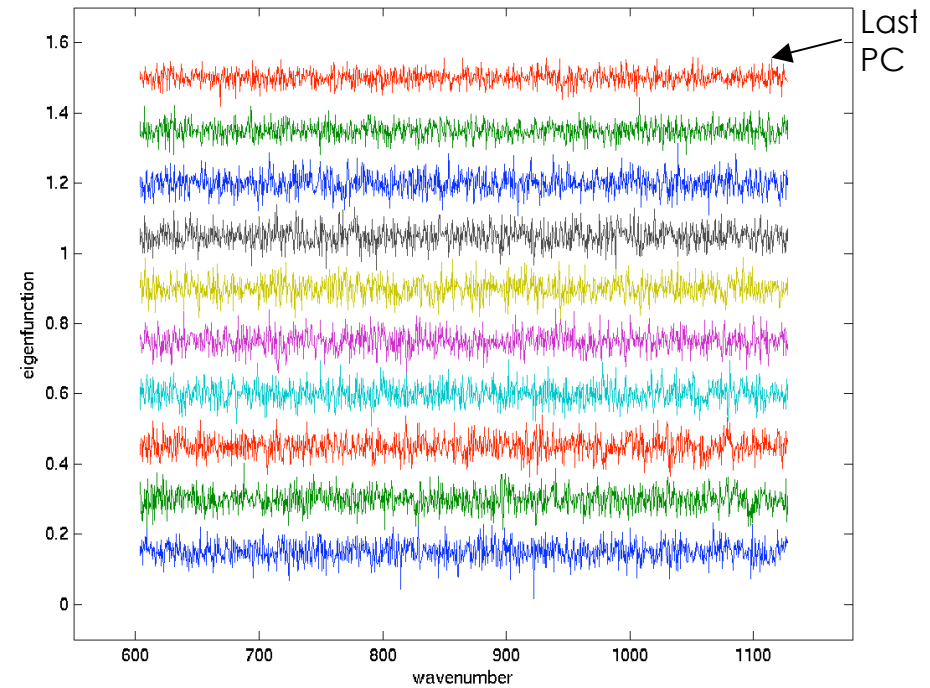
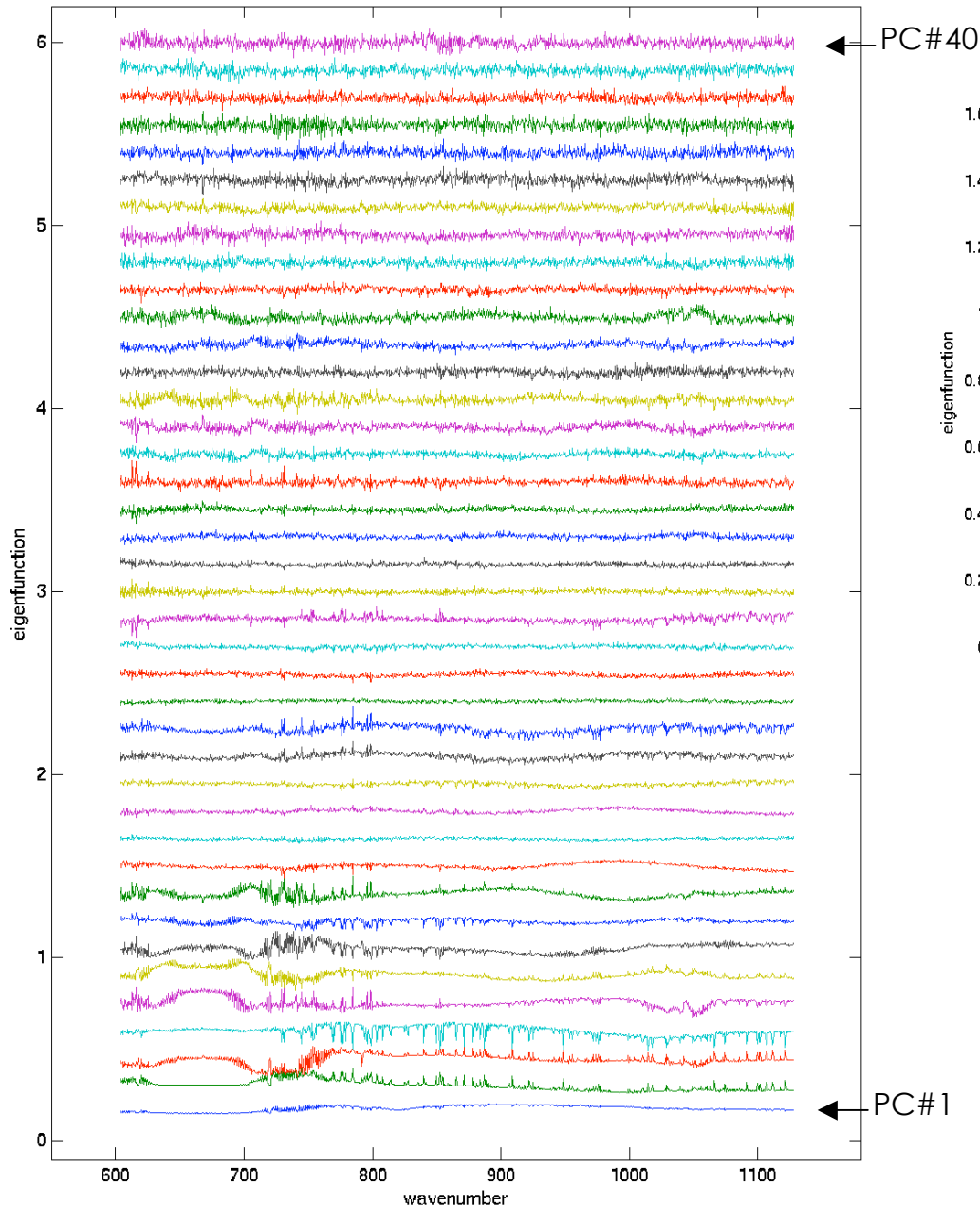
# AIRS Principle Components, granule 195







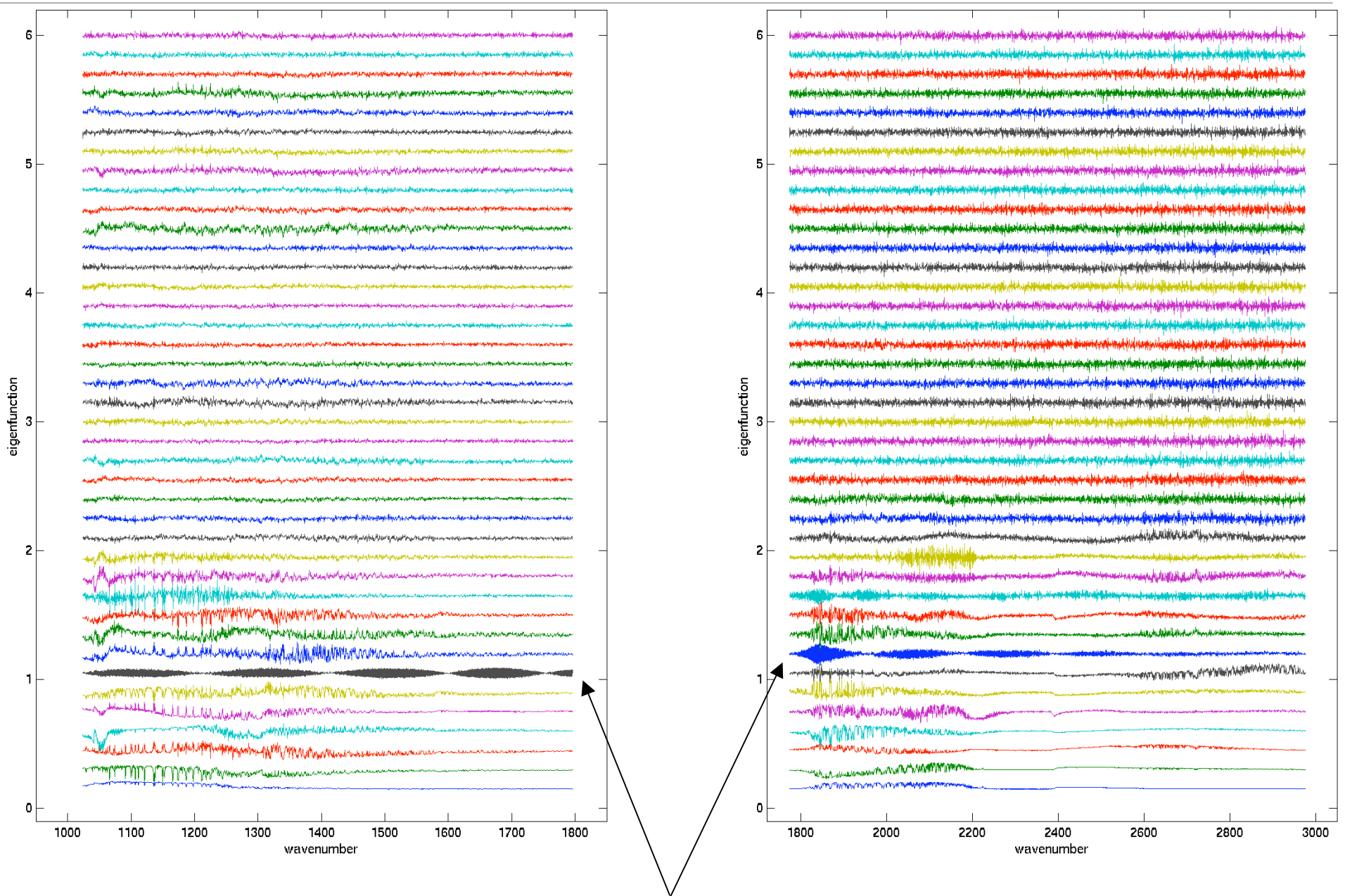
# Scanning-HIS Principle Components, Longwave



Spectral signatures in low order PCs are clean, indicative of real atmospheric characteristics

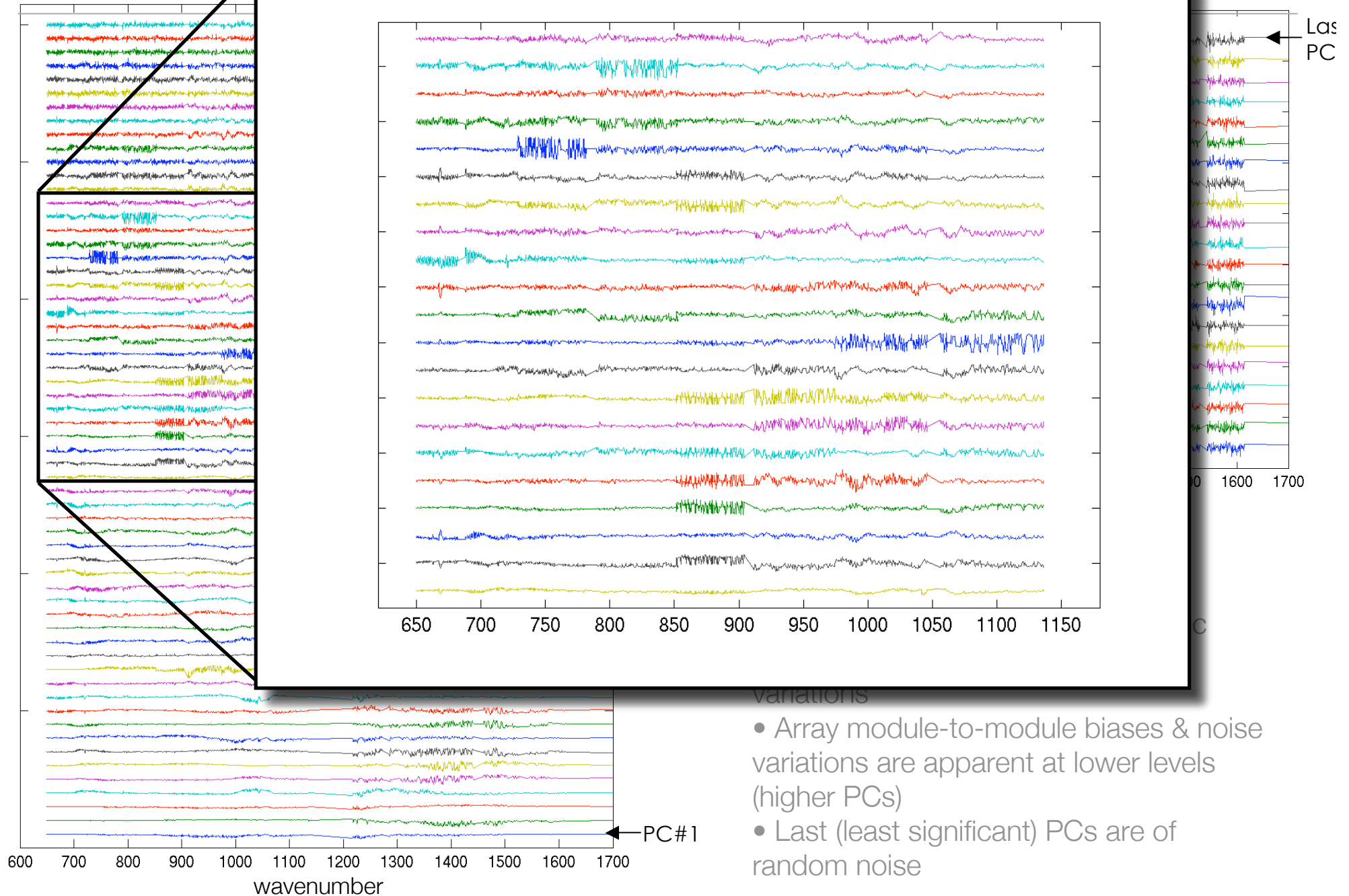


# Scanning-HIS PCs, Midwave and Shortwave

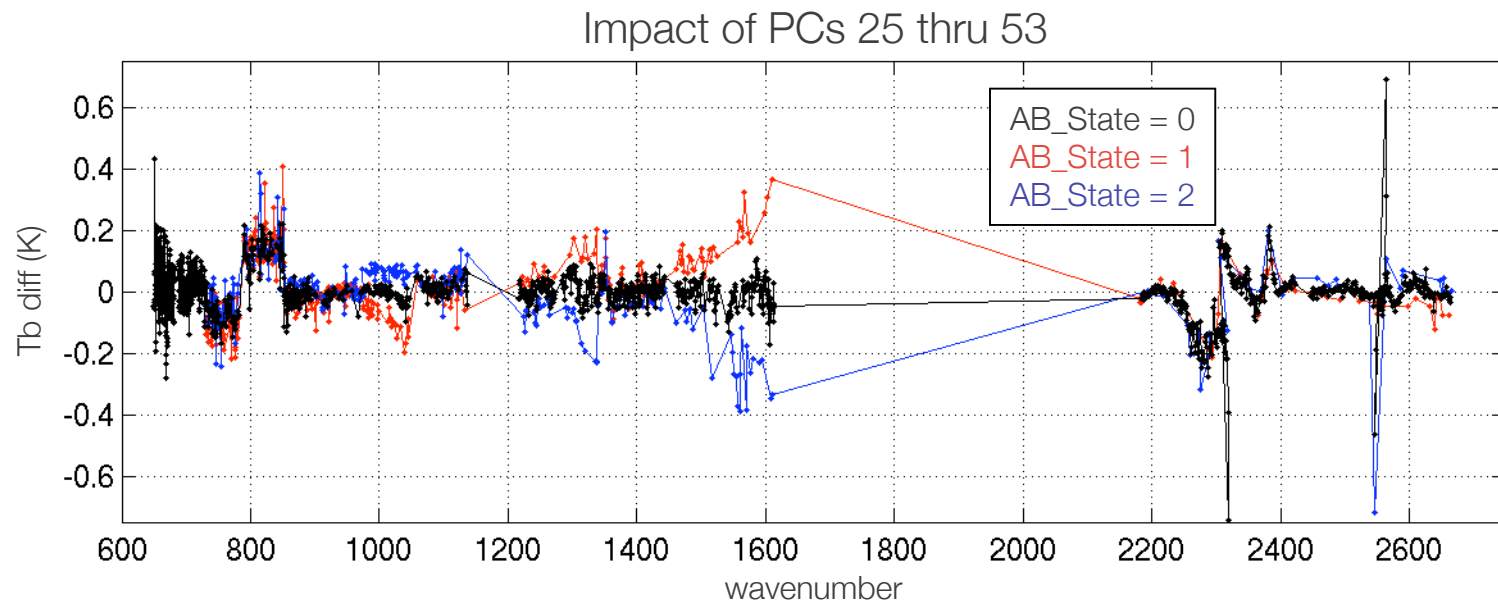
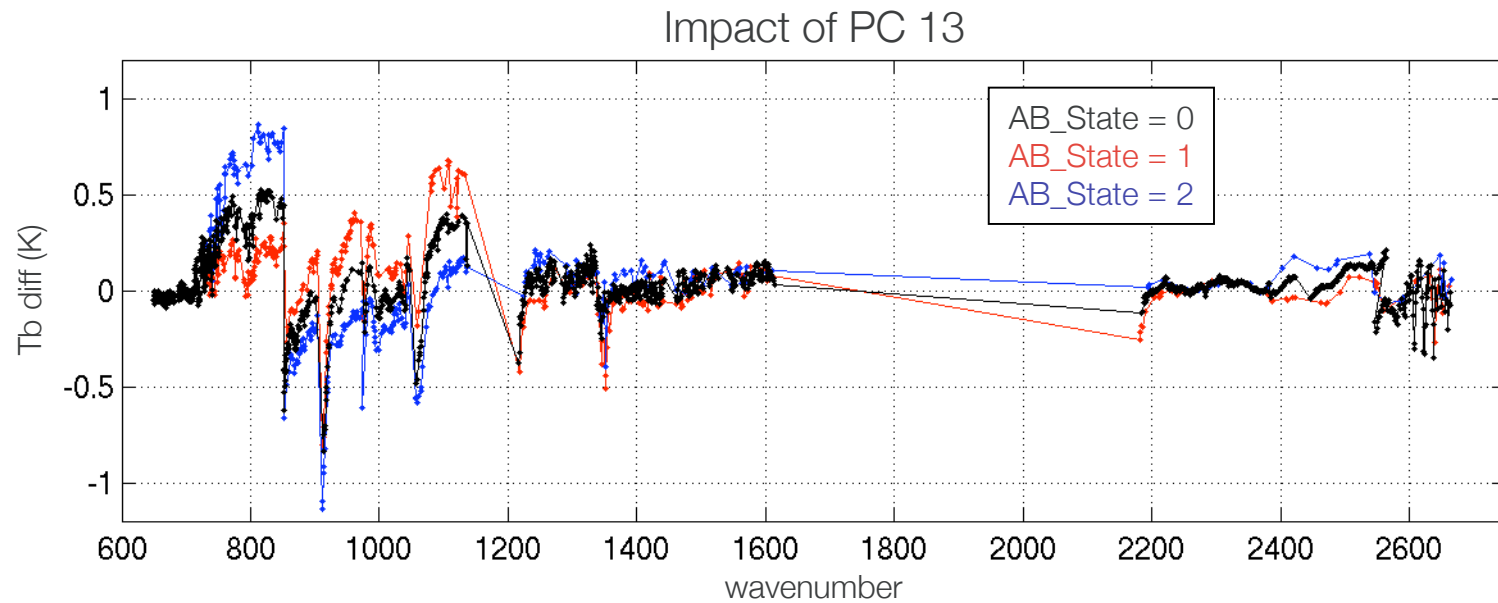


Ringing is indicative of spectral resampling processing artifact- easily fixed by band guard position mod

# AIRS Principle Components granule 195



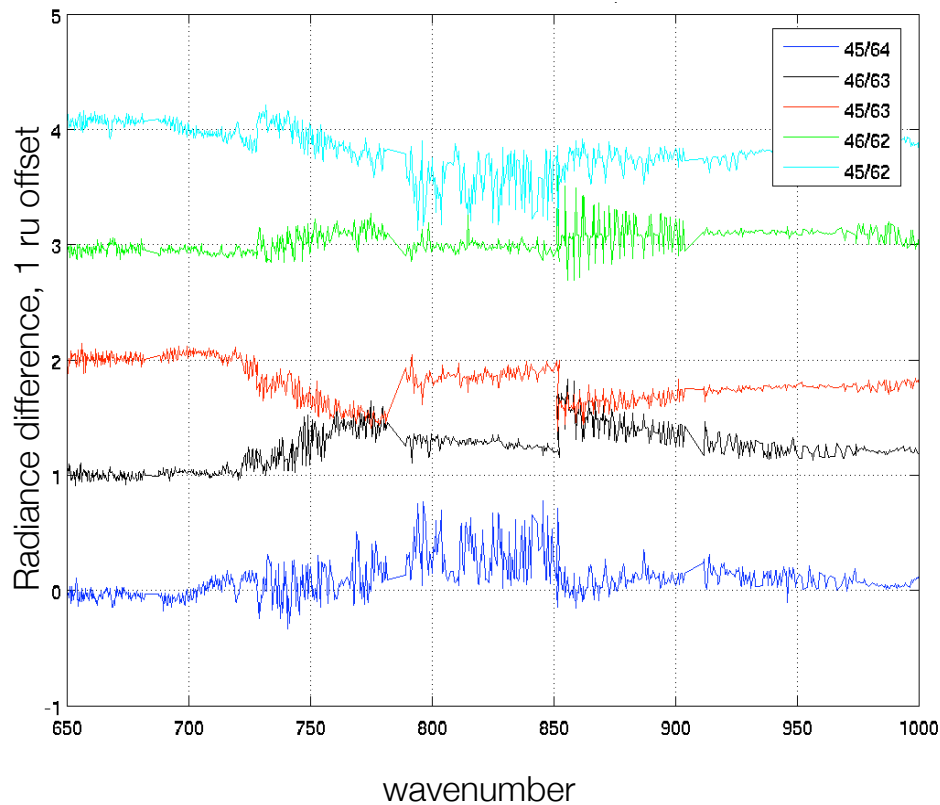
# Impact of PC 13 and 25-53 on an example spectrum



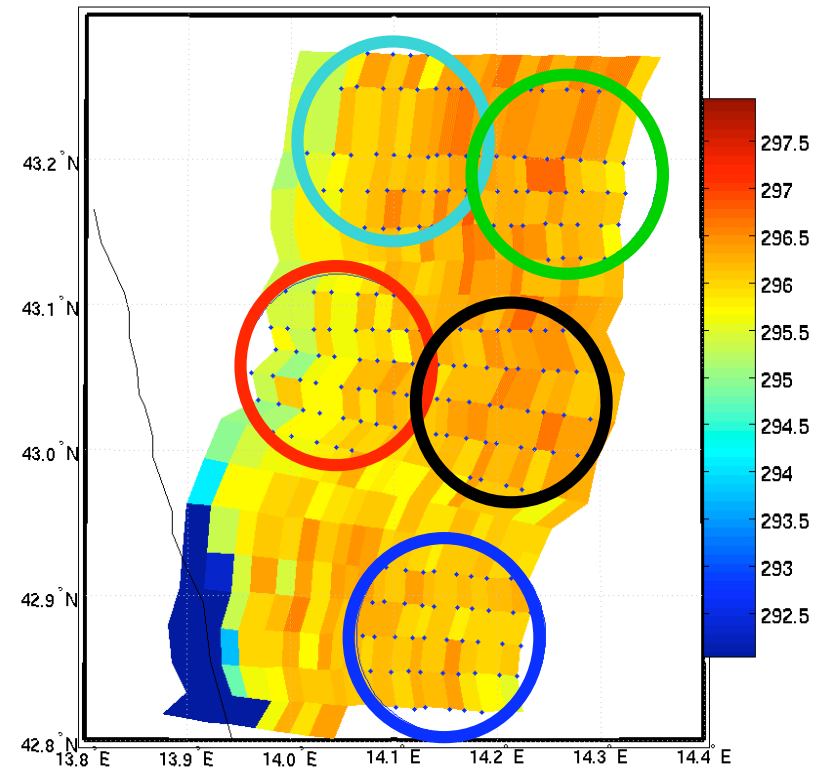
# Variations in individual spectra. 2004.09.07 EAQUATE case

## AIRS

Differences from mean spectrum



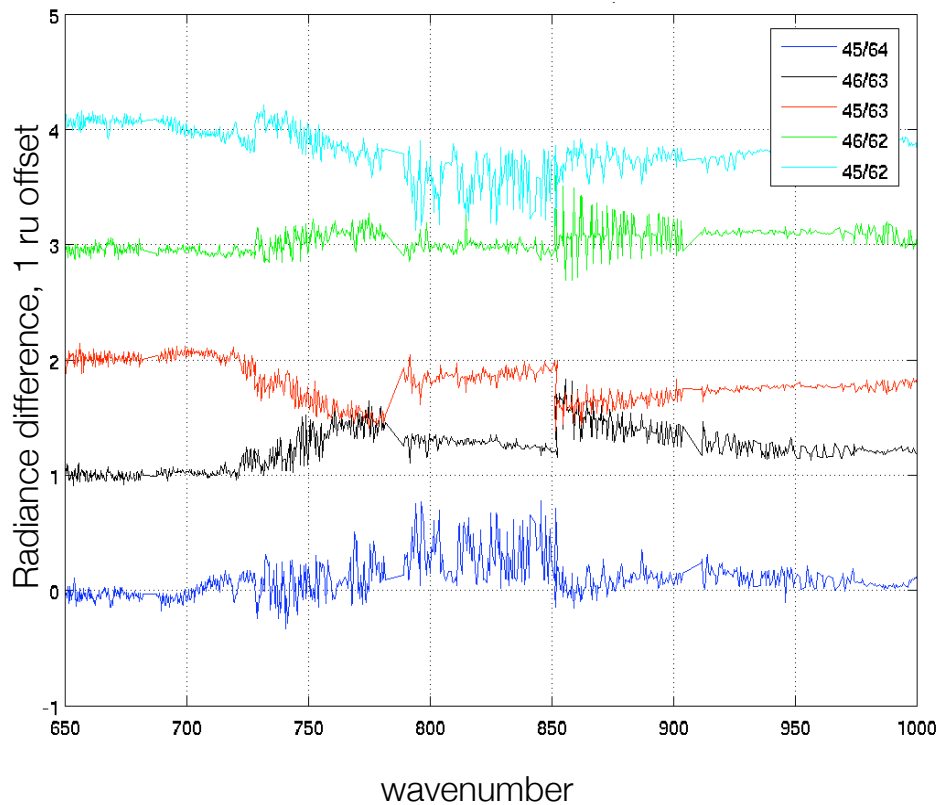
S-HIS brightness temperatures and AIRS FOV locations



# Variations in individual spectra. 2004.09.07 EAQUATE case

## AIRS

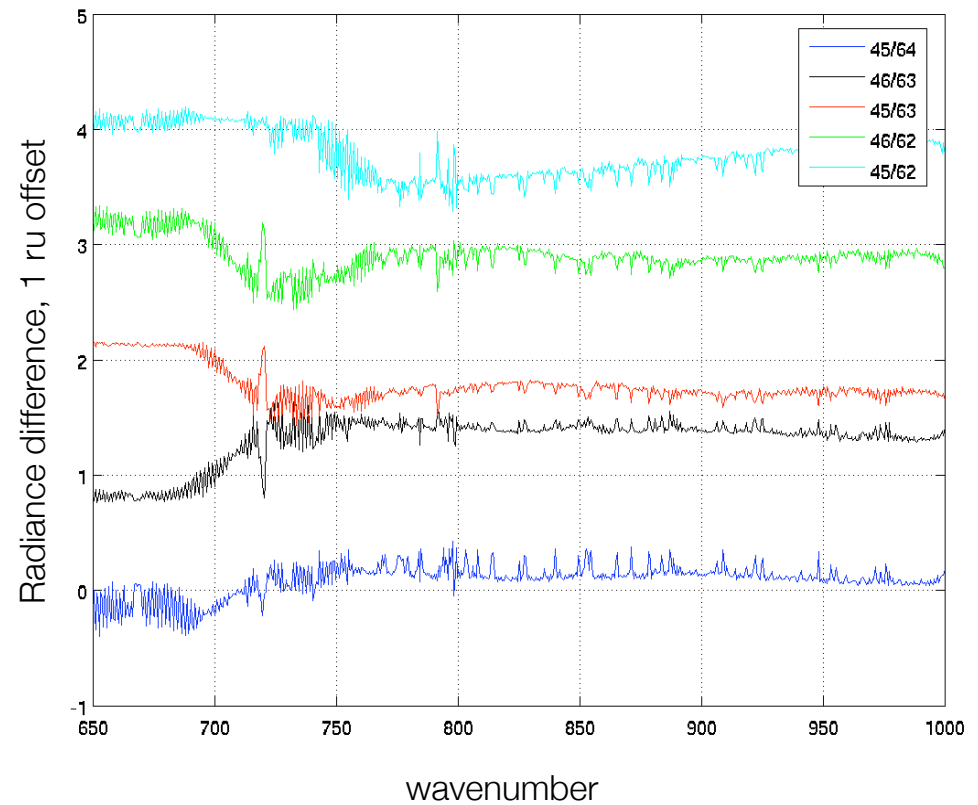
Differences from mean spectrum



A/B state and array correlated artifacts

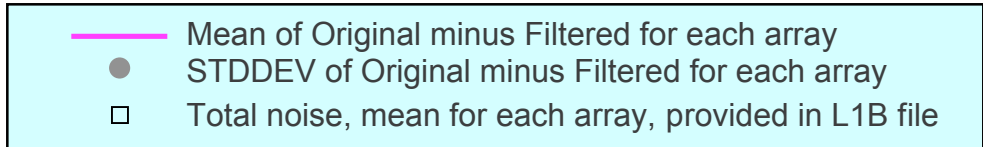
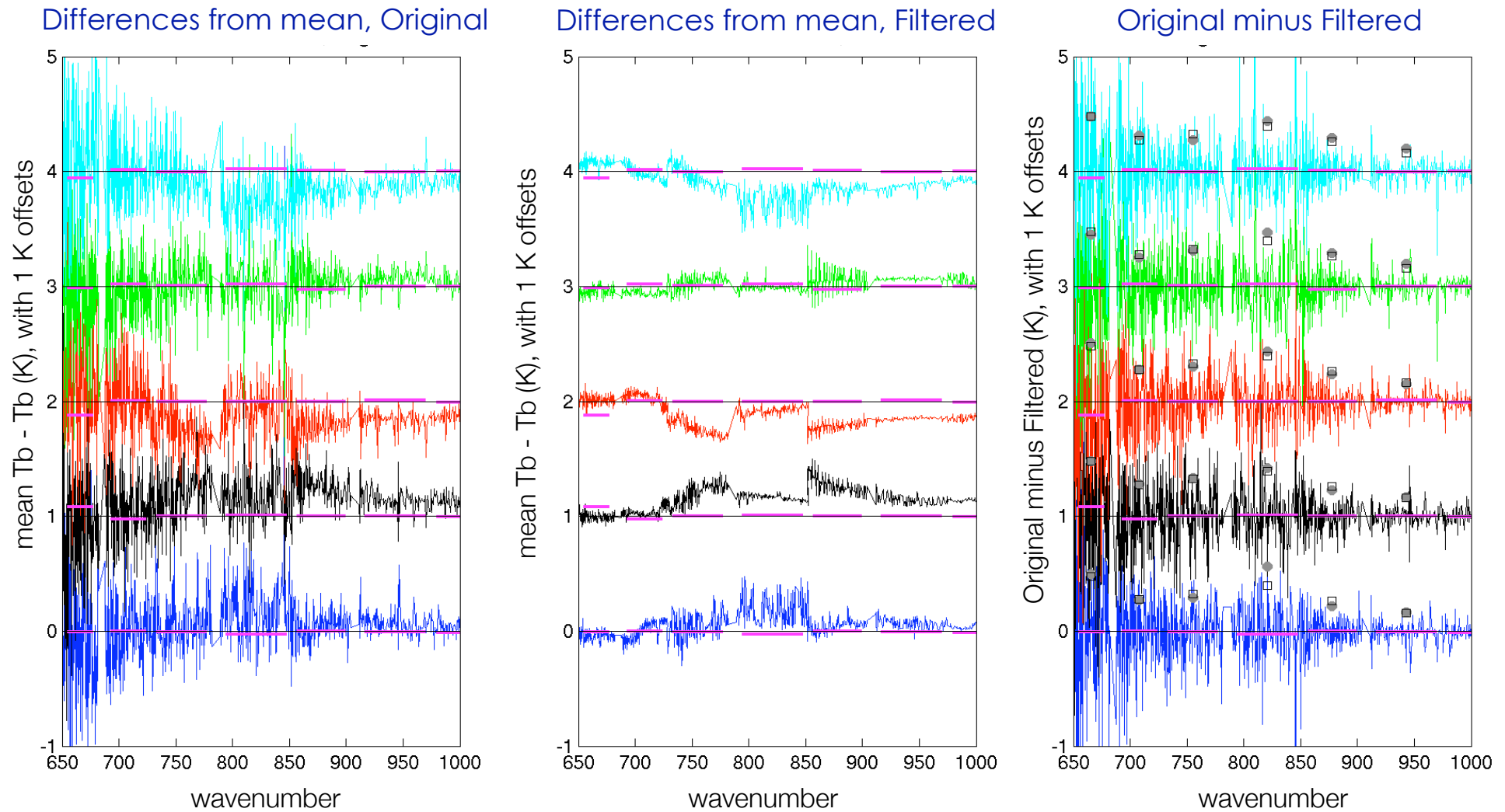
## S-HIS

Differences from mean spectrum

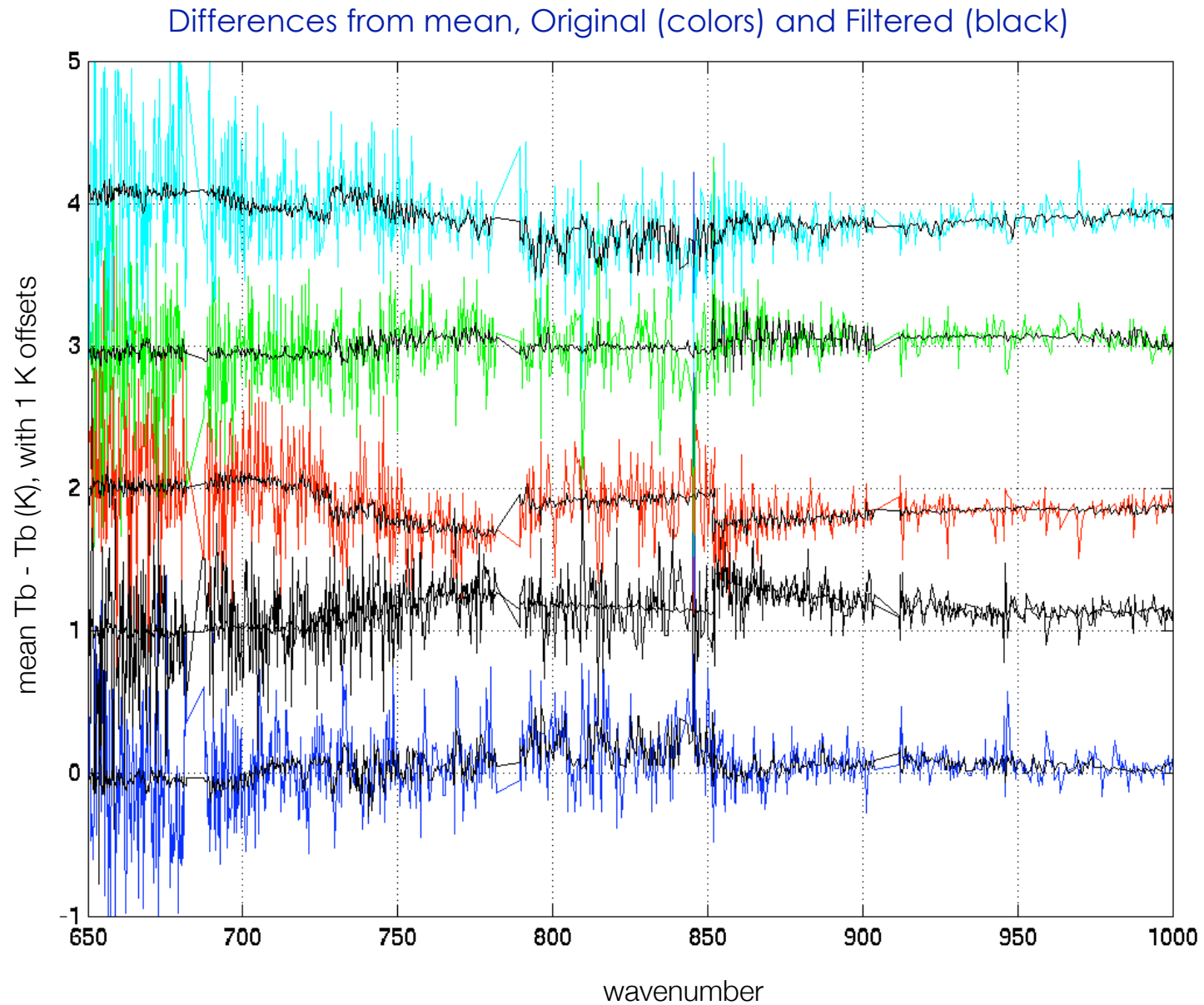


Smooth and physically reasonable

# Variations in individual spectra. 2004.09.07 EAQUATE case



# Variations in individual spectra. 2004.09.07 EAQUATE case

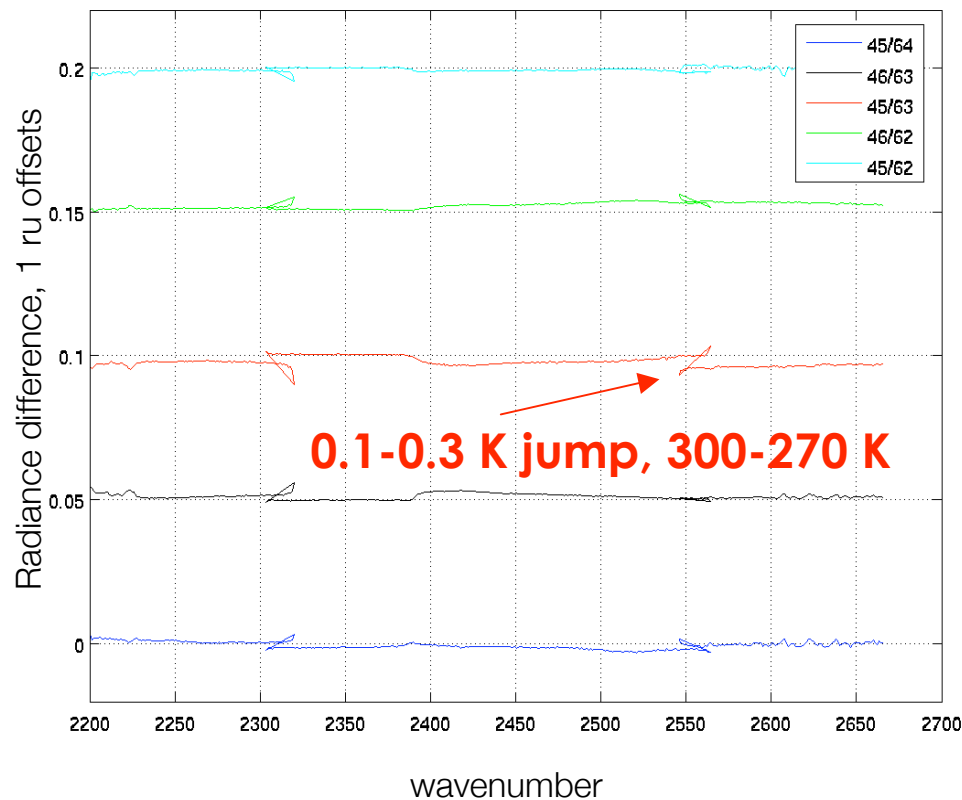




# Variations in individual spectra. 2004.09.07 EAQUATE case

## AIRS

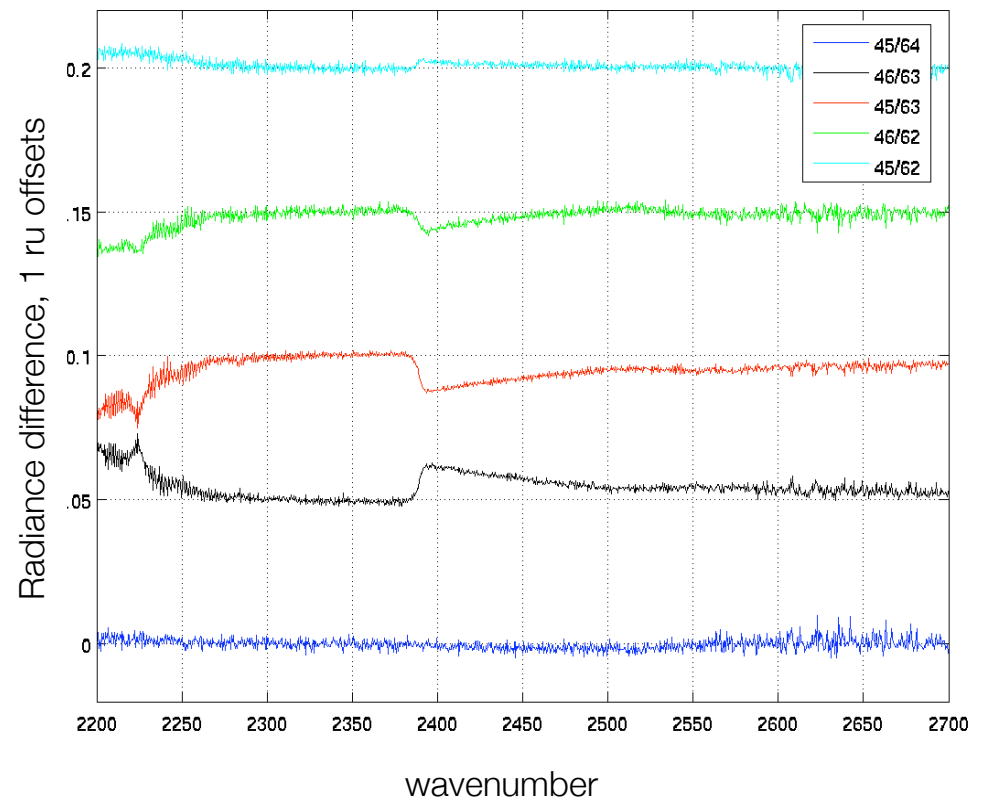
Differences from mean spectrum



Low random noise, but significant array-to-array jumps

## S-HIS

Differences from mean spectrum



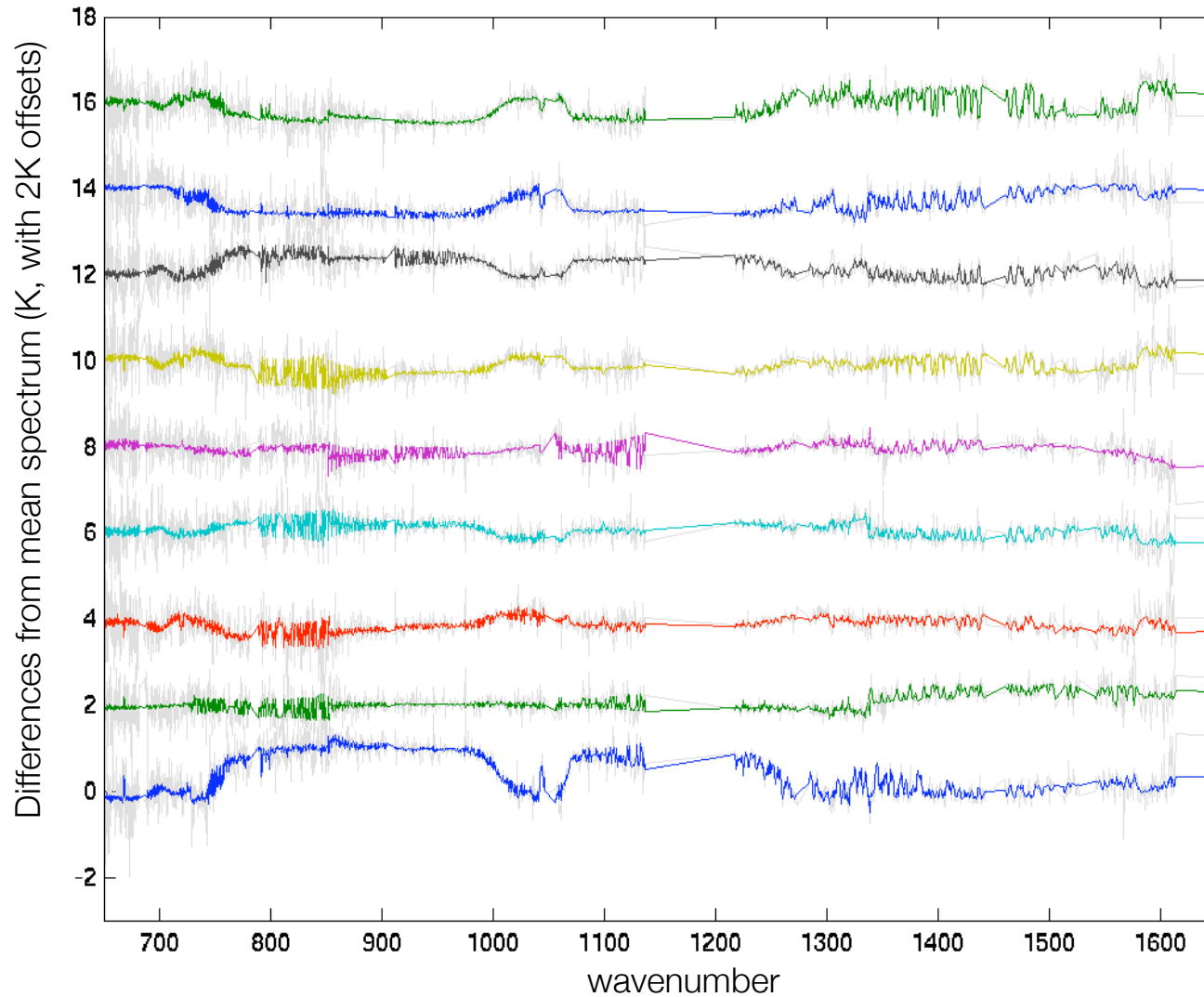
Higher random noise, but 4x spectral resolution and spectrally smooth



# More individual AIRS spectra, 2005.04.01 granule 200

---

BT differences from mean spectrum



# Summary, Conclusions

---

Exploiting the redundancy in high spectral resolution observations, PCA is a simple yet very powerful tool not only for noise filtering and lossy compression, but also for the characterization of sensor noise and other variable artifacts using Earth scene data. Many of the findings presented here are consistent with analyses performed using pre-flight and on-orbit blackbody and space views, providing strong evidence for the validity of the PCA approach and results.

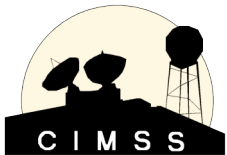
Specific findings:

- PCA estimates of AIRS spectrally random and spectrally correlated NEDN compare well with estimates computed from the on-board blackbody and space views.
  - The signal dependence of AIRS NEDN can be accurately parameterized in terms of the scene radiance (e.g.  $\gamma_{\text{photon}}$ ,  $\text{NEDN}_{\text{Thermal}}$ ). AIRS shortwave NEDN for a 300K scene is  $\sim 2x$  larger than for a 250K scene.
  - The PCA estimate is of the spectrally random noise; estimates of the AIRS spectrally correlated noise using  $[\text{total\_noise}^2 - \text{pca\_noise}^2]^{1/2}$  agree very well with preflight determinations using blackbody data. The spectrally correlated noise is a large fraction of the total noise for several detector arrays.
- Examination of  $N_{\text{orig}} - N_{\text{recon}}$  allows other non-Gaussian phenomenon to be characterized.
  - Many longwave and midwave PV detectors exhibit “popping” behavior above that expected from pure Gaussian behavior; shortwave channels do not exhibit this “popping”.
  - For v4 L1B data, only a small percentage (14 out of 2378) of channels exhibit “striping”.
- Inspection of the PCs and individual PC filtered radiance spectra reveal effects that lie in the less understood domain between calibration (long average) and spectrally random, repeatable noise.
  - The radiometric performance of AIRS at the level of the NEN contains artifacts not described by spectrally and temporally random noise, or by long-term calibration uncertainty.
  - Large ensemble averages show A / B state dependent artifacts on the order of  $\pm 0.4K$  for M-08.
  - For several arrays, the spectrally correlated noise is large, and dependent on A / B state (i.e. A-A and B-B channel correlation, but not A-B), generally consistent with Weiler ADFM#620.

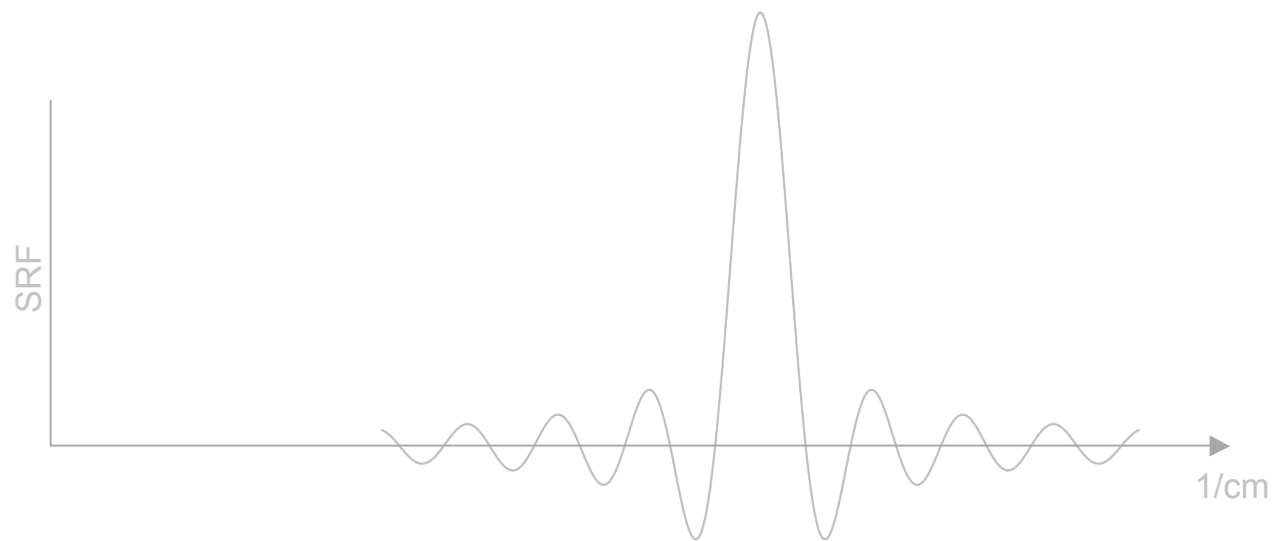
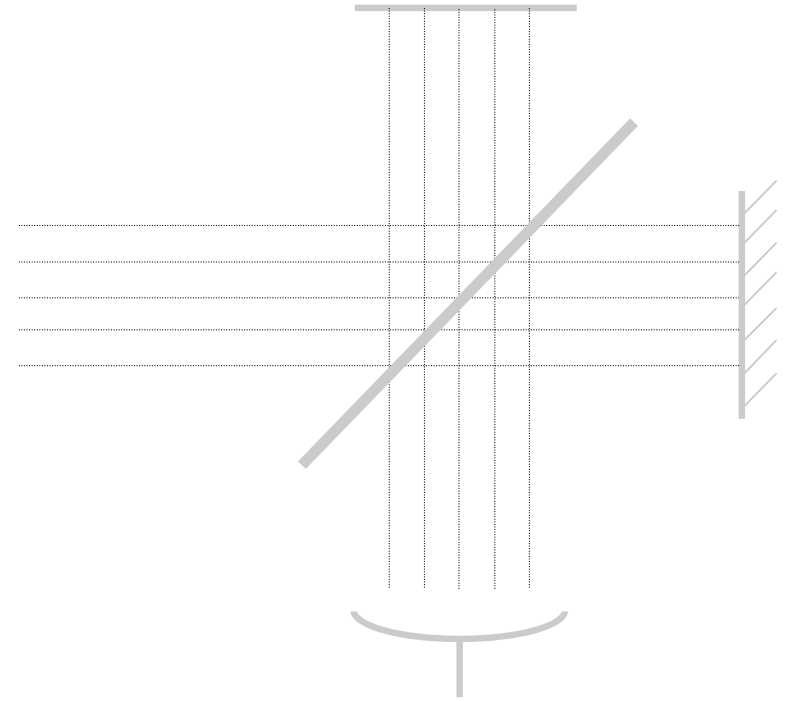
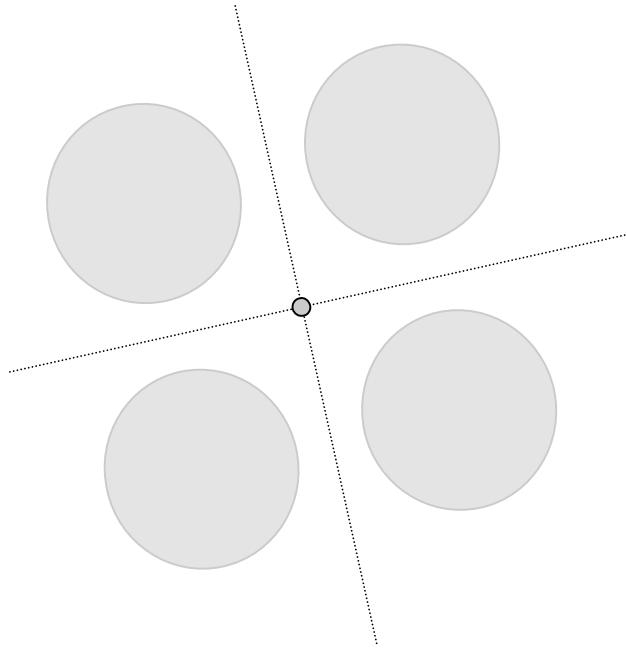
# Preliminary PCA-based investigations of IASI spectra

---

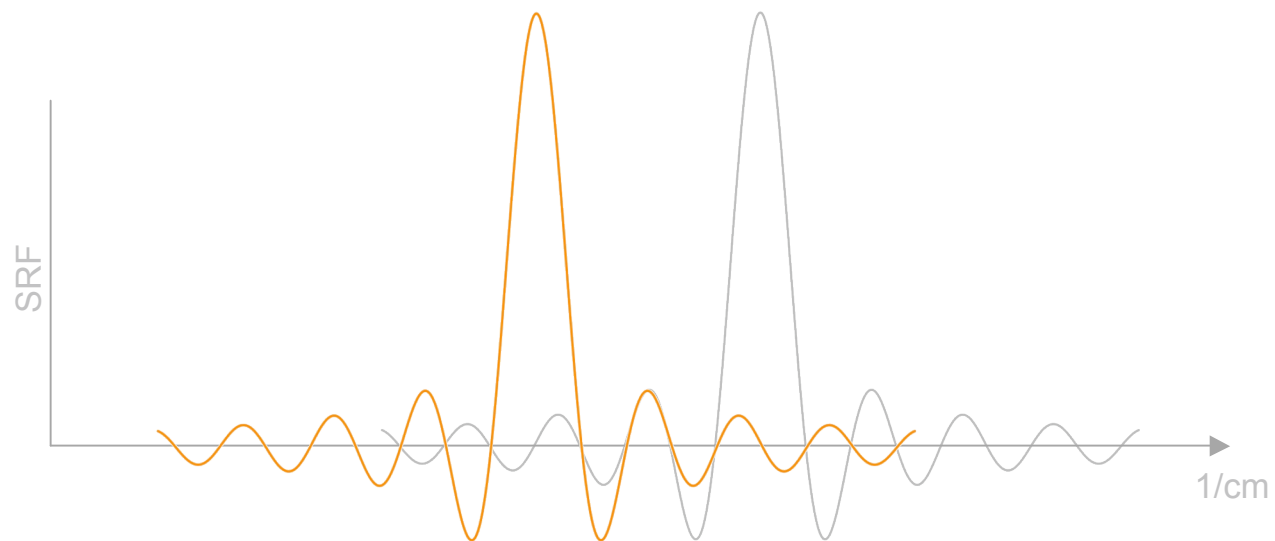
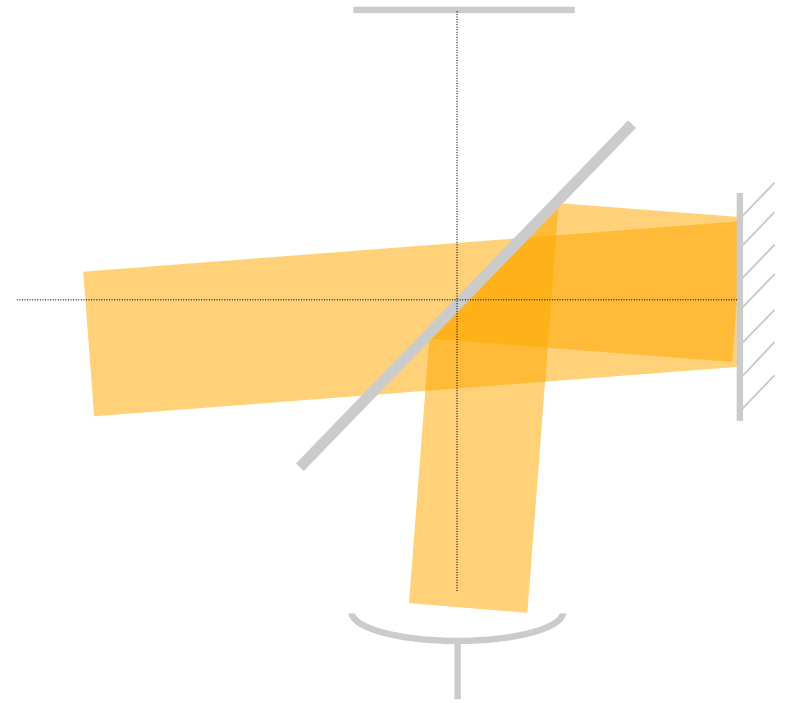
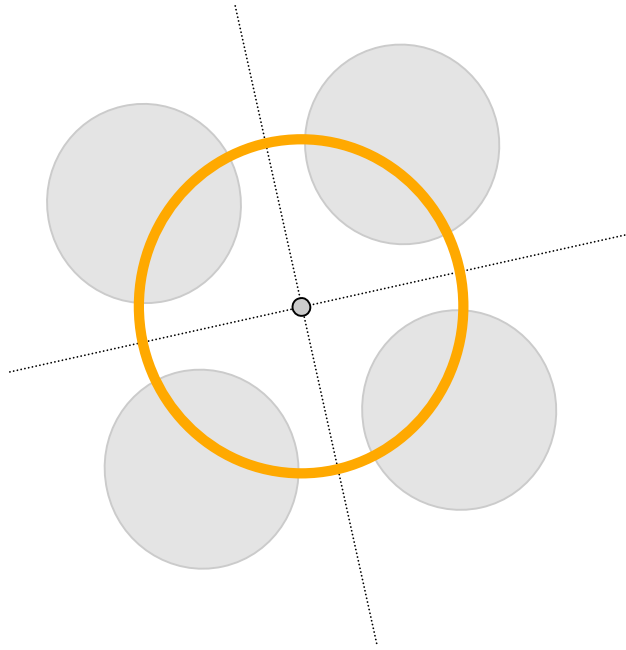
- Dave Tobin, Paolo Antonelli, Hank Revercomb, Bob Knuteson



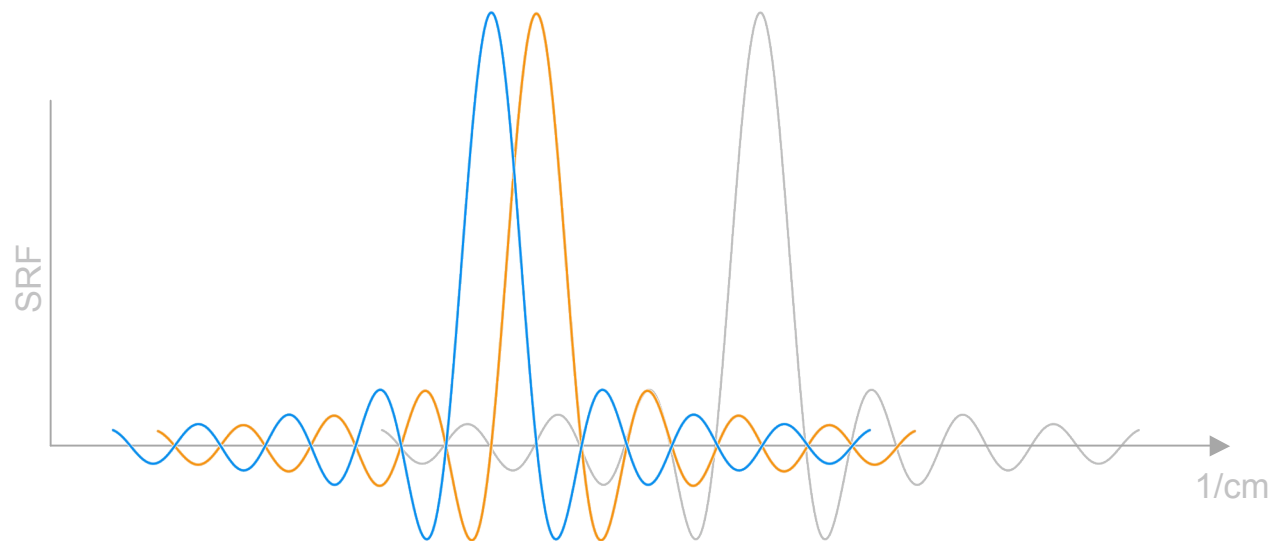
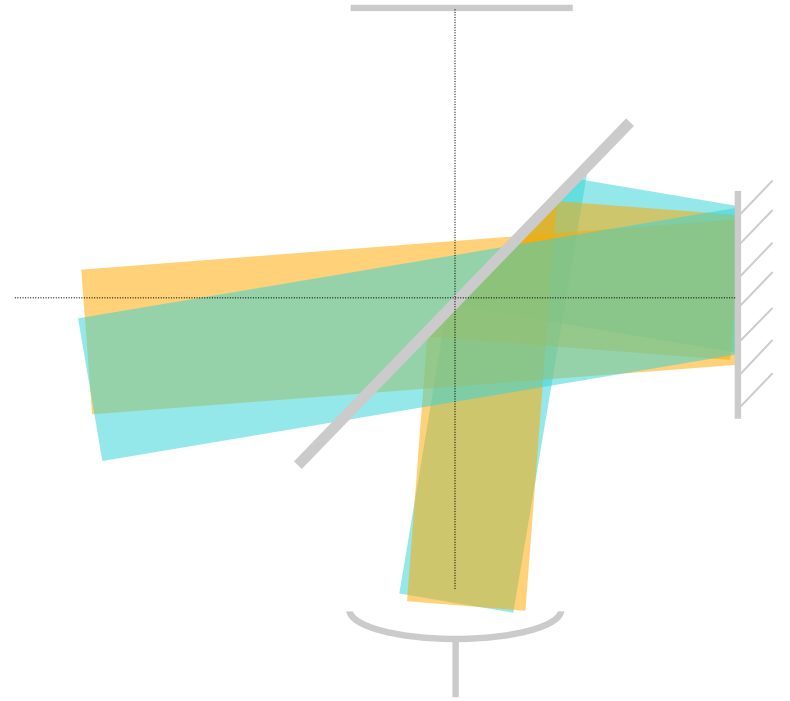
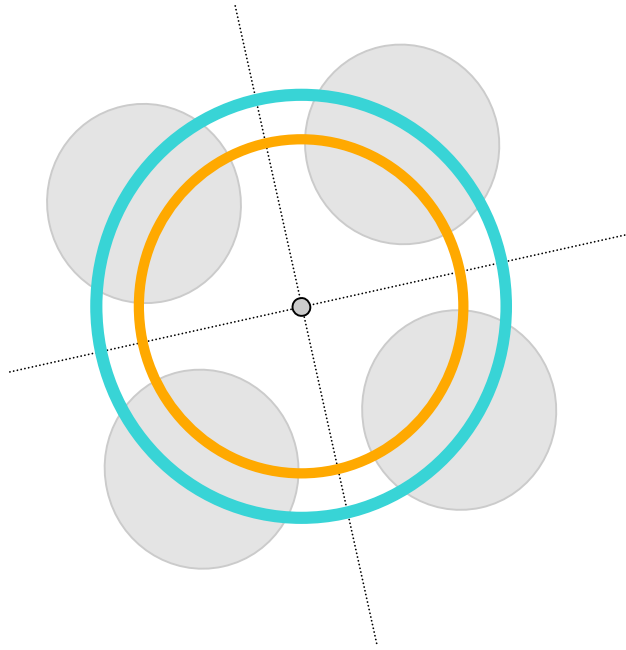
# On-axis beam

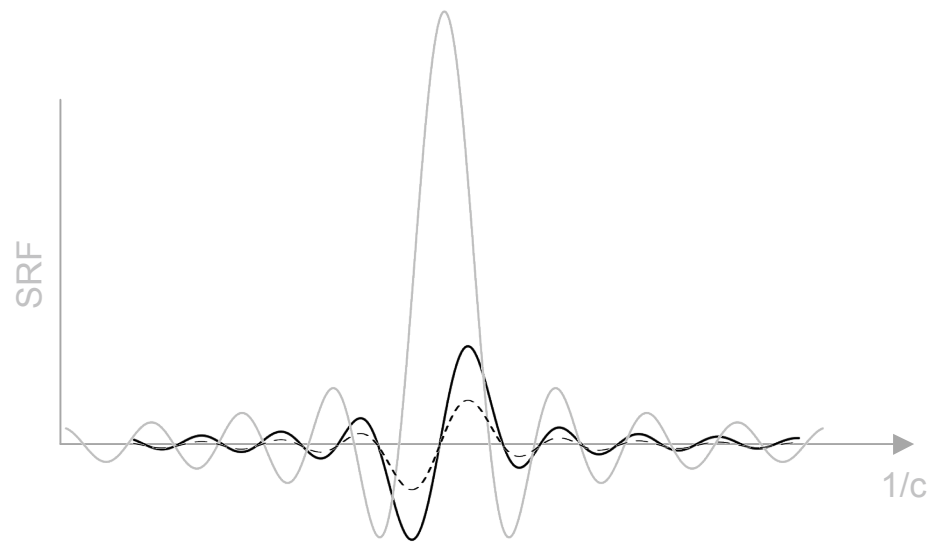
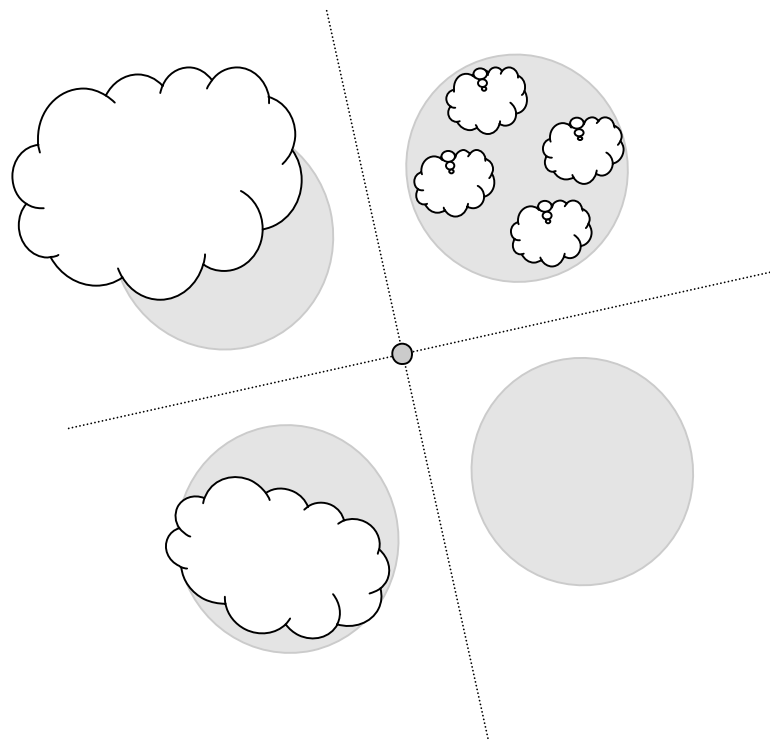
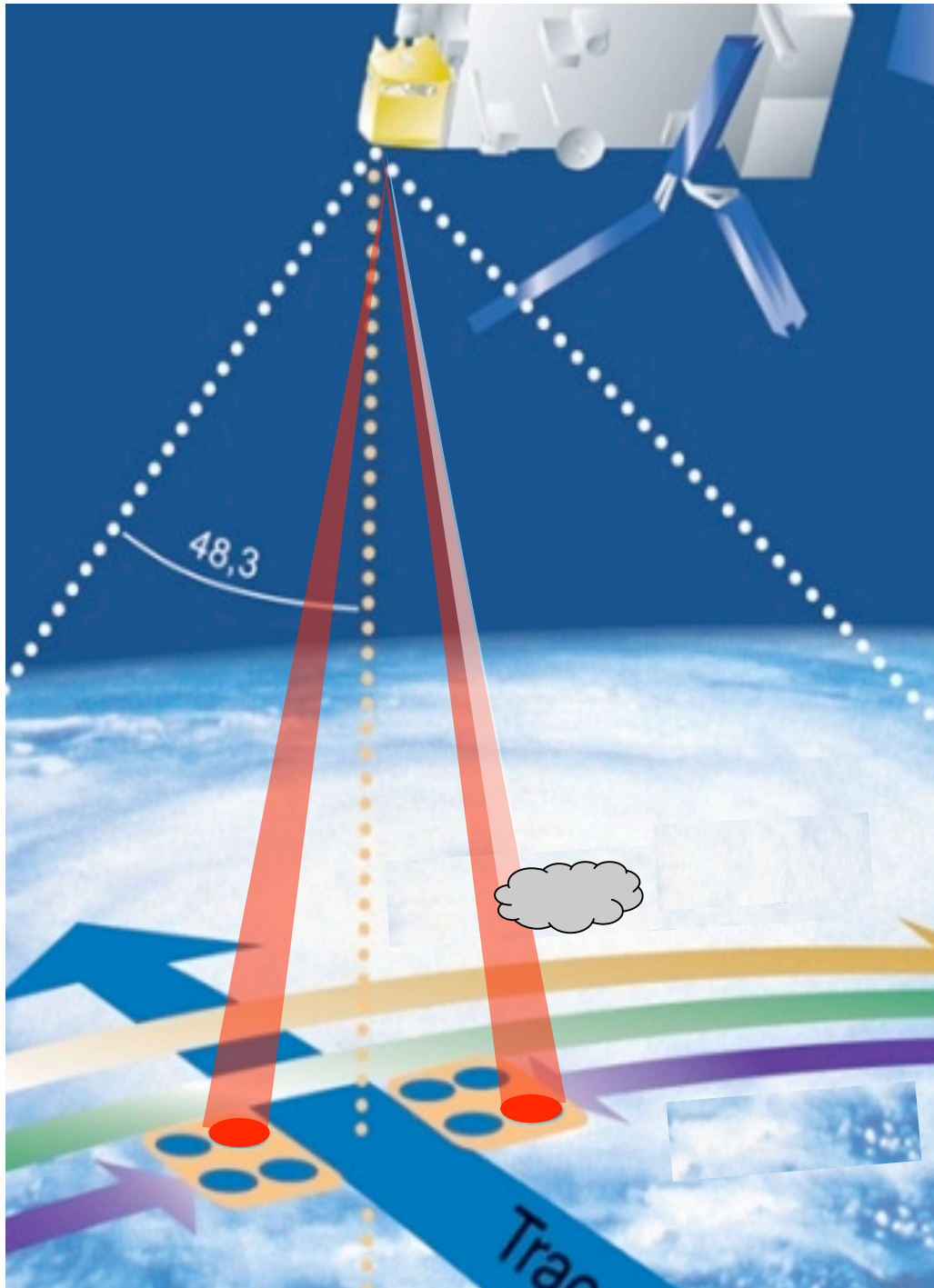


# Off-axis beam



# Off-axis beams





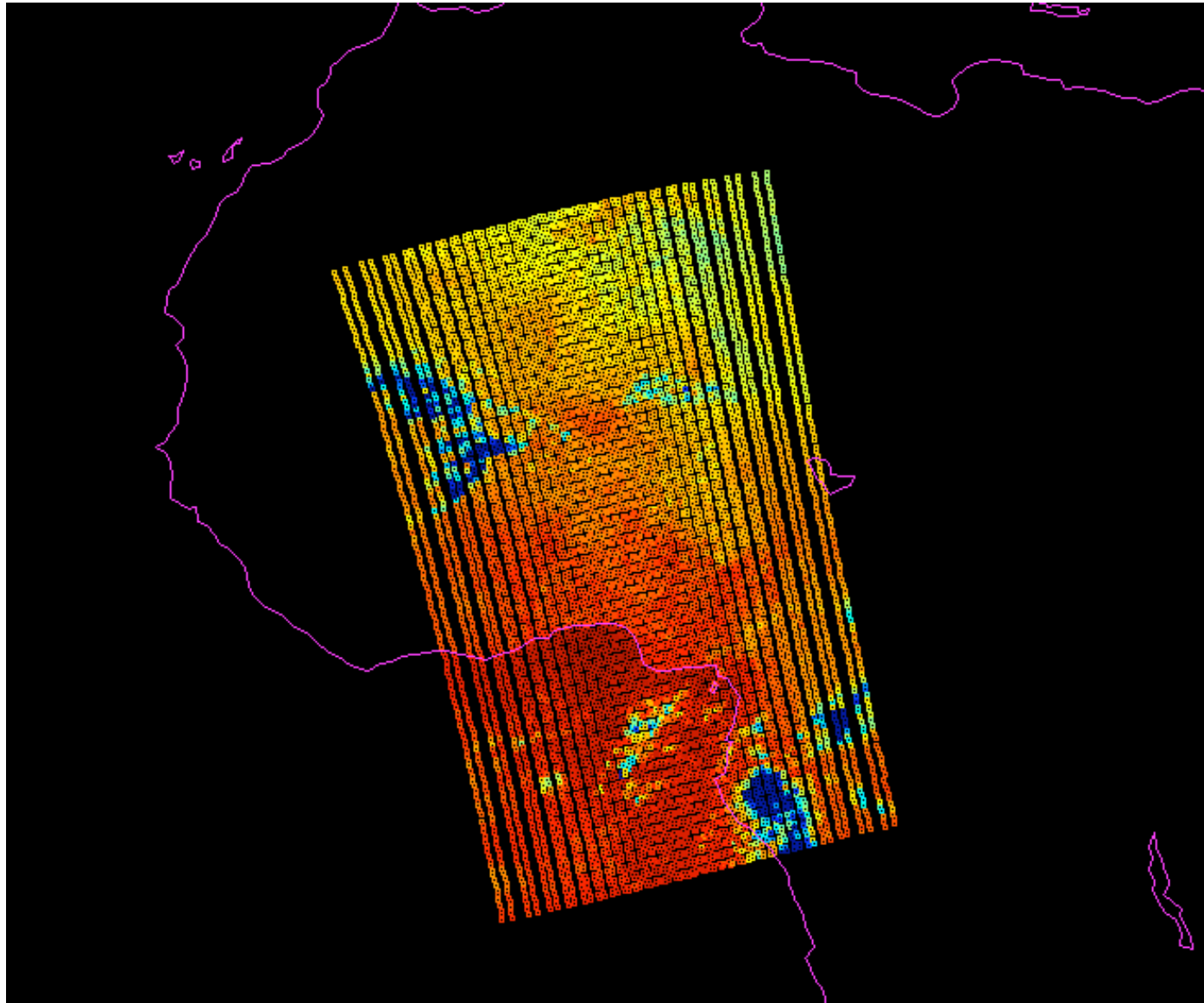
# Data

---

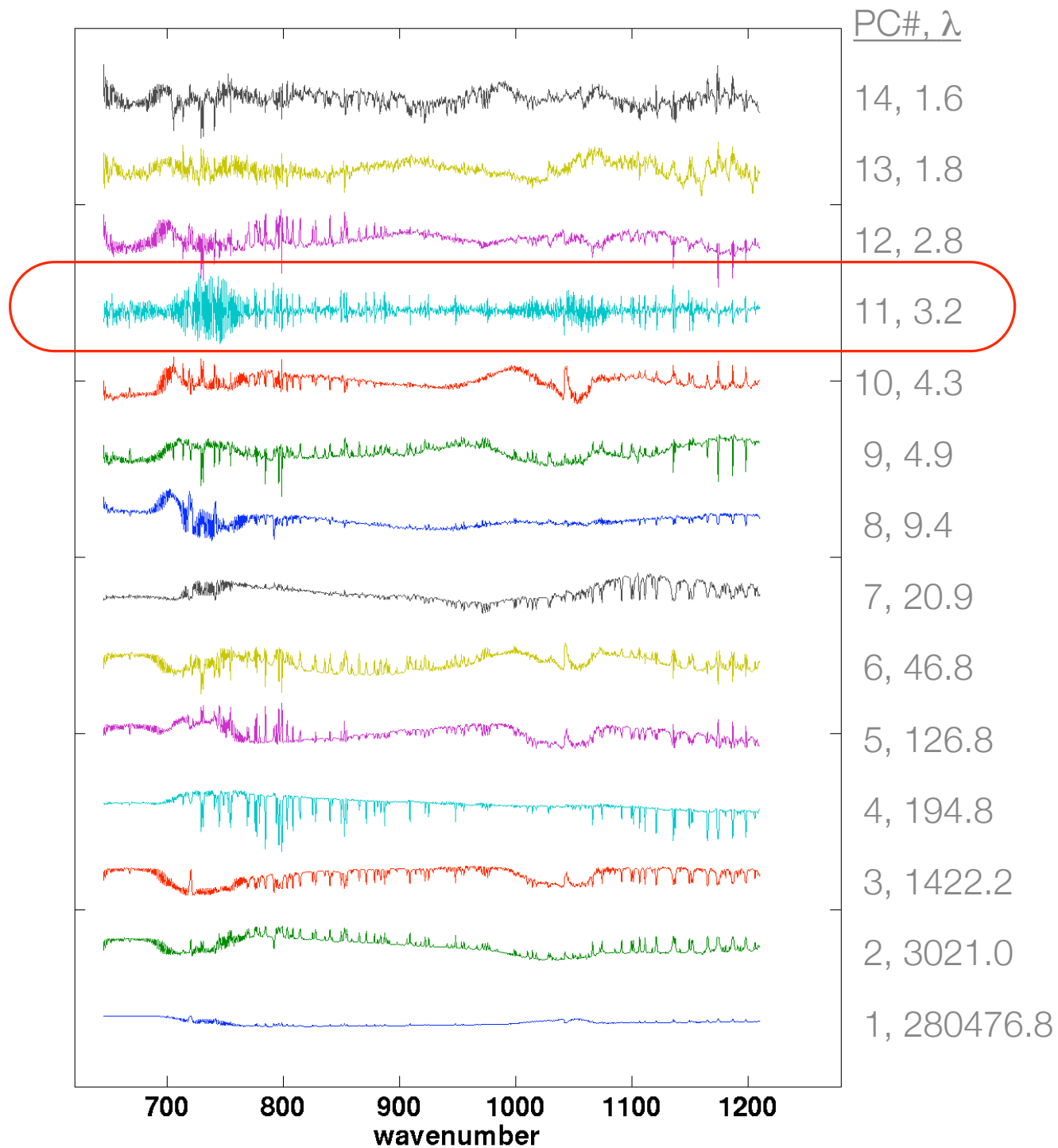
- 3 “granule” (22 scan lines, 22\*30\*4 footprints) NetCDF files from the test orbit
- Data provided to us via NOAA



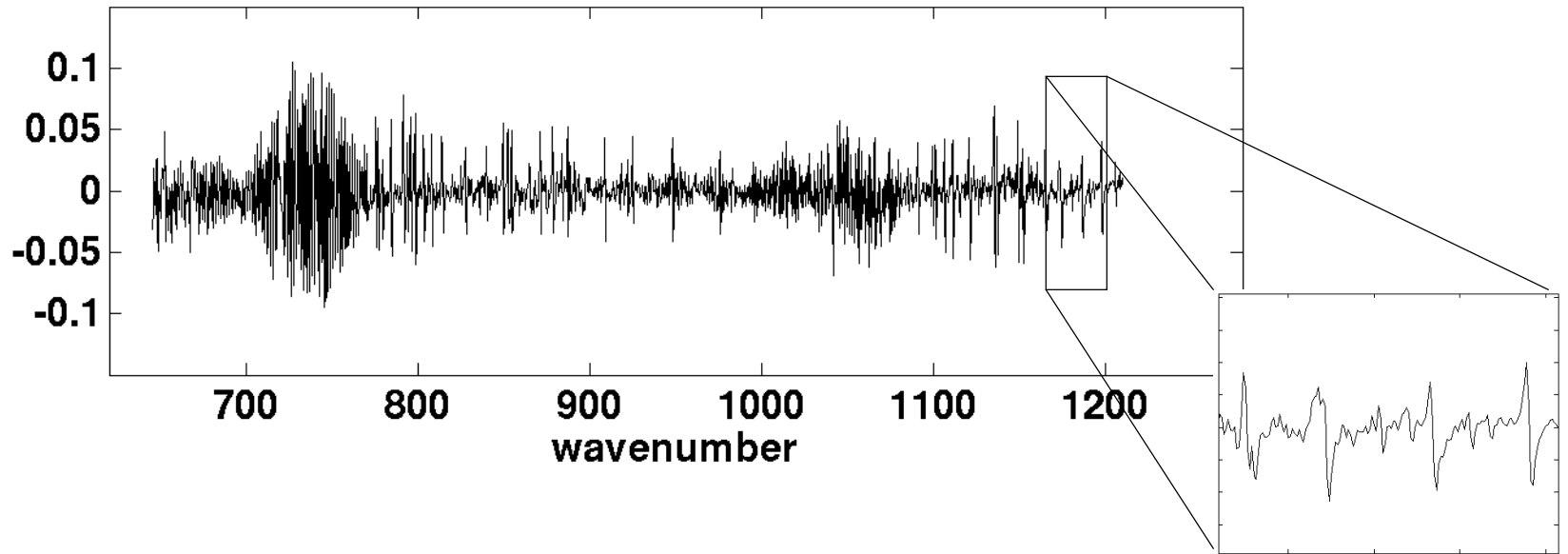
900  $\text{cm}^{-1}$  brightness temperatures



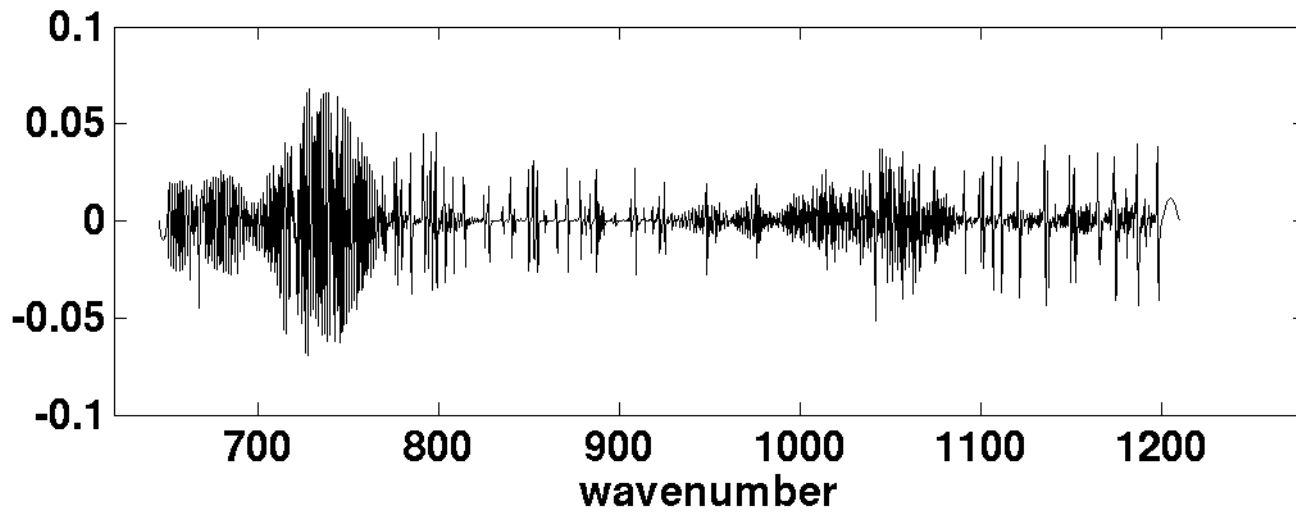
# Longwave PCs



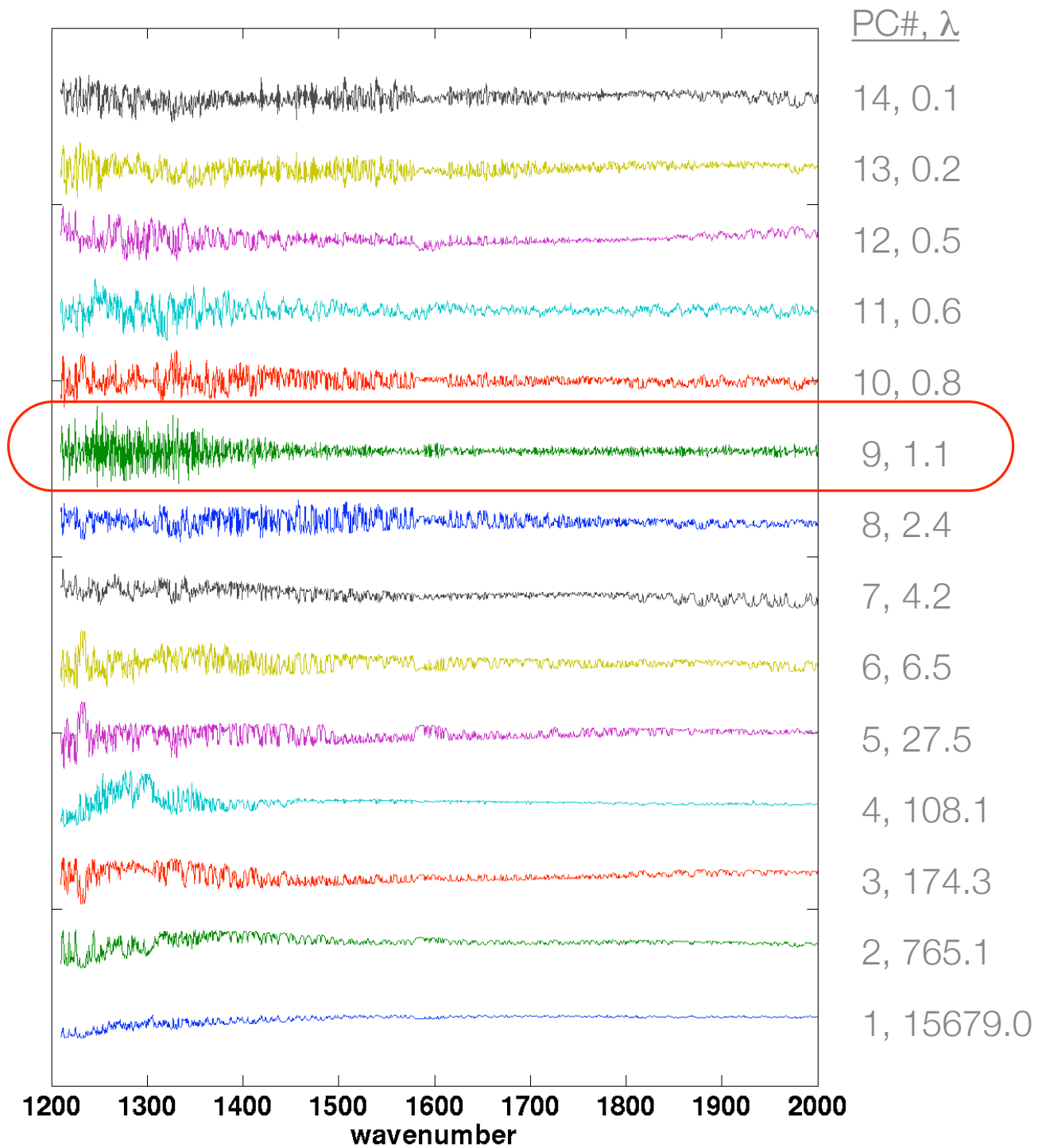
Longwave PC#11



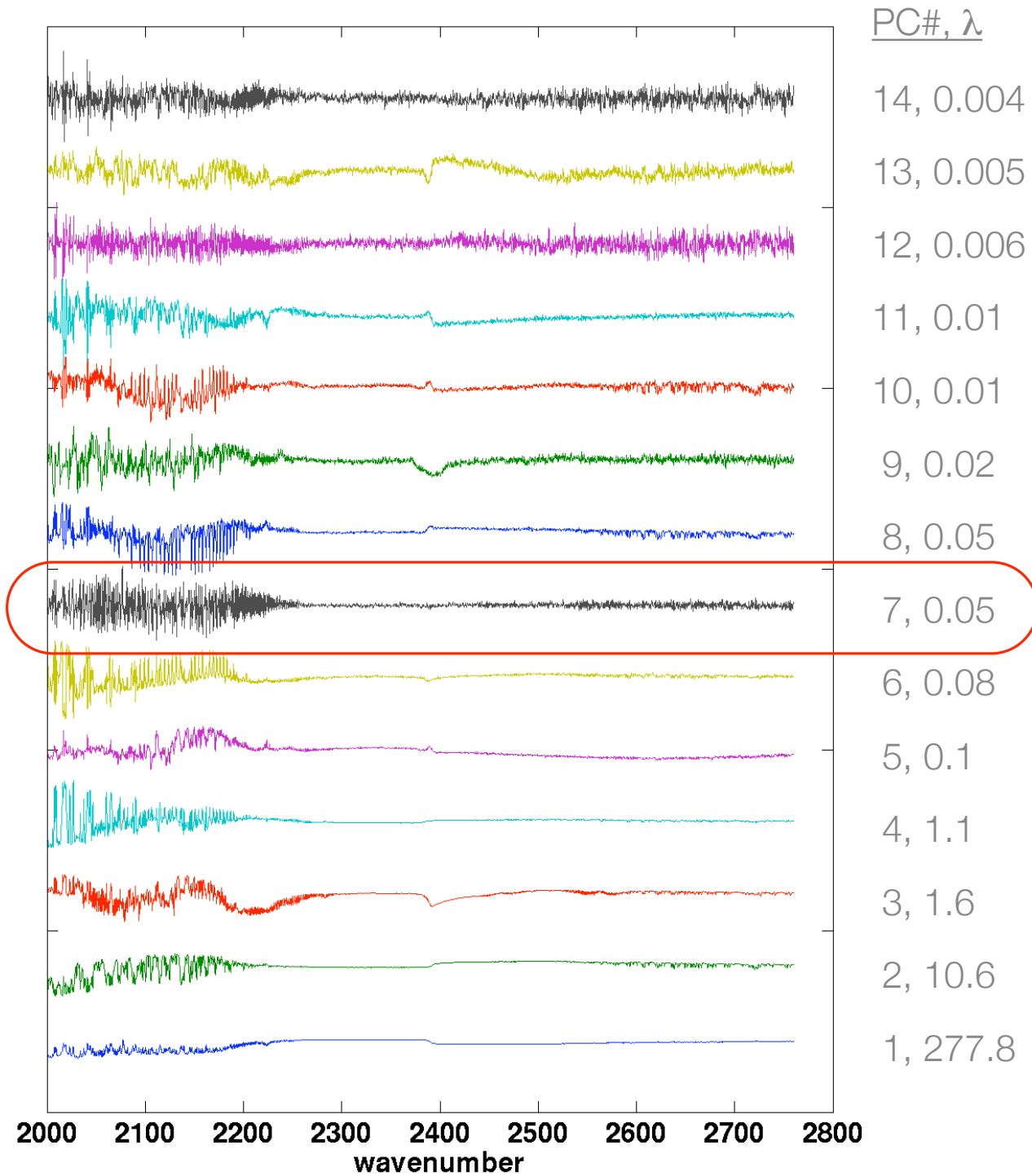
Effect of 1 ppm spectral shift on mean spectrum



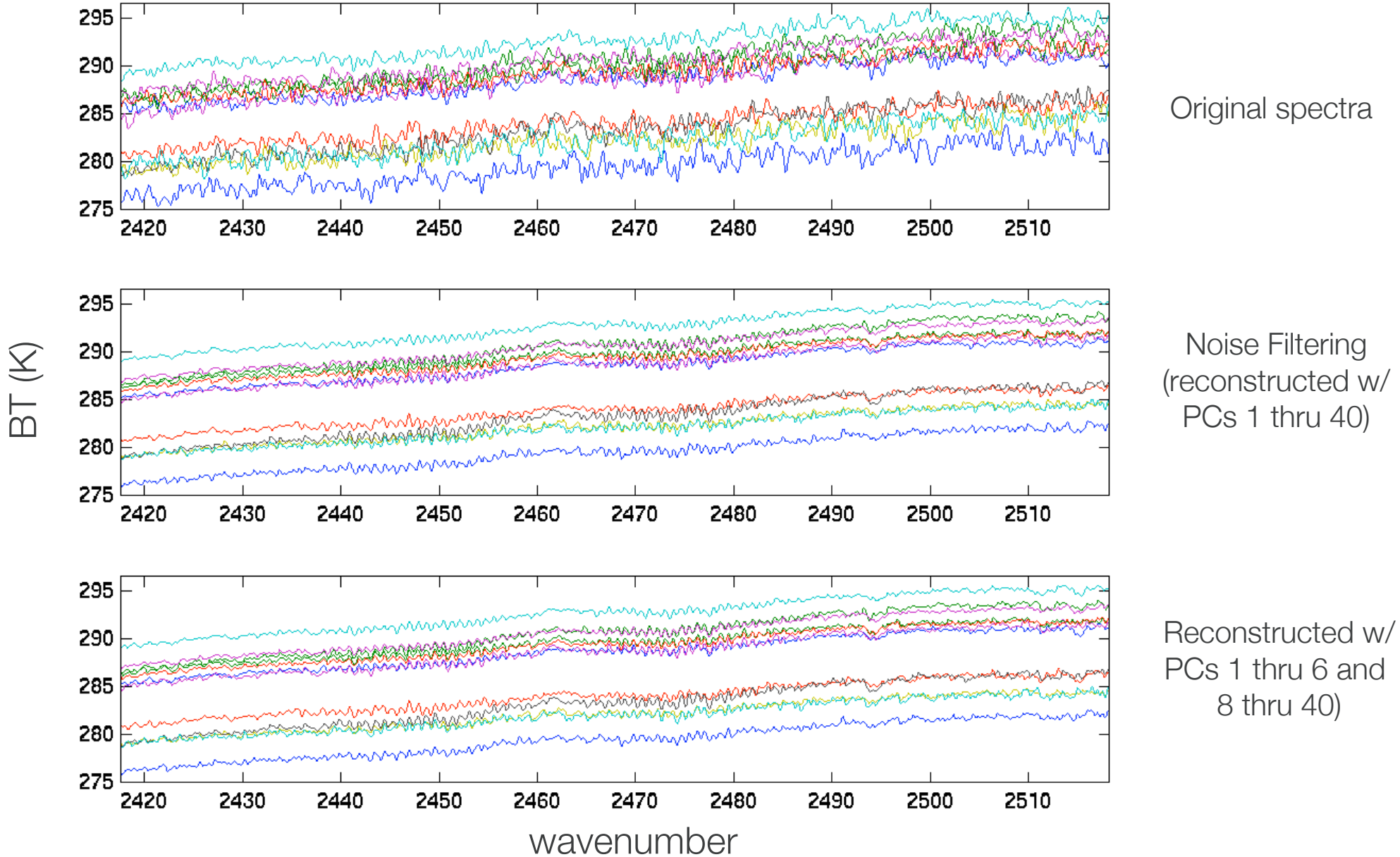
# Midwave PCs



# Shortwave PCs



# Sample SW spectra

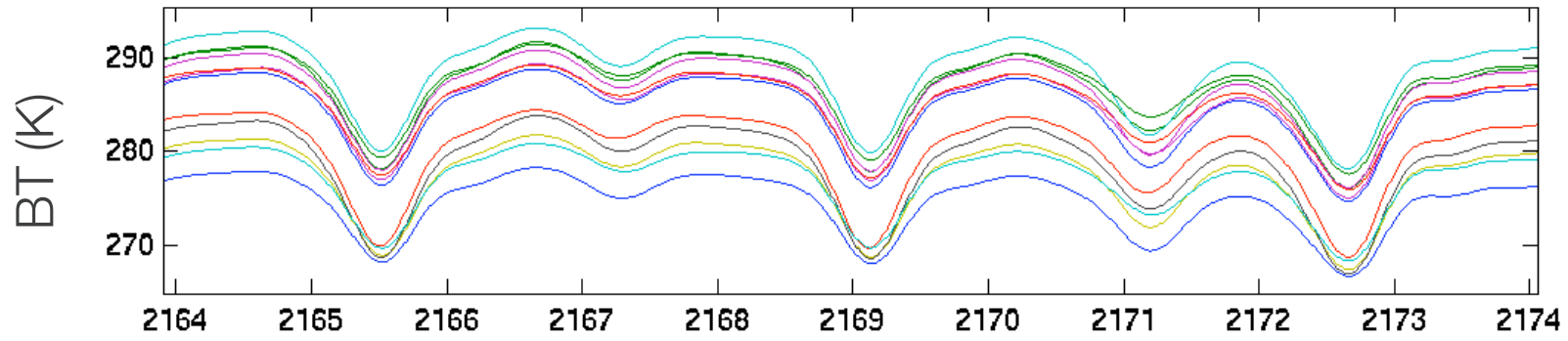
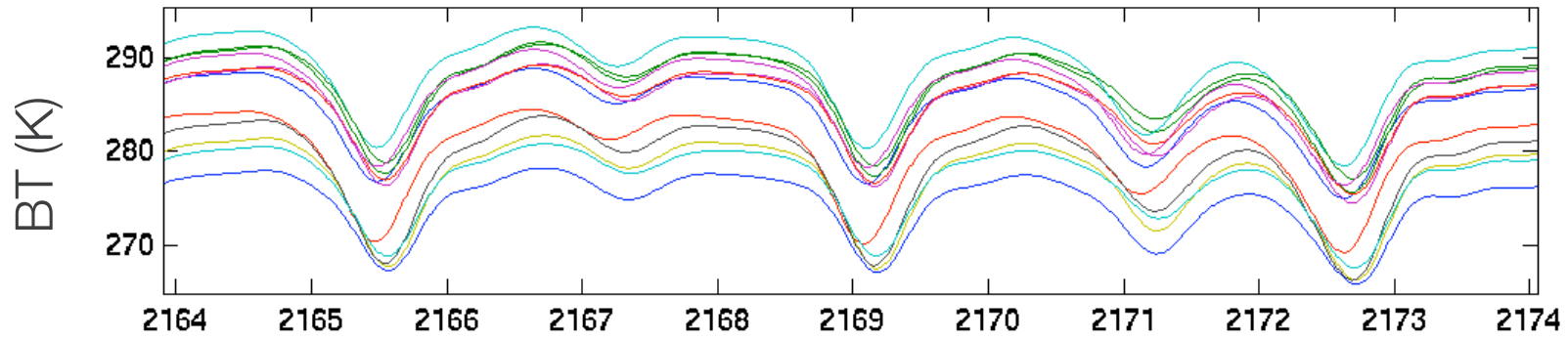


Original spectra

Noise Filtering  
(reconstructed w/  
PCs 1 thru 40)

Reconstructed w/  
PCs 1 thru 6 and  
8 thru 40)

Sample IASI spectra



wavenumber

# Summary, Preliminary Conclusions

---

The IASI spectra look very good !

Dependent set PC noise filtering is a powerful tool for greatly reducing random noise and should be exploited in retrieval and other data applications.

PCA is also a powerful tool for identifying and characterizing sensor characteristics. The primary feature investigated here is the expected effects of ILS variations due to scene inhomogeneity.

Varying self-apodization effects due to scene inhomogeneity within the IASI footprints manifests primarily in a spectral shift, and this effect is found to be largely characterized by a single PC/eigenvector in the dependent set PCA shown here.

Preliminary studies suggest that the spectra can be reconstructed without the “spectral shift” PC included to remove a large portion of the effects of ILS variations due to scene inhomogeneity. More work needs to be done to study the accuracy and computational efficiency of this approach.

For the Shortwave band, higher order PCs also show line broadening and asymmetry effects due to the varying self apodization.

Instrument specific characteristics, such as spectral shifting appear to be orthogonal to environmental variability.



# Next

---

- Further characterization and parameterization of the instrument noise using PCA:
  - Further application of PCA to characterize the correlated component of the instrument noise;
  - Further application of PCA to IASI data.
- Study the impact of PCA on the true, natural compressed version of hyperspectral data: physically retrieved atmospheric variables:
  - hyperspectral data inversion system based on LBLRTM and following C. Rodger's recipe has been developed in the past 2 years;
  - comparison of physical retrievals obtained from filtered and unfiltered radiances;
  - impact of PCA on the hyperspectral data information content.

# Background

---

- Noise estimation/characterization using Earth scene data is made possible by PCA noise filtering
  - Huang et al., Application of Principle Component Analysis to High-Resolution Infrared Measurement Compression and Retrieval, *JAM*, 40, 365-388, 2001.
  - Antonelli et al., A principle component noise filter for high spectral resolution infrared measurements, *JGR*, 109, D23102, 2004.
  - Goldberg et al., Principle Component Analysis of AIRS Data, Workshop on Assimilation of high spectral resolution sounders in NWP, ECMWF, June 2004.
  - Turner et al., Noise reduction of Atmospheric Emitted Radiance Interferometer (AERI) observations using principal component analysis. *Journal of Atmospheric and Oceanic Technology*, in press, 2006.
- PCA is also very useful for diagnosing instrument performance and characteristics
  - Rodgers, Application of Singular Value Decomposition to High Spectral Resolution Measurements, ASSFTS 2005.
  - Tobin et al., Recent efforts to validate EOS observations. Hyperspectral data noise characterization using PCA: application to AIRS, Proc. SPIE Vol. 6301, 2006.
    - *The following analyses follow that of Tobin et al. 2006 for dependent set PCA, but without noise normalization of the radiance spectra at this point.*

# The End

---

- Thank you